National Library
of Canada

Acquisitions and
Bibliographic Services Branch

395 Wellington Street
Ottawa, Ontario
K1A 0N4

Bibliothèque nationale
du Canada

Direction des acquisitions et
des services bibliographiques

395, rue Wellington
Ottawa (Ontario)
K1A 0N4

Your file Votre référence

Our file Notre référence

NOTICE

The quality of this microform is heavily dependent upon the quality of the original thesis submitted for microfilming. Every effort has been made to ensure the highest quality of reproduction possible.

If pages are missing, contact the university which granted the degree.

Some pages may have indistinct print especially if the original pages were typed with a poor typewriter ribbon or if the university sent us an inferior photocopy.

Reproduction in full or in part of this microform is governed by the Canadian Copyright Act, R.S.C. 1970, c. C-30, and subsequent amendments.

AVIS

La qualité de cette microforme dépend grandement de la qualité de la thèse soumise au microfilmage. Nous avons tout fait pour assurer une qualité supérieure de reproduction.

S'il manque des pages, veuillez communiquer avec l'université qui a conféré le grade.

La qualité d'impression de certaines pages peut laisser à désirer, surtout si les pages originales ont été dactylographiées à l'aide d'un ruban usé ou si l'université nous a fait parvenir une photocopie de qualité inférieure.

La reproduction, même partielle, de cette microforme est soumise à la Loi canadienne sur le droit d'auteur, SRC 1970, c. C-30, et ses amendements subséquents.

Canada

DEPARTURE PROCESS CHARACTERIZATION ANALYSIS OF A LEAKY BUCKET SCHEME

Yuan Chen

A Thesis

in

The Department

of

Electrical & Computer Engineering

Presented in Partial Fulfillment of the Requirements

for the Degree of Master of Applied Science at

Concordia University

Montreal, Quebec, Canada

April 1996

ISBN 0-612-10831-7

Canada

ABSTRACT

Departure Process Characterization Analysis of a Leaky Bucket Scheme

Yuan Chen

This thesis presents the statistical characterization analysis of the departure process of a Leaky Bucket scheme in ATM networks. There are few analyses in the literature on the departure process. Most of the previous studies on the interdeparture time distribution of a Leaky Bucket were based on the Laplace transform under simple Poisson arrival assumption. In this thesis, a simple Modified Geometric (MGeo) model based on a mapping procedure is proposed for the interdeparture time distribution of a Leaky Bucket. The burstiness and correlation control effects of a Leaky Bucket are extensively discussed through various statistics such as Squared Coefficient of Variation (SCV), autocorrelation coefficient and Index Dispersion for Counts (IDC). The analyses are carried out under a wide range of traffic sources such as Poisson, Generalized Geometric (GGeo) and Markov Modulated Poisson Process (MMPP) arrival processes. Simulation results are provided to verify the accuracy of the various mapping procedures. Numerical results are obtained in order to investigate how the traffic characteristics of the departure process are affected by the token pool size, the token generation rate, the burst and correlation degree of the arrival process. The trade-off between the burstiness of the departure process and the cell delay is examined. Finally, a two-state MMPP model is suggested to approximate the departure process of a Leaky Bucket.

ACKNOWLEDGEMENTS

I would like to express my profound gratitude to my thesis supervisor, Professor Jeremiah F. Hayes, and co-supervisor, Professor Mustafa Mehmet Ali, for their invaluable guidance, encouragement and support throughout the course of this work.

My sincere thanks to Dr. Jun Huang for his valuable advice and constant assistance during this work.

I would like to thank many other professors and fellow graduate students at Concordia University for their suggestions and help. My acknowledgements to all the examiners for their time and valuable comments. I appreciate the financial assistance from the National Centre of Excellence in Telecommunications during my study.

My heartfelt thanks to my parents and my brothers' for their love and constant encouragement, and many thanks to all my friends for their friendship and help throughout the course of my studies.

Dedicated to

My parents, *Shuhua and Fugeng*

TABLE OF CONTENTS

LIST OF FIGURES

LIST OF TABLES

LIST OF SYMBOLS

M	token pool size
r	token generation rate
λ_j	arrival rate of MMPP in phase j
σ_i	total transition rate of leaving phase i
R	transition rate matrix for the underlying Markov process
Λ	arrival rate matrix for the MMPP
x_i	steady-state probability of system in state i
ρ	load intensity of the system
N	input buffer size
m	number of tokens in the token pool
n	number of cells in the input buffer
$X(m, n, t)$	probability of having m tokens in the token pool and n cells in the buffer at time t ($t = 0, 1, 2, \ldots$ slot)
a_i	probability of i arrivals during a slot
$p_{i,j}$	state transition probabilities, from state i to state j
T	average number of cells entering to the system at the slot boundary
P_L	cell loss probability
SCV	Squared Coefficient of Variation
V	interdeparture time between two departures
C^2	squared coefficient of variation (SCV) of MGeo distribution
C^3	cubed coefficient of variation of MGeo distribution
$P(V = k)$	probability of interdeparture time of k slots
σ, τ, d	parameters of MGeo distribution

J	total number of arrival phases
I	$J \times J$ identity matrix
π	invariant probability vector of phase
e	unity column vector with J components
λ_a	average number of cell arrivals per slot
λ^{-1}	mean of MGeo distribution
C_a^2	squared coefficient of variation (SCV) of the interarrival time
C_d^2	squared coefficient of variation (SCV) of the interdeparture time
$V(z)$	probability generation function of the interdeparture time (slot)
$V^{(m)}$	the mth factorial moment of the interdeparture time (slot)
a	interarrival time of the arrival process
L	average queue length in the system
$\overline{delay}$	mean cell delay in the system
TI	token generation interval (one slot)
SM	smoothness of the departure flow from the Leaky Bucket
V^k	interdeparture time between $(k-1)$th and kth departure
V^{k+1}	interdeparture time between kth and $(k+1)$th departure
$Var(V)$	variance of the interdeparture time
$Q_I(i,j)$	joint probability distribution of two consecutive interdeparture times
R_{I1}	autocorrelation of the two consecutive interdeparture times
C_{I1}	autocovariance of the two consecutive interdeparture times
r_{I1}	autocorrelation coefficient of the two consecutive interdeparture times
D	number of cells departing from the Leaky Bucket at the end of a slot
$\overline{D}$	average number of cell departures at the end of a slot
$\overline{D^2}$	the second moment of the number of cell departures at the end of a slot

$Var(D)$	variance of the number of cell departures at the end of a slot
VMR	Variance to Mean Ratio of the number of departures
$\overline{D^3}$	the third moment of the number of cell departures at the end of a slot
D^k	number of cells departing at the end of k th slot
$Q_C(i,j)$	joint probability of the number of departures at two consecutive slots
R_{C1}	autocorrelation of the number of departures between two consecutive slots
C_{C1}	autocovariance of the number of departures between two consecutive slots
r_{C1}	autocorrelation coefficient of the number of departures between two consecutive slot
$D_{i,j}$	number of cells departing at the end of a slot due to the $i \rightarrow j$ state transition
$i(k)$	state of system at the end of $(k-1)$th slot and just before the beginning of the kth slot
$j(k)$	state of the system at the end of kth slot, just before the beginning of the $(k+1)$th slot
$p_{j,l}^{(i)}$	the j, l th entry of the multiple step transition probability matrix $P^{(i)}$
R_{Cn}	autocorrelation of the number of cell departures at lag n
C_{Cn}	autocovariance of the number of cell departures at lag n
r_{Cn}	autocorrelation coefficient of the number of cell departures at lag n
IDC	Index of Dispersion for Counts
$(\hat{\lambda}_1, \hat{\lambda}_2)$	departure rate of the two-state MMPP departure process
$(\hat{\sigma}_1, \hat{\sigma}_2)$	transition rate of the two-state MMPP departure process
$\hat{R}$	transition rate matrix for the underlying Markov departure process
λ_d	average departure rate of the Leaky Bucket

Chapter 1

INTRODUCTION

1.1 Background

The concept of the Integrated Services Digital Network (ISDN) has been evolving since CCITT (the International Consultative Committee for Telecommunications and Telegraphy) adopted the first set of ISDN recommendations in 1984 [1]. The main feature of the ISDN concept is the support of a wide range of voice and non-voice applications in the same network. Two ISDN standard interfaces were defined and called basic access, primary rate access. The basic access interface, comprising two 64 kbit/s B channels and a 16 kbit/s signalling D channel, has a total bit rate of 144 kbps. The primary rate access interfaces, with a gross bit rate of 1.544 Mbit/s (T1 bandwidth) or 2 Mbit/s (E1 bandwidth), offers the flexibility to allocate high speed H channels or mixtures of B and H channels and a 64 kbit/s signalling channel.

It was soon realized that higher bit rates were required for applications such as interconnection of local area networks, video, image, and so forth, bringing the standardization process to the introduction of Broadband ISDN (B-ISDN) concepts. B-ISDN includes 64 kbit/s ISDN capabilities but in addition opens the door to applications utilizing bit rates above 1.5 Mbit/s or 2 Mbit/s respectively [2]. The upper limit of the bit rate available to a

broadband user will be somewhat above 100 Mbit/s. B-ISDN is conceived as all-purpose digital network. It will provide an integrated access that will support a wide variety of applications for its customers in a flexible and cost-effective manner. B-ISDN is required to support transmission of both asynchronous data and synchronous real-time traffic on a single transmission network. It will provide such diverse services as interactive and distributive services, broadband and narrowband rates, support for bursty and continuous traffic, connection oriented and connectionless transfers, and point-to-point and complex communications. B-ISDN is also required to meet the performance requirements of multimedia traffic.

1.1.1 ATM Networks

In the past few years, Broadband ISDN (B-ISDN) has received increased attention as a communication architecture capable of supporting multimedia applications. Among the techniques proposed to implement B-ISDN, Asynchronous Transfer Mode (ATM) is considered to be the most promising transfer technique because of its efficiency and flexibility. It has been recommended by CCITT as the transfer mode of choice for B-ISDN.

In ATM, all information is organized into fixed-size blocks called "cells", each consisting of a header and an information field. As defined by CCITT, a cell consists of 53 octets, 5 of which are called header and are reserved for the network and 48 which are for the user information with respect to the ATM layer and are termed as the payload. Figure 1.1 is the cell format in ATM networks. The header of each cell contains among others, the virtual channel and virtual path identifiers. The payload contains all the user data and ATM adaptation layer information. The header format is different at a B-ISDN User Network Interface (UNI) than it is in a B-ISDN Network Node Interface (NNI), as illustrated in Figure 1.2.

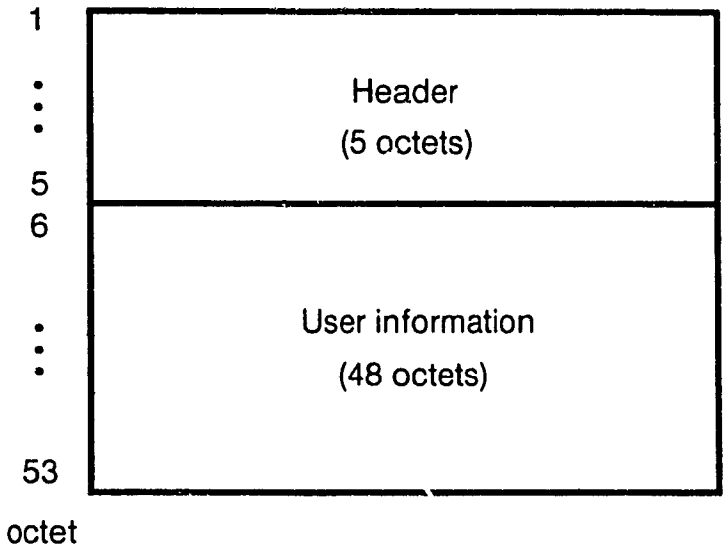

Figure 1.1 ATM cell structure

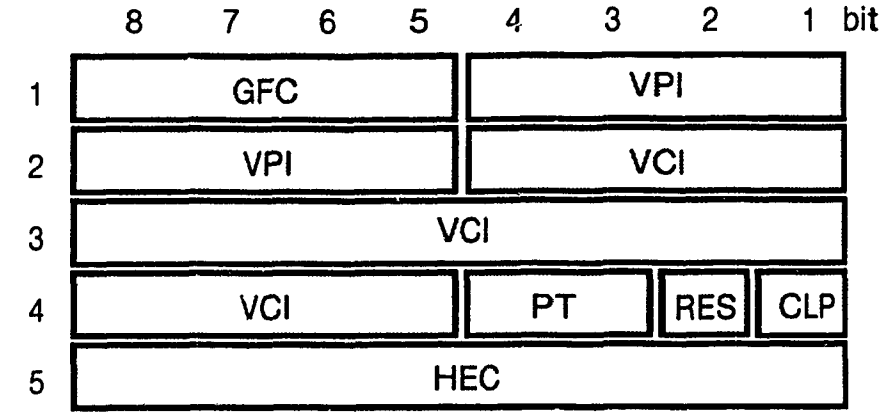

(a) User-Network Interface (UNI)

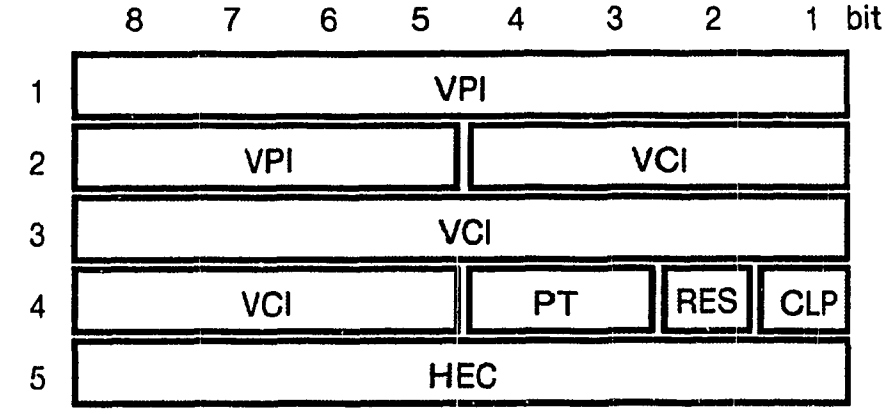

(b) Network Node Interface (NNI)

GFC	Generic Flow Control	RES	Reserved
VPI	Virtual Path Identifier	CLP	Cell Loss Priority
VCI	Virtual Channel Identifier	HEC	Header Error Control
PT	Payload Type		

Figure 1.2 Cell header format at UNI and NNI

1.1.2 Congestion Control in ATM Networks

Many of the traffic sources that ATM is expected to support are bursty, such as voice, interactive video and high-speed data. A bursty source may generate cells at a near-peak rate for a while, and shortly afterwards, it may become inactive, generate no cells. Such a bursty traffic source will not require continuous allocation of bandwidth at its peak rate. Since an ATM network supports a large number of such bursty traffic sources, statistical multiplexing can be used to gain bandwidth efficiency, allowing more traffic sources to share the bandwidth. Due to the dynamic nature of the bursty traffic, severe network congestion can result. Therefore, congestion control is very important in ATM networks in order to provide a desirable level of performance.

Congestion control in ATM based B-ISDN is difficult because of the high link speed, diverse service requirements, and various characteristics of the traffic ATM is expected to support. In recent years, congestion control has been an important and active area of research. Various congestion control mechanisms proposed for ATM networks fall into two classes: reactive and preventive control [3].

Reactive control reacts to the congestion after it happens and tries to bring the degree of network congestion to an acceptable level. It uses the feedback information from the network to adjust the input transmission rate. However, a major problem with reactive control in high-speed networks is the slow feedback. The effects of high-speed channels make the overhead due to propagation delay significant; therefore, by the time that feedback reaches the source nodes and the control is triggered, it may be too late to react effectively. Reactive control based on feedback is generally accepted as inappropriate in the ATM environments.

Unlike reactive control, preventive control does not wait until congestion actually occurs, but rather tries to prevent the network from reaching an unacceptable level of con-

gestion. However, due to the bursty and unpredictable nature of traffic, this preventive approach is not sufficient to control the congestion, and additive reactive controls may be necessary in the network [5].

Preventive control for ATM can be performed in two ways: admission control and bandwidth enforcement. Admission control determines whether to accept or reject a new connection at the time of call setup. This decision is based on traffic characteristics of the new connection and the current network load. The bandwidth enforcement, also called policing, monitors individual connections to ensure that the actual traffic flow conforms with that reported at call establishment.

1.1.3 Leaky Bucket Algorithm as a Policing Function in ATM Networks

Since users may deliberately exceed the traffic volume declared at the call setup (i.e. values of their traffic descriptors), and thus easily overload the network, admission control is not sufficient to prevent congestion. After a connection is accepted, traffic flow of the connection must be monitored to ensure it stays within its contracted parameters (various parameters for the transmitting such as the mean and peak bit rate), negotiated between the user and the network at the connection set-up phase. The policing function is used to prevent the user from exceeding the contracted parameters, which could result in network congestion. If a user transmits cells not conforming to the contract then the policing mechanism detects this and the cells in violation are either immediately discarded or tagged (they might be discarded later if congestion occurs) in order to protect the Quality of Service (QoS) of the other users. The policing function is implemented at each User-Network Interface (UNI) and Network-Node Interface (NNI). For "well-behaving" users or subnetworks, the policing should be transparent, while all violations should be caught.

Various policing methods have been proposed and discussed. Among the proposed policing mechanisms, there are the Leaky Bucket and window-based schemes such as the jumping window, the triggered jumping window, the moving window, the exponentially weighed moving-average. It is generally agreed that the Leaky Bucket scheme performs better than the window based schemes under the conditions that prevail in ATM networks. In fact, the Leaky Bucket scheme has been recommended by CCITT as the policing mechanism of choice in ATM networks. Generic Cell Rate Algorithm (GCRA), a different term but similar approach, is used in the ATM Forum.

The basic idea of the Leaky Bucket mechanism is that a cell, before entering the network, must obtain a token from the token pool. If the token pool is empty, then the cell must wait for a token before it is delivered to the network. Tokens are generated at a fixed rate of r and stored in a token pool. The pool has a finite buffer size of M. After filling the pool, tokens arriving to the pool are discarded. The token generation rate (r) is a measure of the average bit rate of the connection. The token pool size (M) corresponds to the maximum allowable burst length. Thus, it is guaranteed that the long term average bit rate does not exceed the pre-specified rate of the connection. However, over short periods, the scheme permits bursts of higher rate. Essentially, the choice of M determines the burstiness of the transmission, it could be set according to the application requirement. A value of $M = 0$ maximizes the "smoothness" of the traffic, which refers to the rate-based control scheme.

1.2 Research Objectives

A Leaky Bucket scheme is one of the typical bandwidth enforcement mechanisms used for ATM networks; this scheme can enforce the average bandwidth and burst factor of a traffic source. The performance metrics of interest for the Leaky Bucket scheme are:

- Cell loss probability;
- Delay characteristics at the buffer;
- The interdeparture time characteristics of cells.

The Leaky Bucket scheme was first introduced by Turner [4], without the provision of an input queue. Since then a number of its variants have been proposed. In [9], the input buffer is suggested to provide better control of the trade-off between the cell waiting times and the cell loss probabilities. Recently, a good deal of effort has been expended in modeling the Leaky Bucket in ATM networks [5] [6] [7] [8] [9] [10] [11] [12] [13] [14] [15] [29] [32] [33] [40] [47] [48] [49]. An exact analysis of Leaky Bucket methods with finite and infinite input buffer size is presented in [6], providing the Laplace transforms for the waiting time and the inter-departure time of cells from the system. The expected waiting time, the cell loss probability and the variance of inter-departure times are also obtained. However, a Poisson process is assumed for the cell arrival process in their analysis. Berger [10] gives the analysis to continuous time Markovian Arrival Process (MAP). For the regulation of packets during a user's session, Eckberg et. al [11] consider a Leaky Bucket that acts as a throughput-burstiness filter for ATM cells in the network. Cells that arrive to an empty token pool are not blocked but rather are marked, are allowed through and may be discarded if a subsequent node is congested. W. Matragi and K. Sohraby [5] propose an adaptive rate based Leaky Bucket scheme as a combination of preventive and reactive congestion control mechanism. The effects of propagation delay and parameters of the control scheme on the performance are presented by simulation since an exact analysis is rather impossible. The numerical results are given for an ON-OFF arrival process.

An appropriate characterization of the departure process of a Leaky Bucket is very important for the network performance evaluation. The interdeparture time distribution of the Leaky Bucket has been determined in the Laplace domain [6] [7]. Calculating the

moments and the Squared Coefficient of Variation (SCV) for the interdeparture time is very time consuming, especially for the complicated arrival processes. Therefore, our interest is to find a simple model to characterize the interdeparture time distribution of the Leaky Bucket for real-time control.

However, the characterization of burstiness and correlation are not only captured by simple burstiness index such as the SCV and the short term covariance. It is necessary to look at the long term covariance such as long term Index of Dispersion for Counts (IDC) in order to accurately characterize the departure process of the Leaky Bucket. The auto-covariance function of the Leaky Bucket departure process are presented in [8]. We will discuss the IDC and take it into account for modeling the departure process of a Leaky Bucket to a 2-state MMPP process.

1.3 Scope of the Thesis

The objectives of this thesis are to analyze the departure process of the Leaky Bucket algorithm. We provide the detail mapping procedures to analyze the departure process of the Leaky Bucket scheme.

The thesis is organized as follows:

A Modified Geometric (MGeo) model for the interdeparture time distribution of the Leaky Bucket is proposed in Chapter 2. The control effects of a Leaky Bucket are extensively examined from the viewpoint of smoothing out the burstiness of the input traffic. The smoothing effect is characterized by the Squared Coefficient of Variation (SCV) of the interdeparture time of the Leaky Bucket. We also look at the correlation effect between two consecutive interdeparture times. The trade-off between the burstiness of the departure process and the cell delay is examined.

Chapter 3 provides the detailed mapping procedures for the distribution of the number of departures and the correlation of the number of departures between two consecutive slots. The auto-covariance function of the number of departures and the Index of Dispersion for Counts (IDC) are analyzed under different arrival processes with various parameters. A statistical matching method is suggested for the departure process of a Leaky Bucket scheme by considering the IDC.

Finally, the conclusions and recommendations for future work are given in Chapter 4.

Chapter 2

STATISTICAL CHARACTERIZATION OF THE INTERDEPARTURE TIME OF A LEAKY BUCKET

2.1 Introduction

The study of departure process of the Leaky Bucket is important for the performance of the whole network. The departure flow from Leaky Bucket is the arrival to the rest of the network. Since the ATM traffic is very bursty, the Leaky Bucket scheme is expected to reduce the burstiness of the traffic flow to the network. An appropriate characterization of the departure process of the Leaky Bucket is very useful in analyzing the network performance.

A number of studies have investigated the behavior and the performance of the Leaky Bucket scheme in recent years [5]-[15], [29] [32] [33] [40] [47]-[49]. Usually, the quantities studied in these investigations are the input buffer occupancy and the waiting time experienced by cells in the input buffer. Only a few studies focus on the characteristics of the output traffic of the Leaky Bucket [6], [7] and [8]. The Leaky Bucket can be analyzed as a G/D/1/N queue with finite input buffer N and a suitable arrival process. In most of the past research on the departure process of the Leaky Bucket scheme, it has been assumed that input traffic follows a Poisson process. However, bursty traffic expected to be sup-

ported by ATM networks has the squared coefficient of variation (SCV) of interarrival time much higher than 1 (for Poisson arrival). Although the SCV of interarrival time is not the same as burstiness by definition, it is clear that highly bursty traffic would have a high SCV. The smoothing effect of the Leaky Bucket scheme is extensively studied in [6] by characterizing the SCV of the interdeparture time of the Leaky Bucket. Under the assumption of Poisson arrivals, Sidi et. al derived the characteristics of the departure process in terms of the token generation time, the size of the token pool and the buffer size. The trade-off between the smoothness of the departure process and the cell waiting time is studied. Leung et. al [7] analyzed the departure process under a more general assumption of renewal arrival process, but they only give the Laplace transform of the interdeparture time distribution and the numerical results are carried out only for the special case of the Poisson process. In [8], the performance of the Leaky Bucket scheme is analyzed under batch data input traffic. The mean, variance and autocovariance of the Leaky Bucket output process are presented. However, calculation of the covariance is time consuming. A two mini-source model is proposed to characterize the Leaky Bucket output process and to evaluate the network performance.

Most of the analysis of the interdeparture time characterization from Leaky Bucket is in terms of the Laplace transform, obtaining the moments and the coefficient of variation for the interdeparture time is very time consuming since Laplace transforms for departure processes usually are very complicated. This is especially true when complicated arrival processes are involved since differentiation becomes complicated.

The purpose of this chapter is to introduce a new discrete model (Modified Geometric) to characterize the interdeparture time distribution of the departure process from a Leaky Bucket. We offer a mapping procedure to fit the interdeparture time distribution to the MGeo (Modified Geometric) model.

Also, a mapping procedure to derive the joint probability of two consecutive interdeparture times is given. From this, closed form expressions can be obtained for the autocorrelation coefficient between two consecutive interdeparture times. The numerical calculation of the obtained formulas is simple and not time consuming, even for more complicated traffic sources such as Markov Modulated Poisson Process (MMPP) [18].

The analysis is carried out in the discrete time domain which is representative of the ATM environment. We assume that cells arrive and depart only at the slot boundary. Cell arrivals are modeled as Poisson, GGeo (Generalized Geometric) [28] and MMPP processes respectively. The control effects of Leaky Bucket are extensively examined from the viewpoint of smoothing out the burstiness of the input traffic. The smoothing effect is characterized by the squared coefficient of variation (SCV) of the interdeparture time of the departure process from the Leaky Bucket. Since the analysis is an approximation, we also provide the simulation results to assess its accuracy.

The major difference between our work and the previous works of the Leaky Bucket scheme such as [6] [7] and [8] is that we build a Modified Geometric (MGeo) model to characterize the interdeparture time distribution of the departure process from the Leaky Bucket. Our MGeo model could simplify the computations of the probability distribution and the Squared Coefficient of Variation (SCV) of the interdeparture time from the Leaky Bucket. The merits of this MGeo departure process model is that it is mathematically tractable when it is fed into the next queue as a new traffic stream, and it does take the burstiness into account. Another potential advantage of this approach is that it might be used for real-time control due to its easier calculation, since the policing function must be available for every connection during the entire active phase and must operate in real-time.

The rest of this chapter is organized as follows. Section 2.2 summarizes the queueing model of the Leaky Bucket presented in [6]. Section 2.3 gives the mathematical model of MGeo. A detailed mapping procedure of interdeparture time from the Leaky Bucket is

provided. Section 2.4 discusses the smoothing effect from the Leaky Bucket in terms of squared coefficient of variation (SCV) of the interdeparture times. The trade-off between the burstiness of the departure process and the cell delay is examined. The mapping procedure for joint probability of two consecutive interdeparture times and the numerical results for the autocorrelation between two consecutive interdeparture times are contained in Section 2.5. Our conclusions are summarized in Section 2.6.

2.2 Queueing Model of the Leaky Bucket

For the purpose of completeness, in this section we summarize the work done by Sidi which presented in reference [6].

As mentioned earlier, the Leaky Bucket scheme was first introduced in [4] without the input buffer. The input buffer has been proposed to allow a trade-off between cell loss probability and cell waiting time. The queueing model for the Leaky Bucket scheme is depicted in Figure 2.1. A pool of tokens that can contain at most M tokens is available. The generation process of tokens is deterministic, i.e., in each slot (of length TI) a new token is generated and stored in the pool if it contains fewer than M tokens. Otherwise, the newly generated token is discarded.

An arriving cell that finds the token pool non-empty, departs the system at the end of current slot and one token is removed from the token pool. An arriving cell that finds the token pool empty joins the queue (buffer size of N, for finite buffer) if the buffer is not full. When the queue is not empty (the token pool must be empty in this case) and a token is generated at the slot boundary, one cell departs the queue immediately (assume a FIFO order) and the token is removed from the pool. Note that when the queue is not empty, the token pool must be empty, or when the token pool is non-empty, the queue must be empty, or both of them may be empty. But both cannot be non-empty at the same time. The cell

departure process from the Leaky Bucket causes the input process to the network to be smoothed.

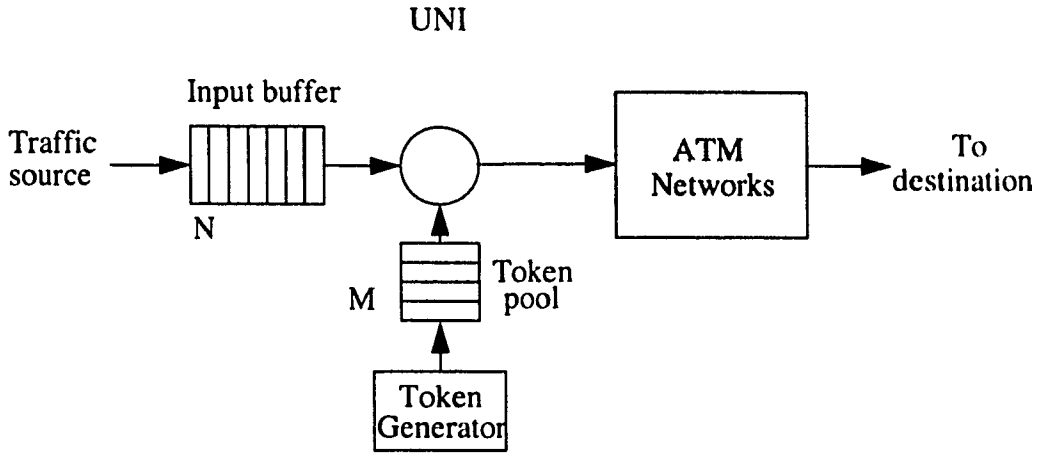

Figure 2.1 Queueing model for the Leaky Bucket scheme

Consider a slotted time axis and a new token is generated at each slot boundary. A generated token joins the token pool if it contains fewer than M tokens, otherwise, it is discarded.

$X(m, n, t)$ is the probability of having m tokens in the token pool and n cells in the buffer at t ($t = 0, 1, 2, \ldots$slot), just prior to the token generation instances. Since the number of tokens cannot exceed M and cells wait in the queue if and only if there are no tokens in the token pool, for all time t:

$$X(m, n, t) = \begin{cases} 0 & m > M \\ 0 & 1 \le m \le M, \quad n \ge 1 \end{cases} \tag{2.1}$$

Since $m \cdot n = 0$ for all the time, for simplicity, one-state variable i is used to represent the state instead of two-state variables (m, n). We have:

$$x(i,t) = \begin{cases} X(M-i,0,t) & 0 \le i \le M \\ X(0,i-M,t) & i \ge M \end{cases} \tag{2.2}$$

Where i is the state of the system which reflects both m and n at time t, $x_i\,(i \ge 0)$ is the corresponding steady-state probability, $x_i = \lim_{t \to \infty} x(i,t)$.

For better understanding, Table 2.1 is given to present the relationship among the number of tokens (m), the number of cells (n) and the state of the system $(i = M - m + n)$ for all possible cases.

TABLE 1.

Two-state variable (m, n)		**One-state variable (i)**
m (# of token)	**n (# of cell in Q)**	**i =M-m+n (state of system)**
M	0	0
M-1	0	1
M-2	0	2
:	:	:
2	0	M-2
1	0	M-1
0	0	M
0	1	M+1
0	2	M+2
:	:	:
0	N	M+N
:	:	:
0	∞	∞

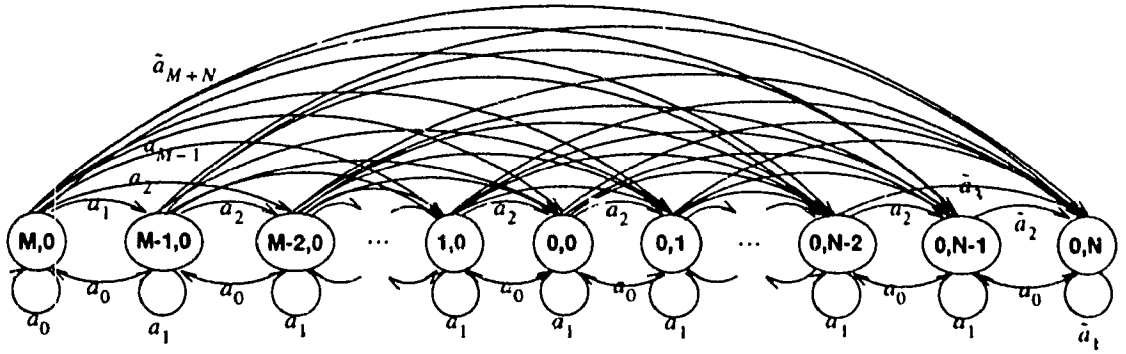

(a) with two-state variables (m, n)

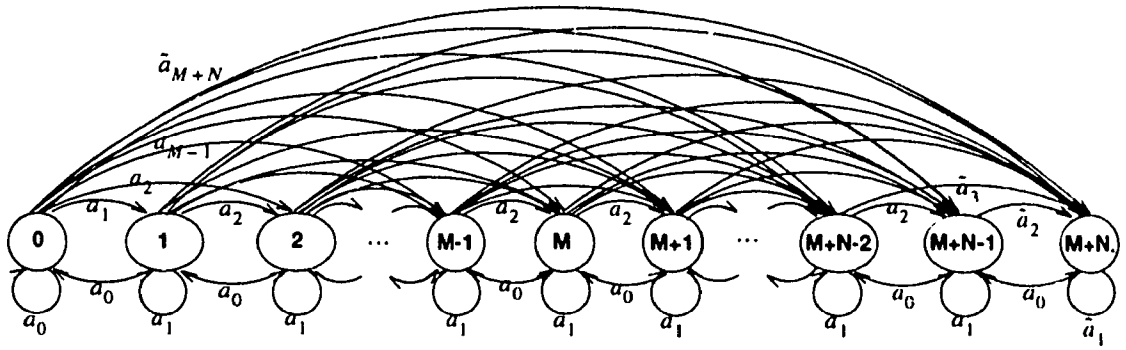

(b) with one-state variable i

Figure 2.2 State Transition Diagram for Leaky Bucket with finite input buffer

Figure 2.2 (a) shows the state transition diagram of the Leaky Bucket model with two-state variables, where (m, n) is the state corresponding to having m tokens in the token pool and n cells in the input buffer, M is the token pool size, N is the input buffer size, a_i is the probability of i arrivals during a slot. Clearly, the arriving cell that finds

there is no token left and the buffer full is discarded. $\tilde{a}_i = 1 - \sum_{j=0}^{i-1} a_j$. Figure 2.2 (b) is the simplified state transition diagram with one-state variable i ($i = M - m + n$) .

Then the stationary transition probability matrix P of finite buffer case can be obtained from Figure 2.2 (b):

$$P = [p_{i,j}] = \begin{bmatrix} a_0 & a_1 & a_2 & \cdots & a_{M-1} & a_M & a_{M+1} & \cdots & a_{M+N-2} & a_{M+N-1} & \tilde{a}_{M+N} \\ a_0 & a_1 & a_2 & \cdots & a_{M-1} & a_M & a_{M+1} & \cdots & a_{M+N-2} & a_{M+N-1} & \tilde{a}_{M+N} \\ 0 & a_0 & a_1 & \cdots & a_{M-2} & a_{M-1} & a_M & \cdots & a_{M+N-3} & a_{M+N-2} & \tilde{a}_{M+N-1} \\ \cdots & \cdots & \cdots & \cdots & \cdots & \cdots & \cdots & \cdots & \cdots & \cdots & \cdots \\ 0 & 0 & 0 & \cdots & a_1 & a_2 & a_3 & \cdots & a_N & a_{N+1} & \tilde{a}_{N+2} \\ 0 & 0 & 0 & \cdots & a_0 & a_1 & a_2 & \cdots & a_{N-1} & a_N & \tilde{a}_{N+1} \\ 0 & 0 & 0 & \cdots & 0 & a_0 & a_1 & \cdots & a_{N-2} & a_{N-1} & \tilde{a}_N \\ \cdots & \cdots & \cdots & \cdots & \cdots & \cdots & \cdots & \cdots & \cdots & \cdots & \cdots \\ 0 & 0 & 0 & \cdots & 0 & 0 & 0 & \cdots & a_1 & a_2 & \tilde{a}_3 \\ 0 & 0 & 0 & \cdots & 0 & 0 & 0 & \cdots & a_0 & a_1 & \tilde{a}_2 \\ 0 & 0 & 0 & \cdots & 0 & 0 & 0 & \cdots & 0 & a_0 & \tilde{a}_1 \end{bmatrix} \quad (2.3)$$

where $p_{i,j}$ is the state transition probabilities, from state i to state j.

For finite buffer size (N), once x_0 is assumed a value, x_i ($1 \le i \le M+N$) can be computed recursively via

$$x_i = \frac{x_{i-1} - x_0 a_{i-1} - \sum_{j=0}^{i-2} x_{j+1} a_{i-1-j}}{a_0} \quad (2.4)$$

and finally all quantities are normalized by $\sum_{i=0}^{M+N} x_i = 1$.

The average number of cells entering to the system (throughput) is given by:

$$T = x_0\left(\sum_{i=0}^{M+N} i a_i + (M+N)\tilde{a}_{M+N}\right) + \sum_{j=1}^{M+N} x_j\left(\sum_{i=0}^{M+N-j+1} i a_i + (M+N-j+1)\tilde{a}_{M+N-j+1}\right) \tag{2.5}$$

Since service time is one slot, the load intensity of the system ρ also represents the average number of cells arrived during one slot. Then cell loss probability is given by:

$$P_L = 1 - \frac{T}{\rho} \tag{2.6}$$

For infinite buffer, the steady-state probability x_i is easily seen to be

$$x_i = x_0 a_i + \sum_{j=0}^{i} x_{j+1} a_{i-j}, \qquad i \geq 0 \tag{2.7}$$

where $x_0 = 1 - \rho$, then other probabilities can be computed recursively from (2.7).

The above queueing model can also be extended to matrix version for the MMPP arrival process. The detailed presentation is given in [14] and [40].

2.3 Interdeparture Time Distribution with Modified Geometric Model

2.3.1 The Modified Geometric Distribution

The Modified Geometric (MGeo) distribution is a discrete distribution (Figure 2.3) with the probability density function:

$$Prob(V = k) = \begin{cases} 1-\tau-d, & k = 0 \\ d+\tau(1-\sigma), & k = 1 \\ \tau(1-\sigma)\sigma^{k-1}, & k \geq 2 \end{cases} \tag{2.8}$$

We define

$$\lambda = \frac{1}{\bar{V}} \tag{2.9}$$

$$C^2 = \frac{E(V-\bar{V})^2}{(\bar{V})^2} = \frac{\overline{V^2}-(\bar{V})^2}{(\bar{V})^2} \tag{2.10}$$

$$C^3 = \frac{E(V-\bar{V})^3}{(\bar{V})^3} = \frac{\overline{V^3}-3\overline{V^2}\bar{V}+2(\bar{V})^3}{(\bar{V})^3} \tag{2.11}$$

where

$$\bar{V} = \sum_{k=0}^{\infty} kP(k) \tag{2.12}$$

$$\overline{V^2} = \sum_{k=0}^{\infty} k^2P(k) \tag{2.13}$$

$$\overline{V^3} = \sum_{k=0}^{\infty} k^3P(k) \tag{2.14}$$

λ^{-1} is the mean, C^2 is the squared coefficient of variation (SCV) of MGeo distribution, C^3 is the cubed coefficient of variation MGeo distribution. These three parameters can describe the departure flow with MGeo distribution completely.

The first two moments provide the squared coefficient of variation which can be used to capture the burstiness of the departure process from the Leaky Bucket. The idea of MGeo model is an extension of Generalized Geometric (GGeo) model studied in [28] and [30]. GGeo model is a special case of MGeo model by setting $d = 0$.

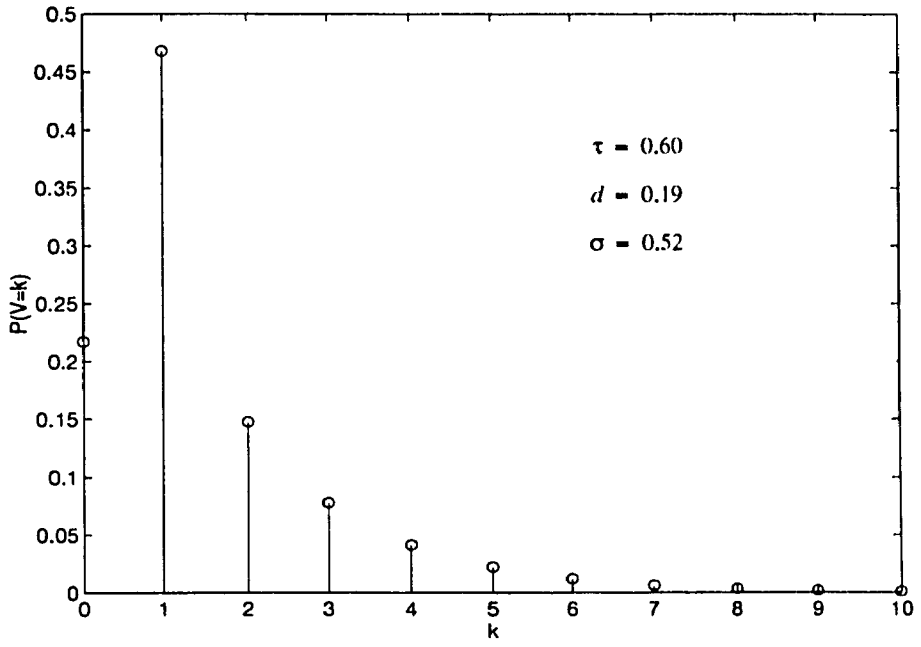

Figure 2.3 Modified Geometric (MGeo) distribution

2.3.2 Mapping Procedure

The MGeo model is a discrete probability distribution implying a special bulk departure pattern and the interdeparture time for a single departure is geometrically distributed with parameter σ.

The dynamics of the Leaky Bucket's operation are such that we can map the departure process of Leaky Bucket to the MGeo distribution given by (2.8).

First we consider the case of an infinite input buffer. Since each departing cell is accompanied by a single token, the departure process of cells is the same as the process of departing tokens. Hence, the interdeparture time V is the slots between the departure epoch of the tagged token and the subsequent departure.

Before giving the derivation, some notation is defined:

m: number of tokens in the bucket, when the tagged token departs;

n: number of cells in the input buffer, when the tagged token departs;

M: token pool size;

x_i: steady-state probability of the system in state i which reflects both token number and cell number, $(i = M - m + n)$;

a_i: probability of i arrivals during a token generation interval;

V: interdeparture time between the tagged and subsequent token departures, Figure 2.4;

$P(V = k)$: probability of interdeparture time of k slots.

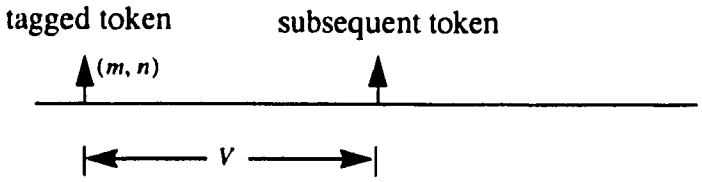

Figure 2.4

We assume that tokens depart in a FIFO order. Our assumption is based on the discrete slot boundary which means cells arrive and depart only at the slot boundary. The

arrivals during the slot is independent from slot to slot conditioned on the state of the arrival process. We also assume that tokens are generated and depart at the slot boundary. Our embedded point is the slot boundary, just after the token departure.

We consider an arbitrary token that departs from the token pool and tag it. In order that this token will ever depart the system, it must join the token pool (the probability of this event is $1 - x_0$). Conditioned on the event that the tagged token joins the token pool at the embedded point, we may find the system in one of the following states.

1. The queue is not empty and the token pool is empty $(n \geq 1, m = 0)$ *:*

There are n $(n \geq 1)$ cells and no tokens in the system.

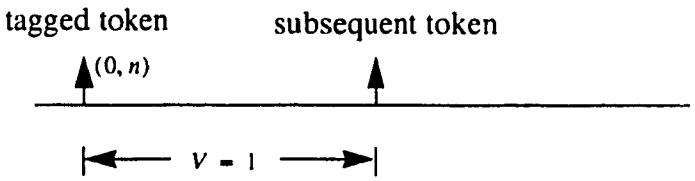

Figure 2.5

In Figure 2.5, the subsequent token generated at the next slot boundary will depart immediately. The interdeparture time V is one slot, the probability of this event is:

$$P(V = 1) = Pr[\text{no tokens in the system}] = \sum_{i=M+1}^{\infty} x_i \qquad (2.15)$$

2. Both the queue and the token pool are empty $(n = 0, m = 0)$ *:*

There are no cells and tokens in the system.

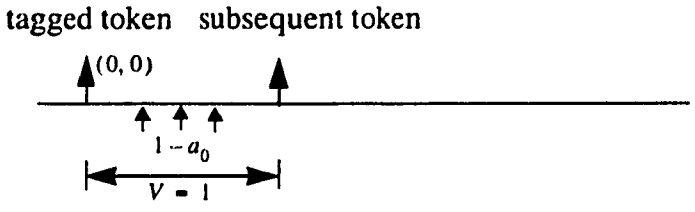

Figure 2.6

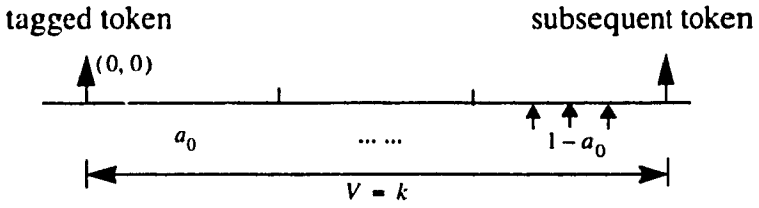

Figure 2.7

In this case, the subsequent token will depart at next slot boundary if there is at least one arrival during the current slot and V is one slot with probability $(1-a_0)$, Figure 2.6. Or next departure will occur at the kth slot boundary if no cells arrive during the previous $k-1$ slots and the V is k slots with the probability $a_0^{k-1}(1-a_0)$, Figure 2.7. Then the probabilities of all these events are:

$$P(V=k) = x_M a_0^{k-1}(1-a_0), \qquad k = 1, 2, 3, \ldots \tag{2.16}$$

3. *The token pool is not empty and the queue is empty* $(n = 0, 1 \le m \le M-1)$ *:*

There are m $(1 \le m \le M-1)$ tokens and no cells in the system. In order to see the interdeparture time between the tagged token and the subsequent departure, the tagged token must depart from the system (the probability of this event is $1-a_0$). Conditioned on the event that the tagged token departs from the token pool, we have the following two cases.

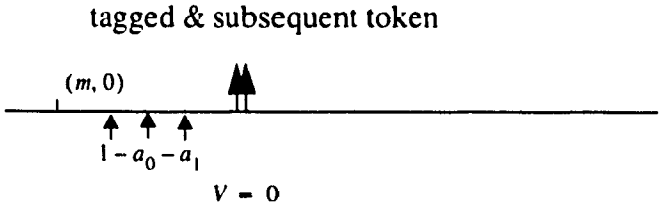

Figure 2.8

a) *If* i $(i \geq 2)$ *cells arrive during the current slot,* then the tagged token and the subsequent token will depart simultaneously at the next slot boundary, see Figure 2.8. Then V is zero slot with probability a_i $(i \geq 2)$, the probability of this event is:

$$P(V=0) = Pr[\text{more than one arrival} \mid \text{at least one arrival}] \sum_{i=1}^{M} \lambda_i$$
$$= \frac{1-a_0-a_1}{1-a_0} \sum_{i=1}^{M-1} x_i \qquad (2.17)$$

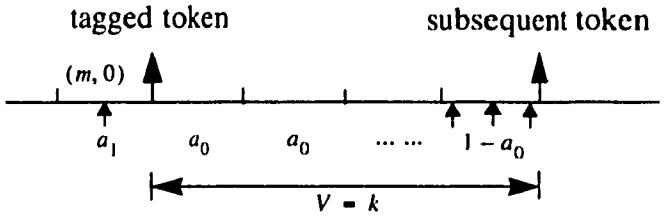

Figure 2.9

b) *If there is only one arrival during the current slot,* then the tagged token will depart at the next slot boundary. The subsequent token will depart at the following kth slot boundary and the interdeparture time V is k slots with probability $a_1 a_0^{k-1}(1-a_0)$, as shown in Figure 2.9. Then the probabilities of all these events are:

$$P(V=k) = Pr[\text{only one arrival} \mid \text{at least one arrival}] \sum_{i=1}^{M-1} x_i$$

$$= \frac{a_1 a_0^{k-1}(1-a_0)}{1-a_0} \sum_{i=1}^{M-1} x_i \tag{2.18}$$

$$= a_1 a_0^{k-1} \sum_{i=1}^{M-1} x_i \qquad k = 1, 2, 3 \ldots$$

In summary, conditioned on the event that the tagged token joins the token pool (the probability of this event is $1 - x_0$), the probability distribution of interdeparture time V is given by:

$$P(V=0) = \frac{(1-a_0-a_1)}{(1-x_0)(1-a_0)} \sum_{i=1}^{M-1} x_i \tag{2.19}$$

$$P(V=1) = \frac{1}{1-x0}\left(\sum_{i=M+1}^{\infty} x_i + \Omega(1-a_0) \right) \tag{2.20}$$

$$P(V=k) = \frac{\Omega a_0^{k-1}(1-a_0)}{1-x_0} \qquad k = 2, 3, 4, \ldots \tag{2.21}$$

where

$$\Omega = x_M + \frac{a_1}{1-a_0} \sum_{i=1}^{M-1} x_i \tag{2.22}$$

Now we get the probability distribution of interdeparture time from Leaky Bucket. For the finite buffer size of N, we just replace ∞ by $M+N$ in (2.20).

From the equations (2.19), (2.20), (2.21)and (2.22), we can see that the interdeparture time of a Leaky Bucket has the same distribution pattern as the MGeo model. Next we try

to determine the parameters τ, d and σ in the MGeo distribution. From (2.8), (2.19), (2.20), (2.21)and (2.22), we know that σ, d and τ can be obtained by mapping the departure process of the Leaky Bucket. σ, d and τ are given by:

$$\sigma = a_0 \tag{2.23}$$

$$d = \frac{\sum_{i=M+1}^{\infty} x_i}{1 - x_0} \tag{2.24}$$

$$\tau = \frac{\Omega}{1 - x_0} \tag{2.25}$$

where x_i is the steady-state probability of the system which can be solved by using (2.4).

The vector version derivation for the MMPP arrival process is similar to the scalar case. The MMPP [24] is a generalized Poisson process which allows the arrival rate to be governed by an underlying Markov chain. We make the same assumption as in the scalar case. We assume that tokens depart in a FIFO order. Our assumption is based on the discrete slot boundary which means that cells and tokens arrive and depart only at the slot boundary. Our embedded point is the slot boundary, just after the token's departure. In order to present the derivation for the vector form, some notation is necessary as given below:

J: number of phases of the arrival process in MMPP;

x_i: steady-state probability vector with J elements, $x_i = (x_{i1}, x_{i2}, \ldots, x_{ij}, \ldots x_{iJ})$, where $x_{ij} (1 \le j \le J)$ is the steady-state probability of system in state i when the phase of arrival process is in j;

A_i: probability of i arrivals during a token generation interval with $J \times J$ elements;

e: column vector of 1's, with J elements;

I: $J \times J$ identity matrix;

π: invariant probability vector of phase.

Conditioned on the event that the tagged token joins the token pool (the probability of this event is $1 - x_0 e$) and at the embedded point, we may find the system in one of the following states.

1. The queue is not empty and the token pool is empty $(n \geq 1, m = 0)$ *:*

There are n $(n \geq 1)$ cells and no tokens in the system. In this case the subsequent token generated at the next slot boundary will depart immediately. The interdeparture time V is one slot, the probability of this event is:

$$P(V = 1) = Pr[\text{no tokens in the system}] = \sum_{i=M+1}^{\infty} x_i e \tag{2.26}$$

2. Both the queue and the token pool are empty $(n = 0, m = 0)$ *:*

There are no cells and tokens in the system. In this case the subsequent token will depart at next slot boundary if there is at least one arrival during the current slot and V is one slot with probability $(I - A_0)$. Or next departure will occur at the kth slot boundary if no cells arrive during the previous $k-1$ slot and the V is k slots with the probability $A_0^{k-1}(I - A_0)$. Then the probabilities of all these events are:

$$P(V = k) = x_M A_0^{k-1}(I - A_0)e \qquad \text{k=1, 2, 3, ...} \tag{2.27}$$

3. The token pool is not empty and the queue is empty $(n = 0,\ 1 \leq m \leq M-1)$ *:*

There are $m\,(1 \le m \le M-1)$ tokens and no cells in the system. In order to see the interdeparture time between the tagged token and the subsequent departure, the tagged token must depart from the system (the probability of this event is $I - A_0$). Conditioned on the event that the tagged token departs from the token pool, we have the following two cases.

a) *If $i\,(i \ge 2)$ cells arrive during the current slot*, then the tagged token and the subsequent token will depart simultaneously at the next slot boundary. Then V is zero slot with probability $A_i\,(i \ge 2)$, the probability of this event is:

$$\begin{aligned} P(V=0) &= \left(\sum_{i=1}^{M-1} x_i\right) Pr\,[\text{more than one arrival} \mid \text{at least one arrival}] \\ &= \left(\sum_{i=1}^{M-1} x_i\right)(I-A_0)^{-1}(I-A_0-A_1)\,e \end{aligned} \tag{2.28}$$

b) *If there is only one arrival during the current slot*, then the tagged token will depart at the next slot boundary. The subsequent token will depart at the following kth slot boundary and the interdeparture time V is k slots with probability $A_1 A_0^{k-1}(I-A_0)$. Then the probabilities of all these events are:

$$\begin{aligned} P(V=k) &= \left(\sum_{i=1}^{M-1} x_i\right) Pr\,[\text{only one arrival} \mid \text{at least one arrival}] \\ &= \left(\sum_{i=1}^{M-1} x_i\right)(I-A_0)^{-1} A_1 A_0^{k-1}(I-A_0)\,e \\ & \qquad\qquad k = 1,\ 2,\ 3\ \ldots \end{aligned} \tag{2.29}$$

Finally, conditioned on the event that the tagged token joins the token pool (the probability of this event is $1 - x_0 e$), the probability distribution of interdeparture time V is given by:

$$P(V=0) = \frac{1}{1-x_0 e}\left(\sum_{i=1}^{M-1} x_i\right)(I-A_0)^{-1}(I-A_0-A_1)e \tag{2.30}$$

$$P(V=1) = \frac{1}{1-x_0 e}\left(\sum_{i=M+1}^{\infty} x_i + \Omega(I-A_0)\right)e \tag{2.31}$$

$$P(V=k) = \frac{1}{1-x_0 e}\Omega A_0^{k-1}(I-A_0)e, \qquad k = 2, 3, 4, \ldots \tag{2.32}$$

where

$$\Omega = x_M + \left(\sum_{i=1}^{M-1} x_i\right)(I-A_0)^{-1}A_1 \tag{2.33}$$

As we see from equations (2.19), (2.20), (2.21)and (2.22), the vector case is analogous to the scalar case. Same as before, for the finite buffer size of N, we just replace ∞ by $M+N$ in (2.31). The parameters τ, d and σ in the MGeo distribution for the MMPP arrival process is given by:

$$\sigma = \pi A_0 e \tag{2.34}$$

$$d = \frac{1}{1-x_0 e}\sum_{i=M+1}^{\infty} x_i e \tag{2.35}$$

$$\tau = \frac{\Omega e}{1-x_0 e} \tag{2.36}$$

where x_i is the steady-state probability vector which can be solved by using the extension of (2.4) presented in [14] and [40].

Now we can use the parameters we have obtained [(2.23), (2.24), (2.25) and (2.34), (2.35), (2.36)] to determine the MGeo distribution for the departure process of the Leaky Bucket by using (2.8).

2.3.3 Numerical Results and Discussions

First, we consider the simplest case of Poisson arrival process to see the departure process of the Leaky Bucket by using our derived MGeo model and we will compare the numerical results with Sidi's approach [6]. Later on, we also consider an input traffic model of GGeo-type [28] which takes the burstiness into account. Finally, the correlated arrival process of the MMPP is discussed.

For Poisson arrivals, the probability of i arrivals during a slot is given as by:

$$a_i = \frac{\lambda_a e^{-\lambda_a}}{i!}, \qquad i \geq 0 \tag{2.37}$$

For GGeo-type arrivals, the probability of i arrivals during a slot is given in [28]:

$$a_i = \begin{cases} 1-\eta, & i = 0 \\ \eta\delta(1-\delta)^{i-1}, & i \geq 1 \end{cases} \tag{2.38}$$

where $\delta = \dfrac{2}{C_a^2 + 1 + \lambda_a}$ and $\eta = \dfrac{2\lambda_a}{C_a^2 + 1 + \lambda_a}$. C_a^2 is the squared coefficient of variation (SCV) of the interarrival time and λ_a is the average number of cells arriving in a token generation interval (one slot).

For the MMPP arrivals, the probability of i arrivals during a slot is given in [20]:

$$A_n = \int_0^{\infty} P(n,t) \otimes dH(t) \tag{2.39}$$

where $P(n,t)$ is the probability that n cells will arrive in time $(0,t)$ for J-state MMPP, and $\otimes$ is a Kronecker product defined by $P \otimes H = \{p_{ij}H\}$.

By mapping the departure process of the Leaky Bucket, we know that the interdeparture time distribution of the Leaky Bucket fits to the MGeo distribution (2.8). From (2.23), (2.24), (2.25) and (2.34), (2.35), (2.36), we can easily get the parameters of MGeo distribution.

Figure 2.10 shows the interdeparture time distributions (MGeo) from a Leaky Bucket at different system loads (i.e. average arrival rates) for Poisson arrival process. As we expected, the interdeparture time distribution becomes more concentrated as the system load increases.

Figure 2.11, Figure 2.12 and Figure 2.13 show the interdeparture time distribution for GGeo arrival process. We observe that the interdeparture time distribution is very sensitive to the system load, token pool size and the squared coefficient of variation of the interarrival time. According to the measured data of video-phone given by Rathgeb [29], we consider the SCV of interarrival time running from 1 to 10.6.

Figure 2.14 and Figure 2.15 give the interdeparture time distribution for the MMPP arrival process. We have seen that the traffic load and the token pool size greatly affect the interdeparture time distribution for the MMPP traffic also. Compared with Figure 2.12, we also find the interdeparture time distribution is not very sensitive to the IDC (Index of Dispersion for Counts) of input MMPP traffic.

Simulation results demonstrate that our MGeo approach is a good approximation for the interdeparture time distribution of the Leaky Bucket.

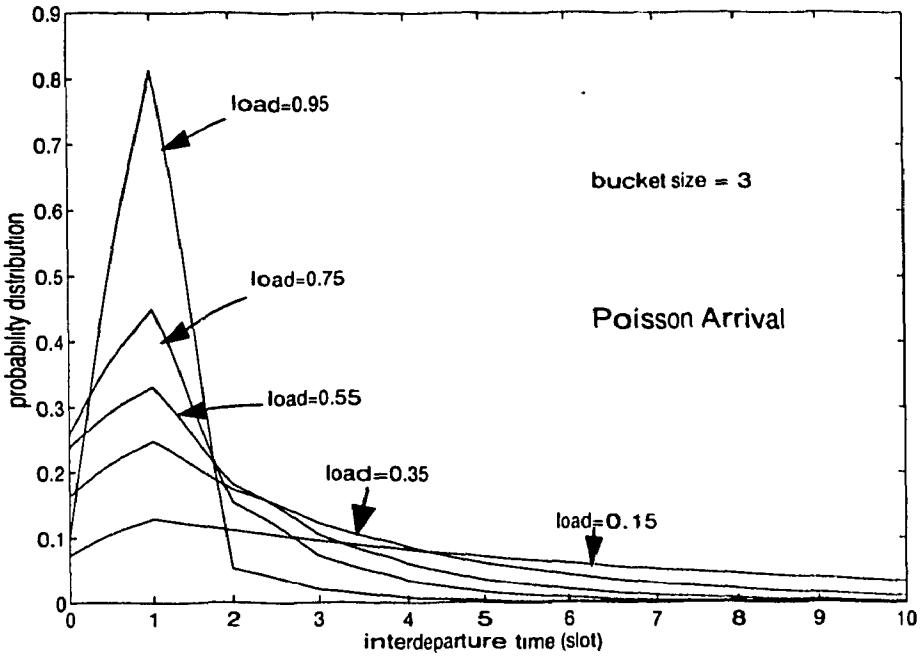

Figure 2.10 Interdeparture time distributions from Leaky Bucket for different system loads (Poisson arrival process)

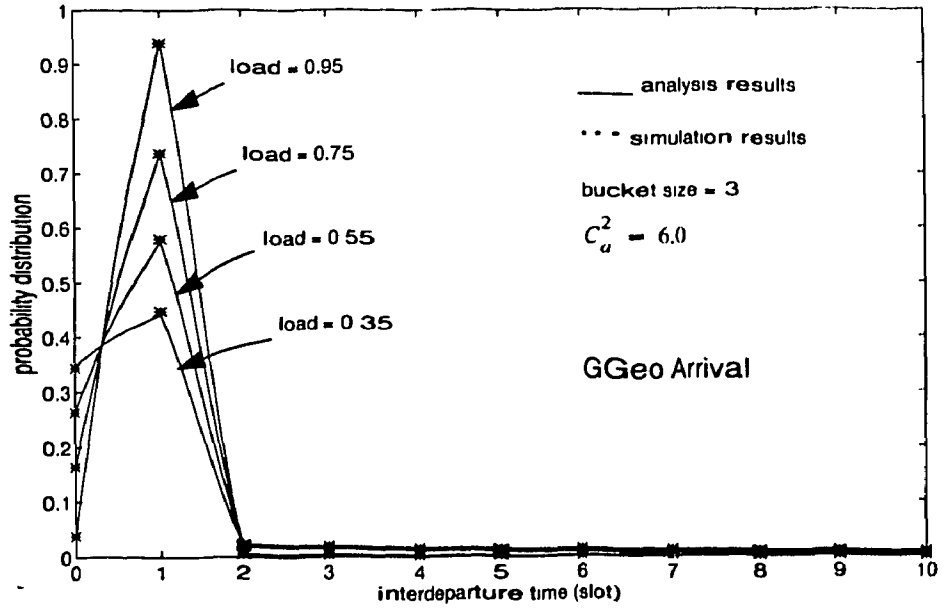

Figure 2.11 Comparison of the analysis results with simulation results for interdeparture time distributions at different system loads for GGeo arrival process (C_a^2 = 6.0, M = 3)

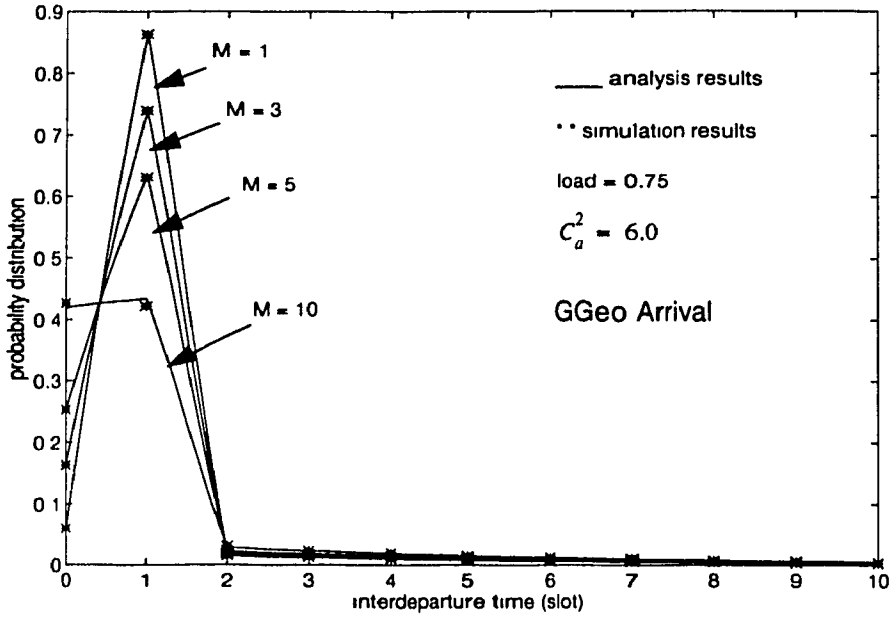

Figure 2.12 Comparison of the analysis results with simulation results for interdeparture time distributions at different token pool sizes M (system load = 0.75, C_a^2 = 6.0)

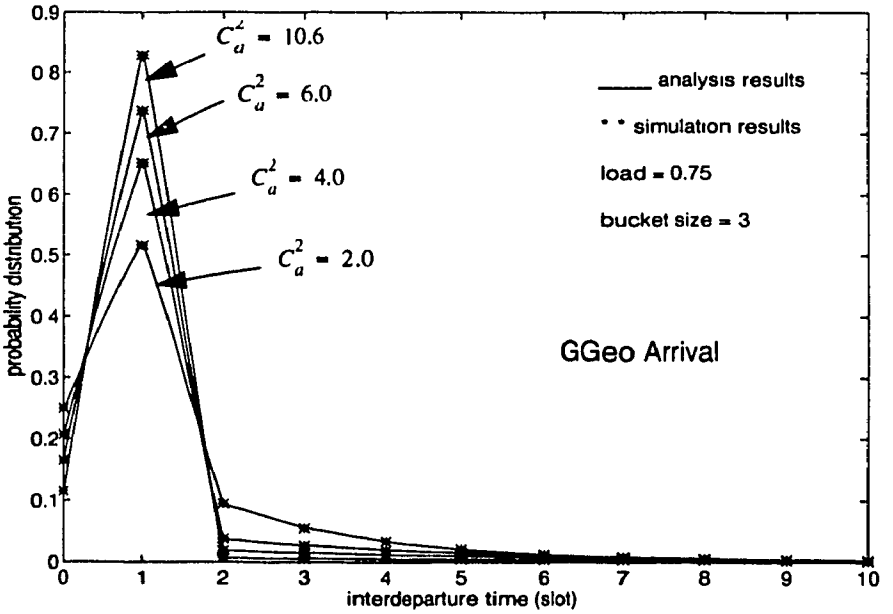

Figure 2.13 Comparison of the analysis results with simulation results for interdeparture time distributions at different SCV of interarrival time C_a^2 (system load = 0.75, M = 3)

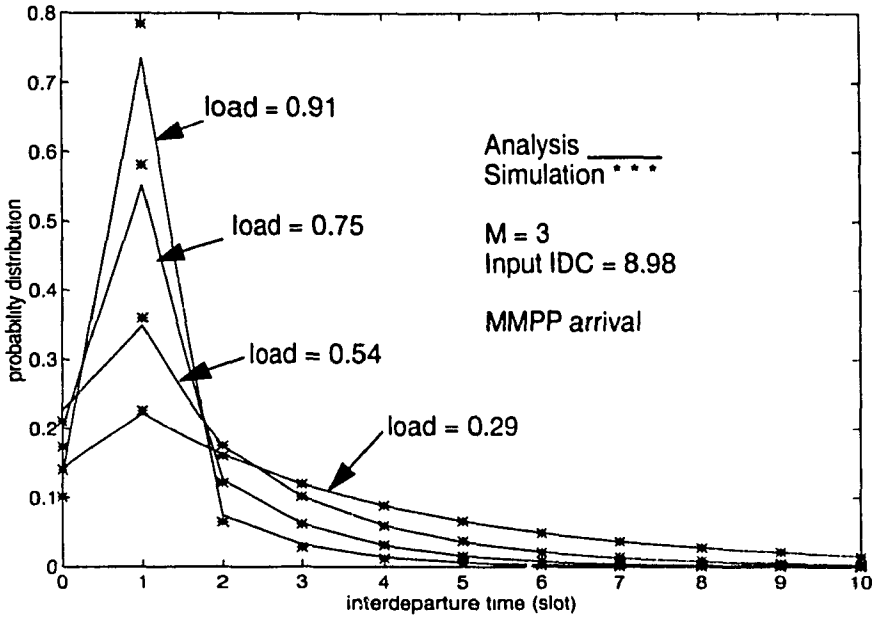

Figure 2.14 Comparison of the analysis results with simulation results for interdeparture time distributions at different system loads for the MMPP arrival process

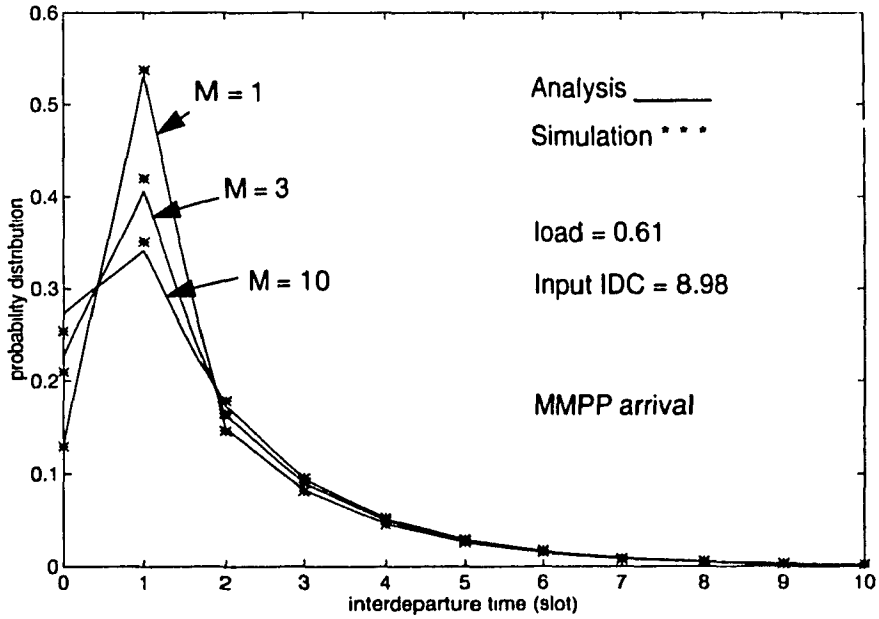

Figure 2.15 Comparison of the analysis results with simulation results for interdeparture time distributions at different token pool size M

2.4 Burstiness of the Departure Process from a Leaky Bucket

2.4.1 The Moments

Let $V(z)$ denote the probability generating function of the interdeparture time in number of slot. From (2.8), we have

$$V(z) = 1 - \tau - d + dz + \frac{\tau(1-\sigma)z}{1-\sigma z} \tag{2.40}$$

Let $V^{(m)}$ denote the mth factorial moment of the interdeparture time (slot), that is

$$V^{(m)} = E(V(V-1)(V-2)\ldots(V-m+1)) \tag{2.41}$$

Taking the first and second derivatives of $V(z)$, we obtain

$$E(V) = d + \frac{\tau}{1-\sigma} \tag{2.42}$$

$$E(V(V-1)) = \frac{2\sigma\tau}{(1-\sigma)^2} \tag{2.43}$$

thus the second moment of the interdeparture time is

$$\begin{aligned} E\left(V^2\right) &= E(V) + E(V(V-1)) \\ &= d + \frac{\tau(1+\sigma)}{(1-\sigma)^2} \end{aligned} \tag{2.44}$$

the variance is

$$Var(V) = \overline{V^2} - (\overline{V})^2$$
$$= d - d^2 + \frac{\tau(1+\sigma-\tau-2d+2d\sigma)}{(1-\sigma)^2} \quad (2.45)$$

where the parameters τ, d and σ are given in (2.23), (2.24), (2.25) and (2.34), (2.35), (2.36).

2.4.2 The Squared Coefficient of Variation (SCV) and Average Cell Delay

ATM traffic is very bursty in nature and capturing this burstiness is essential for an accurate model. The first two moments provide the squared coefficient of variation (SCV) and this parameter can be used to capture the burstiness of ATM traffic.

1. The squared coefficient of variation of interarrival time C_a^2

The squared coefficient of variation (SCV) for interarrival time is given by:

$$C_a^2 = \frac{var(a)}{(\bar{a})^2} \quad (2.46)$$

where a is the interarrival time of the arrival process.

From the interarrival time distribution of a specific traffic, we can easily get the squared coefficient of variation (SCV) of interarrival time. For Poisson arrival, the SCV of interarrival time is simply 1.

For very bursty traffic, such as in a high speed communications network, the SCV of interarrival times would be much higher than 1. According to the measured data of video-phone given by Rathgeb [29], the SCV of interarrival time for highly variable

output stream is around 10.6 and the SCV of interarrival time for smoothest traffic is about 2. The SCV of interarrival time for the actual traffic will be somewhere in between two extremes from 2 to 10.6.

2. The squared coefficient of variation of interdeparture time C_d^2

The SCV of interdeparture time can be obtained by:

$$C_d^2 = \frac{\overline{V^2} - \overline{V}^2}{\overline{V}^2} \tag{2.47}$$

where

$$\overline{V} = d + \frac{\tau}{1-\sigma} \tag{2.48}$$

$$\overline{V^2} = d + \frac{\tau(1+\sigma)}{(1-\sigma)^2} \tag{2.49}$$

the parameters τ, d and σ are given in (2.23), (2.24), (2.25) and (2.34), (2.35), (2.36).

3. Average queue length and mean cell delay

The average queue length in the system is given by:

$$L = \sum_{i=M+1}^{\infty} (i-M)\, x_i \tag{2.50}$$

Since service time is one slot, from Little's formula, the mean cell delay in the system is:

$$\overline{delay} = \frac{L}{\rho} \tag{2.51}$$

For finite buffer case (buffer size of N), just replace ∞ by $M+N$ in (2.50).

Figure 2.16, Figure 2.17 and Figure 2.18 show the effect of traffic load and token pool size (M) on the cell delay in the system and the squared coefficient of variation (SCV) of interdeparture time from a Leaky Bucket for Poisson, GGeo and MMPP arrival processes respectively. Both the cell delay and the SCV of the interdeparture time of cells are greatly affected by system load and token pool size M, and there is a clear trade-off between these two parameters.

We can see that as traffic load increases the cell delay increases while SCV decreases. If the average arrival rate λ_a is fixed, the load ρ varies in direct proportion to TI, the token generation interval. In the extreme case of $\rho \rightarrow 0$, tokens are generated very rapidly $(TI \rightarrow 0)$, $C_d^2 \rightarrow C_a^2$, the Leaky Bucket does not throttle the sources at all. The cell delay goes to zero for Poisson and MMPP arrival process or $C_a^2 = 1$ in GGeo arrival process and remains small for the highly bursty traffic. Clearly, in this case the departure process is the same as the arrival process. Most of the buffering or loss takes place inside the network, potentially affecting the performance of other sources as well. From Figure 2.17, we can see assuming SCV of interarrival time to be 1 gives very optimistic results for cell delay. In the other extreme case of $\rho \rightarrow 1$, tokens are generated very slowly $(TI \rightarrow 1/\lambda_a)$, the Leaky Bucket is "tightly" controlling the source, most of the cells are buffered in the input queues (or lost). The cell delay goes to infinity and $C_d^2 \rightarrow 0$ since each cell waits for a token to be generated and the departure process approaches a deterministic process.

It is clear that the reduction of the burstiness of the traffic flow is larger in heavily loaded systems than it is in lightly loaded ones. Thus, the departure process of a Leaky Bucket in a lightly loaded system with bursty arrival process tends to be bursty too.

The effect of the size of the bucket is also demonstrated in Figure 2.16, Figure 2.17 and Figure 2.18. As M increases, the cell delay decreases while SCV of interdeparture time increases. The small value of cell delay introduced by the highly bursty traffic at the

light load could be diminished to zero by increasing the token pool size M. It is interesting to note that for large values of M ($M \approx 10$), it is only at high load, $\rho \rightarrow 1$, that the effect of the bursty control is seen, i.e. $C_d^2 < C_a^2$. In this range, the system performance is very sensitive to the changes in the load.

Figure 2.16, Figure 2.17 and Figure 2.18 also provide the comparison of the analysis results with simulation results for SCV of the interdeparture time and the cell delay for Poisson and GGeo and MMPP arrival processes respectively. We can observe that our analytical MGeo model approach and simulation give very similar results.

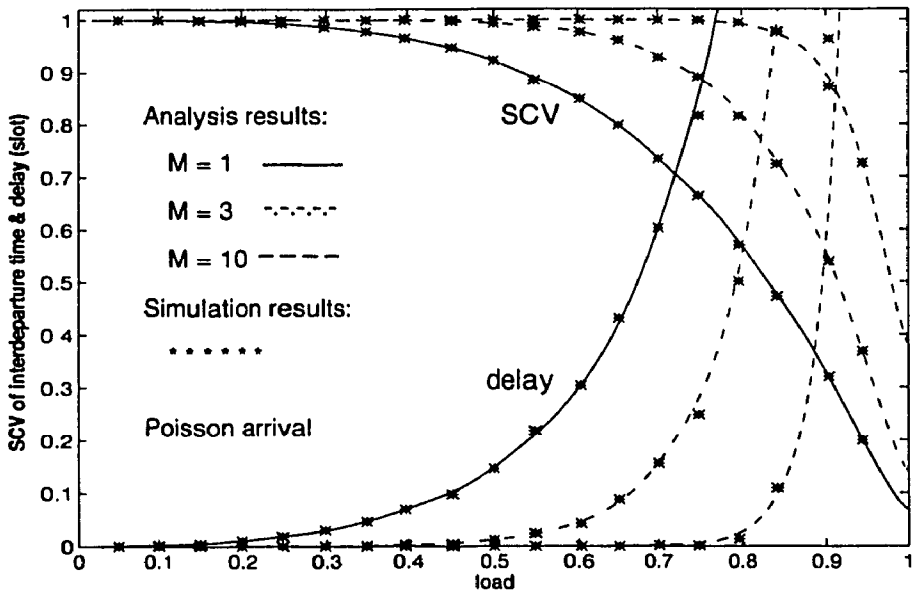

Figure 2.16 SCV of interdeparture time and cell delay vs. traffic load for different token pool sizes M (Poisson arrival)

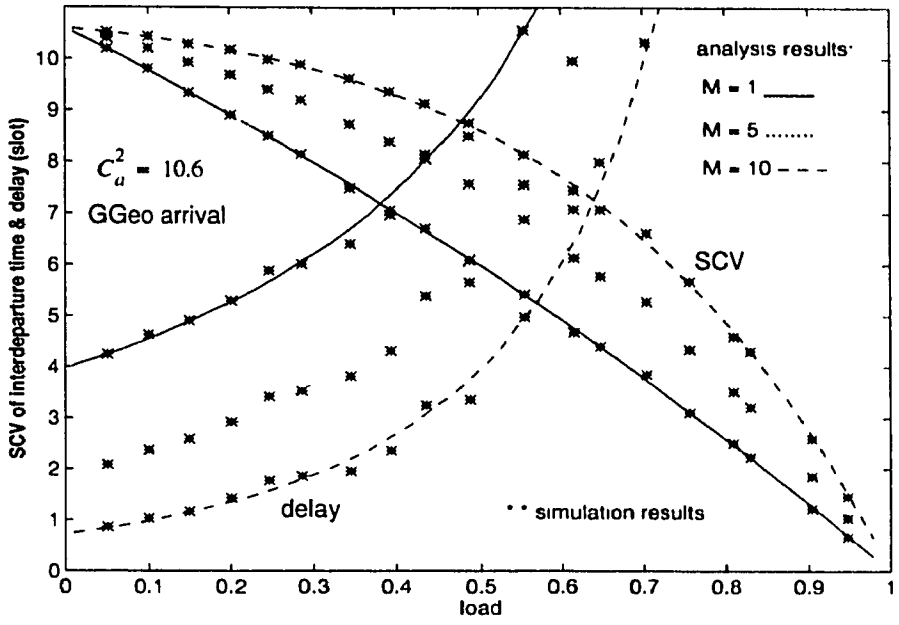

Figure 2.17 SCV of interdeparture time and queueing delay vs. traffic load for different token pool sizes M (GGeo arrival, SCV of interarrival time = 10.6)

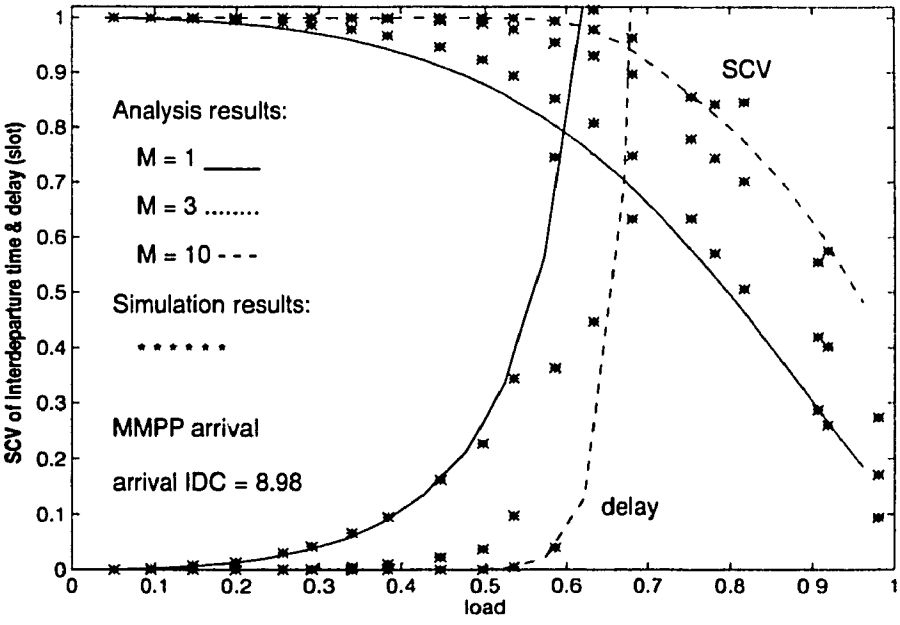

Figure 2.18 SCV of interdeparture time and queueing delay vs. system load for different token pool sizes M (MMPP arrival)

2.4.3 The Smoothness of the Departure Process of a Leaky Bucket

The Leaky Bucket scheme is used to smooth and regulate the incoming traffic, so the smoothness is a very important parameter in the performance evaluation of the Leaky Bucket scheme. We define SM as the smoothness of the departure flow from the Leaky Bucket, which reflects only one departure per slot. From (2.8), we have:

$$SM = \frac{P(1)}{1-P(1)} = \frac{d+\tau(1-\sigma)}{1-d-\tau(1-\sigma)} \tag{2.52}$$

where the parameters τ, d and σ are given in (2.23), (2.24), (2.25) and (2.34), (2.35), (2.36). From the definition of SM, we know that the larger SM is the more smooth the flow is. As we mentioned earlier the SCV is a measure of burstiness of a traffic which also reflects the smoothness of the process. But notice that SM is the inverse of SCV.

Figure 2.19 and Figure 2.20 show the smoothness of departure flow versus traffic load for the different token pool sizes for the GGeo (with SCV of interarrival time to 10.6) and the MMPP arrival process respectively. The smoothness is also greatly affected by the traffic load and the token pool size.

As the traffic load increases, the smoothness increases and the Leaky Bucket scheme has stronger smoothing control on the departure flow. For the fixed average arrival rate, higher smoothness can be obtained by increasing the token generation interval TI. However, the performance degradation on cell delay and cell loss will be expected.

From Figure 2.19 and Figure 2.20, we can see the effect of the token pool size M. As M increases, the smoothness decreases, this means the Leaky Bucket has less control on the smoothness of the departure flow. By means of the token pool size M, the Leaky Bucket scheme still allows for a certain degree of burstiness while limiting the average input rate below some predefined rate. M corresponds to the maximized burstiness of the

departure flow. As M increases, the maximized allowable burstiness increases and the Leaky Bucket has less smoothing control on the traffic. A value of $M = 0$, corresponds to the rate-based control, maximizes the "smoothness" of the traffic.

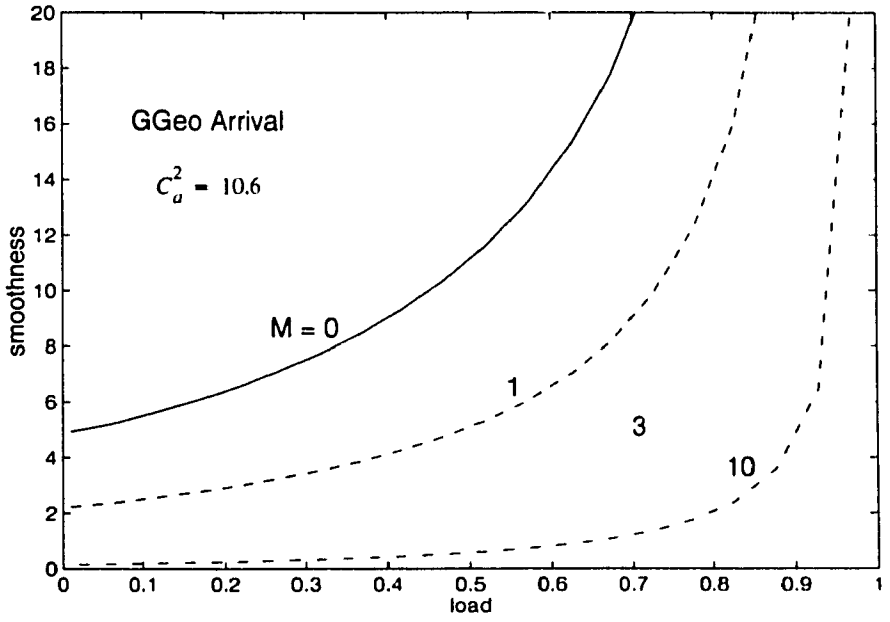

Figure 2.19 Smoothness vs. system load for different token pool size M (SCV of interarrival time = 10.6)

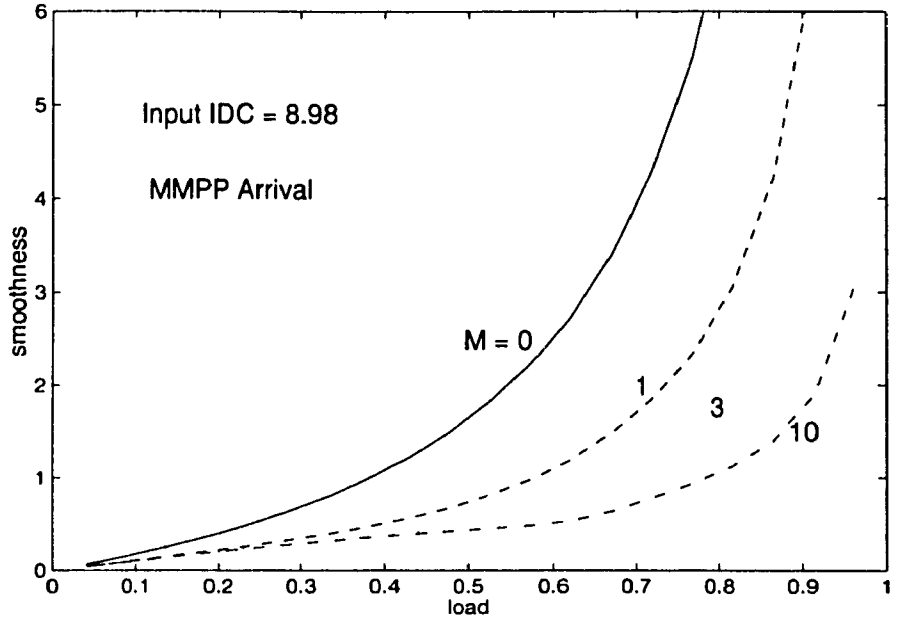

Figure 2.20 Smoothness vs. system load for different token pool size M (MMPP arrival, input IDC=8.98)

2.5 Autocorrelation between Two Consecutive Interdeparture Times

ATM networks are expected to support diverse applications such as voice, video and data transfer with different Quality of Service (QOS) requirement. Many of the traffic sources in ATM are not only bursty but highly correlated as well. It has been shown that neglecting correlations may result in a dramatic underestimation of various performance measures such as the loss probability and the cell delay [31]. Thus, it is important to look at the correlation effect of the departure process of the Leaky Bucket. In this section, in order to see the correlation of the departure process from a Leaky Bucket at lag 1, we provide a mapping procedure for the joint probability of two consecutive interdeparture times.

2.5.1 Mapping Procedure

In order to see the correlation effect of the departure process from a Leaky Bucket, we focus on the autocorrelation between the two consecutive interdeparture times. By definition, the autocorrelation at lag 1 can be determined through the joint probability distribution of two consecutive interdeparture times.

We make the same assumptions as before. Our embedded point is the slot boundary, just after the token's departure. The cells and tokens only arrive and depart at the slot boundaries. In order to have the derivation for the vector form, some notations are given below:

V^k: interdeparture time between $k-1$ th and kth departure, shown in Figure 2.21;

V^{k+1}: interdeparture time between kth and $k+1$ th departure, shown in Figure 2.21.

First, we are going to find the joint probability distribution of two consecutive interdeparture times $Q_1(i,j) = Pr[V^k = i, V^{k+1} = j]$. As before, we let (m, n) denote the number of tokens and cells in the token pool and the input buffer respectively at the $(k-1)$th departure.

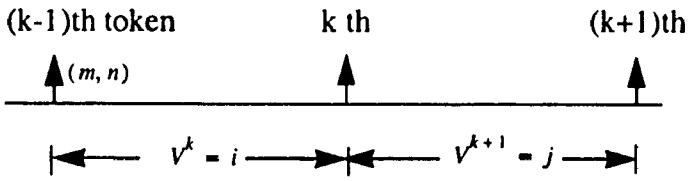

Figure 2.21

As before, conditioned on the event that the $(k-1)$th token joins the token pool at the embedded point, we may find the system in one of the following states.

1. The queue is not empty and the token pool is empty $(n \geq 1, m = 0)$ *:*

a) There are $n \geq 2$ *cells and no tokens in the system.*

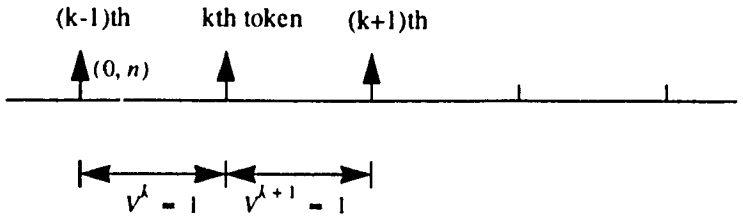

Figure 2.22

In this case, the subsequent token (kth) generated at the next slot boundary will depart immediately, and the $(k+1)$th token generated at the following slot boundary will depart at the following slot boundary as shown in Figure 2.22. Both interdeparture times V^k and V^{k+1} are one slot, the joint probability of this event can be obtained as:

$$Q_1(1,1) = Pr[V^k = 1, V^{k+1} = 1] = \sum_{m=M+2}^{\infty} x_m e \tag{2.53}$$

b) There is $n = 1$ *cell and no tokens in the system.*

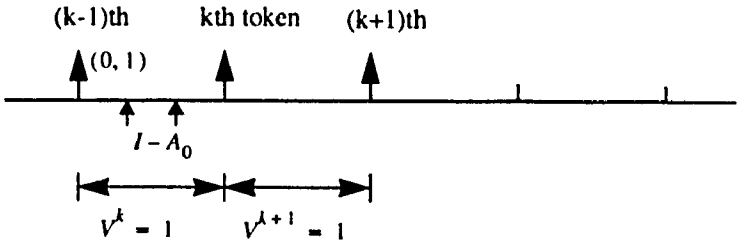

Figure 2.23

If at least one cell arrives at the current slot as in Figure 2.23, the kth token generated at the next slot boundary will depart immediately, and the $(k+1)$th token will depart at the following slot with probability $(I - A_0)$. The joint probability is given by:

$$Q_I(1,1) = Pr[V^k = 1, V^{k+1} = 1] = x_{M+1}(I - A_0)e \tag{2.54}$$

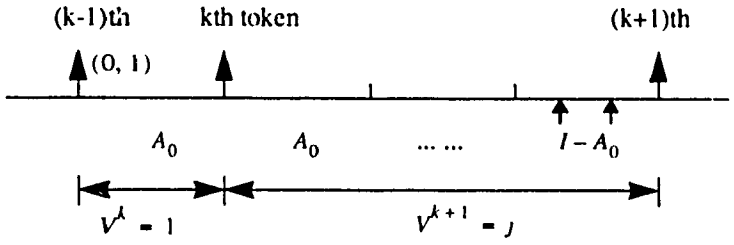

Figure 2.24

If there are no arrivals at the current slot as shown in Figure 2.24, the kth token generated at the next slot boundary will depart immediately and the $(k+1)$th token will depart at the jth slot boundary following the kth departure with probability $A_0 A_0^{j-1}(I - A_0)$. The joint probability of this event is:

$$Q_I(1,j) = Pr[V^k = 1, V^{k+1} = j] = x_{M+1} A_0 A_0^{j-1}(I - A_0)e \qquad j = 1, 2, 3, \ldots \tag{2.55}$$

2. *Both the queue and the token pool are empty* $(n = 0, m = 0)$ *:*

a) There are no cells and tokens in the system and there is at least one arrival during the current slot.

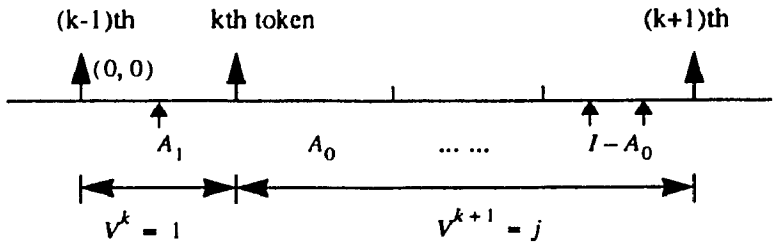

Figure 2.25

As shown in Figure 2.25, if there is only one cell arrival at the current slot, the kth token will depart at the next slot boundary and the $(k+1)$th token will depart at the jth slot boundary following the kth departure with probability $A_1 A_0^{j-1}(I-A_0)$. The joint probability of this event is:

$$Q_I(1,j) = Pr[V^k = 1, V^{k+1} = j] = x_M A_1 A_0^{j-1}(I-A_0)e \qquad j = 1, 2, 3, \ldots \tag{2.56}$$

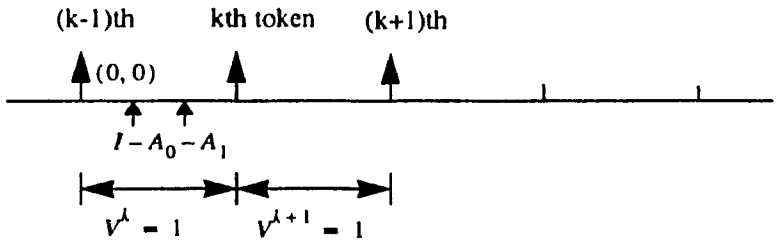

Figure 2.26

If there are more than one arrival at the current slot as shown in Figure 2.26, the kth token will depart at the next slot boundary and the $(k+1)$th token will depart at the one after the next slot boundary with probability $I-A_0-A_1$. The joint probability of this event is:

$$Q_I(1,1) = Pr[V^k = 1, V^{k+1} = 1] = x_M(I - A_0 - A_1)e \tag{2.57}$$

b) There are no cells and tokens in the system and there are no arrivals during the current slot.

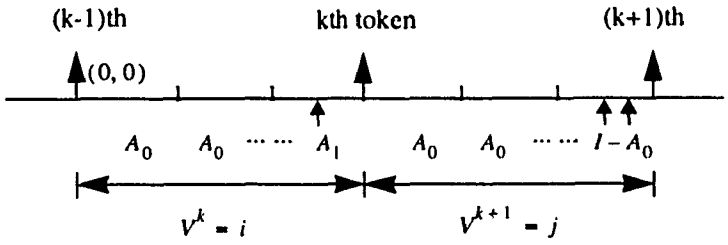

Figure 2.27

If there is only one arrival before the kth departure (Figure 2.27), the kth token will depart at the ith slot boundary following the $(k-1)$th departure and the $(k+1)$th token will depart at the jth slot boundary following the kth departure with probability $A_0^{i-1}A_1A_0^{j-1}(I-A_0)$. The joint probability of this events is:

$$Q_I(i,j) = Pr[V^k = i, V^{k+1} = j] = x_M A_0^{i-1} A_1 A_0^{j-1} (I - A_0)e \tag{2.58}$$
$$i = 2, 3, 4, \ldots \quad j = 1, 2, 3, \ldots$$

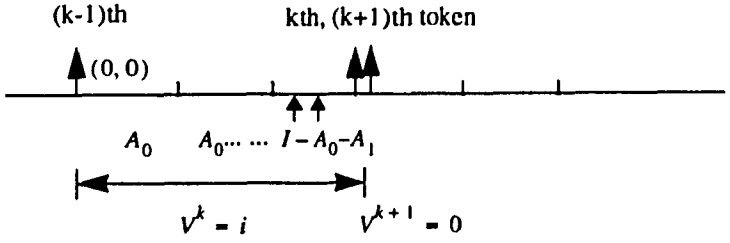

Figure 2.28

If there are more than one arrival before the kth departure, the kth and the $(k+1)$th token will depart at the same time with probability $A_0^{i-1}(I-A_0-A_1)$, see Figure 2.28. The joint probability of this event is:

$$Q_I(i,0) = Pr[V^k = i, V^{k+1} = 0] = x_M A_0^{i-1}(I-A_0-A_1)e \qquad i = 2, 3, 4, \ldots \tag{2.59}$$

3. *The token pool is not empty and the queue is empty* $(n = 0, 1 \le m \le M-1)$ *:*

There are m $(1 \le m \le M-1)$ tokens and no cells in the system. In order to see the joint probability of the interdeparture time between the $(k-1)$th, the kth token and the kth, the $(k+1)$th token, the $(k-1)$th token must depart from the system (the probability of this event is $I-A_0$). Conditioned on the event that the $(k-1)$th token departs from the token pool, we have the following two cases.

a) There are i $(i \ge 2)$ *cells arriving during the current slot.*

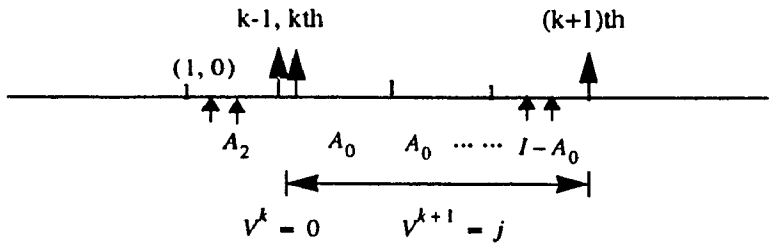

Figure 2.29

If there is only one token $(m = 1)$ *in the system* and there are only two arrivals during the current slot as shown in Figure 2.29, the $(k-1)$th token and the kth token will depart simultaneously at the next slot boundary and the $(k+1)$th token will depart at the jth slot boundary following the kth departure with probability $A_2A_0^{j-1}(I-A_0)$. The joint probability of this event is:

$$Q_I(0,j) = Pr\left[V^k = 0, V^{k+1} = j\right] = x_{M-1}(I-A_0)^{-1}A_2A_0^{j-1}(I-A_0)e \qquad (2.60)$$
$$j = 1, 2, 3, \ldots$$

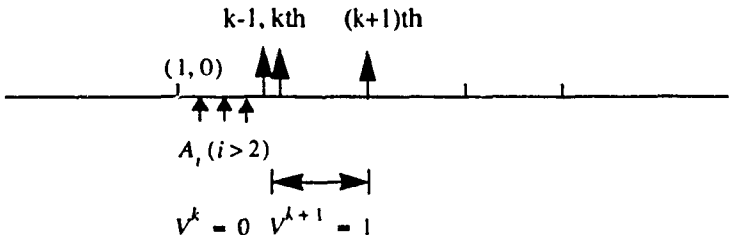

Figure 2.30

If there is only one token $(m = 1)$ *in the system* and there are more than two arrivals at the current slot shown in Figure 2.30, the $(k-1)$th token and the kth token will depart at the same time of next slot boundary and the $k+1$th token will depart at the one after the next slot boundary with probability $I - A_0 - A_1 - A_2$. The joint probability is given by:

$$Q_I(0,1) = Pr\left[V^k = 0, V^{k+1} = 1\right] = x_{M-1}(I-A_0)^{-1}(I-A_0-A_1-A_2)e \qquad (2.61)$$

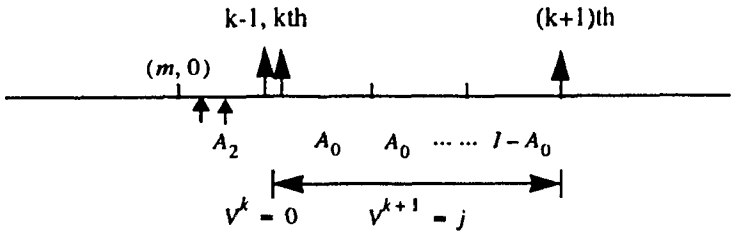

Figure 2.31

If there are more than one token $(m \geq 2)$ *in the system* and there are only two arrivals during the current slot shown in Figure 2.31, then the $(k-1)$th token and the kth token will depart simultaneously at the next slot boundary, and the $(k+1)$th token will depart at the jth slot boundary following the kth departure with probability $A_2 A_0^{j-1}(I - A_0)$. The joint probability of this case is:

$$Q_I(0,j) = Pr[V^k = 0, V^{k+1} = j] = \sum_{m=1}^{M-2} x_m (I - A_0)^{-1} A_2 A_0^{j-1} (I - A_0) e \qquad (2.62)$$

$$j = 1, 2, 3, \ldots$$

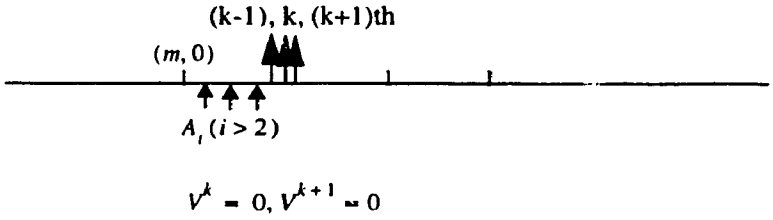

Figure 2.32

If there are more than one token $(m \geq 2)$ *in the system* and there are more than two arrivals during the current slot shown in Figure 2.32, the $(k+1)$th token will depart at the same time as the $(k-1)$th and kth tokens with probability $I - A_0 - A_1 - A_2$. The joint probability of this event is:

$$Q_I(0,0) = Pr[V^k = 0, V^{k+1} = 0] = \sum_{m=1}^{M-2} x_m (I - A_0)^{-1} (I - A_0 - A_1 - A_2) e \qquad (2.63)$$

b) There is only one arrival during the current slot.

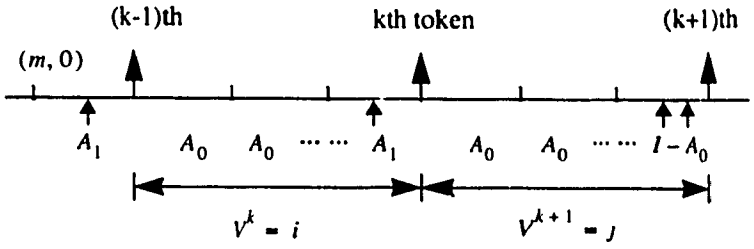

Figure 2.33

Then the $(k-1)$th token will depart at the next slot boundary and the kth token will depart at the ith slot boundary following $(k-1)$th departure. If there is only one arrival before the kth departure, the $(k+1)$th token will depart at the jth slot boundary following kth departure with probability $A_1A_0^{i-1}A_1A_0^{j-1}(I-A_0)$, as shown in Figure 2.33. The joint probability of this case is given by:

$$Q_I(i,j) = Pr[V^k = i, V^{k+1} = j] = \sum_{m=1}^{M-1} x_m (I-A_0)^{-1} A_1 A_0^{i-1} A_1 A_0^{j-1} (I-A_0)\, e \qquad (2.64)$$

$$i, j = 1, 2, 3, \ldots$$

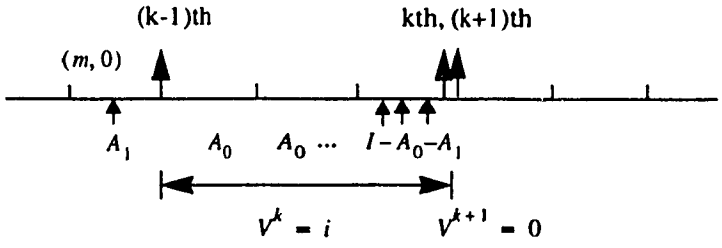

Figure 2.34

If there are more than one arrival before the kth departure (Figure 2.34), the $(k+1)$th token will depart at the same time as the kth token with probability $A_1A_0^{i-1}(I-A_0-A_1)$. Then the joint probabilities of this event is:

$$Q_I(i,0) = Pr[V^k = i, V^{k+1} = 0] = \sum_{m=1}^{M-1} x_m (I-A_0)^{-1} A_1 A_0^{i-1} (I-A_0-A_1) e \qquad (2.65)$$
$$i = 1, 2, 3, \ldots$$

Finally, conditioned on the event that the $(k-1)$th token joins the token pool (the probability of this event is $1 - x_0 e$), the joint probability of two consecutive interdeparture times $Q_I(i,j) = \dfrac{Q_I(i,j)}{1-x_0 e}$.

Then the autocorrelation of the two consecutive interdeparture times is

$$\begin{aligned} R_{I1} = E\{V^k V^{k+1}\} &= \sum_{i=0}^{\infty}\sum_{j=0}^{\infty} ijPr[V^k = i, V^{k+1} = j] \\ &= \sum_{i=0}^{\infty}\sum_{j=0}^{\infty} ijQ_I(i,j) \end{aligned} \qquad (2.66)$$

The autocovariance at lag 1 is defined as:

$$\begin{aligned} C_{I1} &= R_{I1} - (\bar{V})^2 \\ &= \sum_{i=0}^{\infty}\sum_{j=0}^{\infty} ijQ_I(i,j) - (\bar{V})^2 \end{aligned} \qquad (2.67)$$

Then the autocorrelation coefficient is given by

$$r_{I1} = \frac{C_{I1}}{Var(V)} = \frac{\sum_{i=0}^{\infty}\sum_{j=0}^{\infty} ijQ_I(i,j) - (\bar{V})^2}{Var(V)} \qquad (2.68)$$

where $\bar{V}$ is the mean interdeparture time given in (2.42) and $Var(V)$ is the variance of the interdeparture time given in (2.45).

2.5.2 Numerical Results

In Figure 2.35, Figure 2.36, Figure 2.37, Figure 2.38, Figure 2.39 and Figure 2.40, we have plotted the autocorrelation coefficient between two consecutive interdeparture times, at various values of traffic load, token pool size M and arrival IDC, for the Poisson and the MMPP arrival processes.

From Figure 2.35 and Figure 2.39, it is clear that the autocorrelation between two consecutive interdeparture times from Leaky Bucket for Poisson arrival is always (slightly) negative. The Leaky Bucket thus transforms the uncorrelated interarrival times at its input into slightly negatively correlated interdeparture times at its output, which can also be considered as a favorable effect of the Leaky Bucket control. The same conclusion is drawn by Wittevrongel and Bruneel for the ON-OFF source model in [32]. The MMPP arrival process has correlated interarrival times. The autocorrelation coefficient between two consecutive interdeparture times is less than a specific value which corresponding to the autocorrelation coefficient of interarrival times at lag 1. It is clear the Leaky Bucket has a favorable control on correlation between two consecutive interdeparture times.

From Figure 2.35 and Figure 2.36, we can see that the autocorrelation coefficient between two consecutive interdeparture times is greatly affected by traffic load and token pool size M. It decreases when the traffic load increases. It is clear that at heavy loaded systems, the Leaky Bucket has stronger control on the autocorrelation coefficient of the interdeparture time (at lag 1). For the lightly loaded systems with correlated arrival process it tends to be correlated too.

Figure 2.37 depicts the value of autocorrelation coefficient of the interdeparture time at lag 1 versus the arrival IDC for different token pool size of M at traffic load 0.67. Leaky bucket has a stronger control on the correlation when pool size decreases. It is interesting to note that the autocorrelation coefficient of interdeparture times slightly increases when

the arrival IDC increases from 20 to 100. This means that autocorrelation coefficient of interdeparture time at lag 1 becomes less sensitive to arrival IDC when the arrival IDC reaches to 10.

The effect of token pool size M is also demonstrated in Figure 2.38, Figure 2.39 and Figure 2.40. The autocorrelation coefficient between two consecutive interdeparture times increases when M increases. For the large value of M, the autocorrelation coefficient between two consecutive interdeparture times reaches to the autocorrelation coefficient of interarrival times. The Leaky Bucket will have no control on the correlation at lag 1.

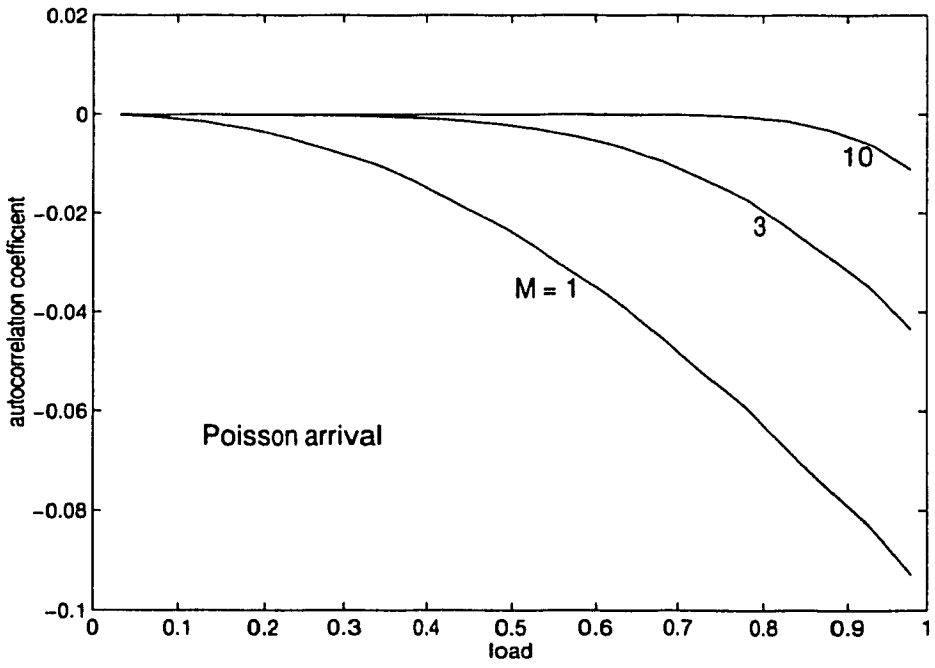

Figure 2.35 Autocorrelation coefficient between consecutive interdeparture times vs. load

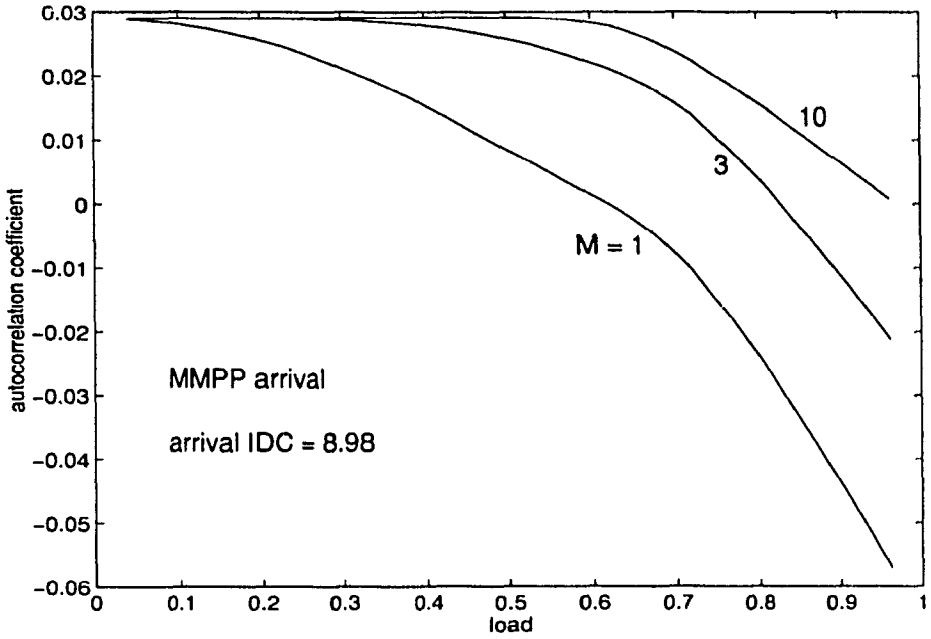

Figure 2.36 Autocorrelation coefficient between consecutive interdeparture times vs. load

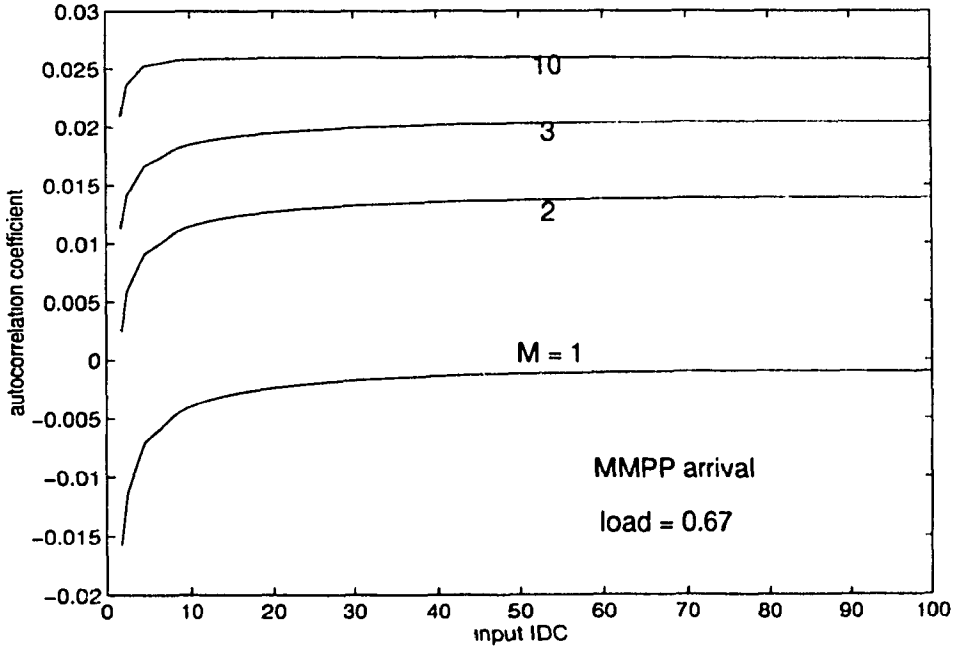

Figure 2.37 Autocorrelation coefficient between consecutive interdeparture times vs. input IDC

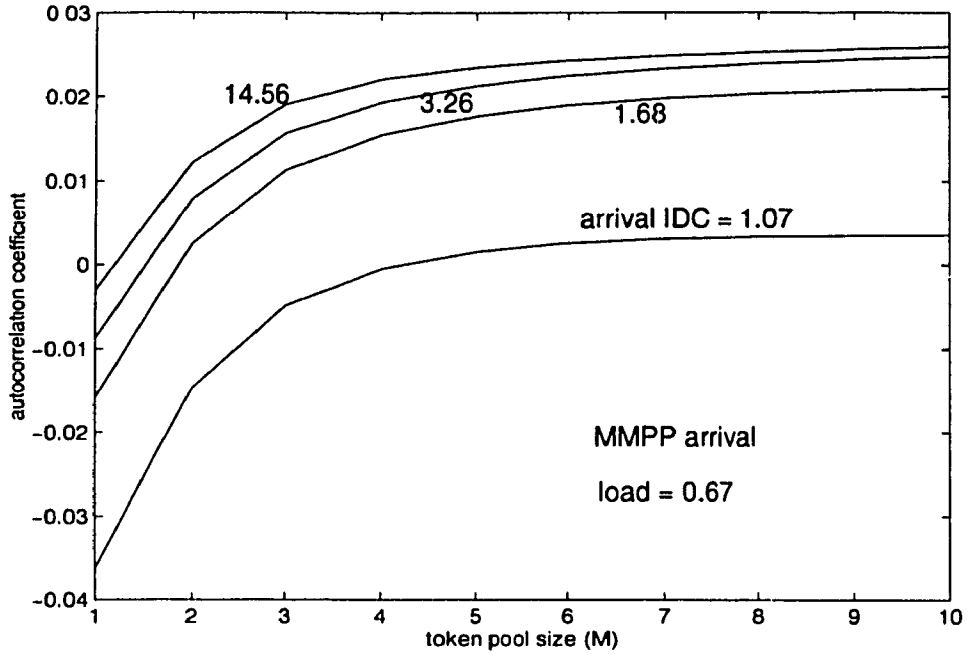

Figure 2.38 Autocorrelation coefficient between consecutive interdeparture times vs. pool size

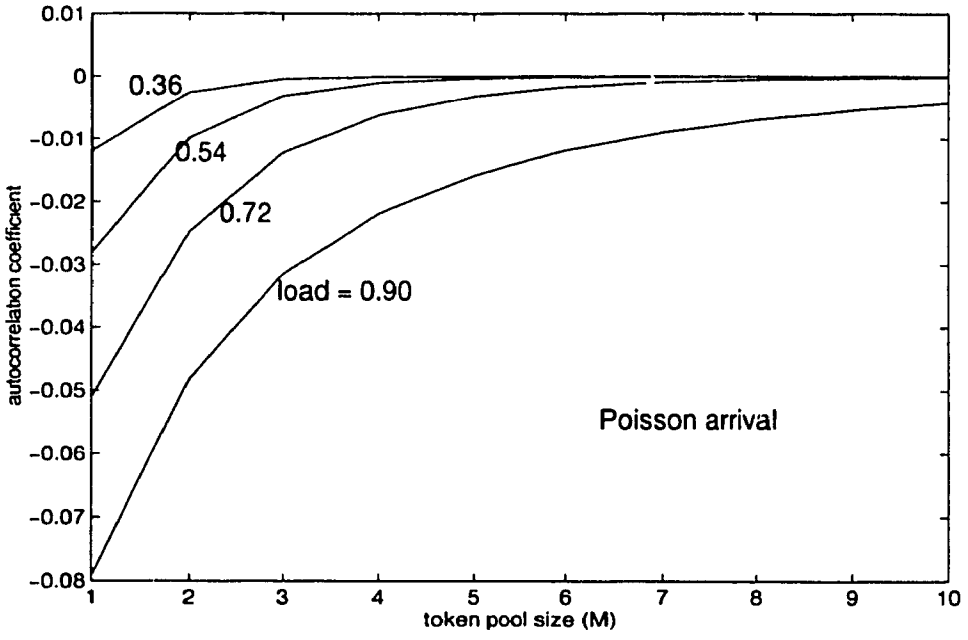

Figure 2.39 Autocorrelation coefficient between consecutive interdeparture times vs. pool size M

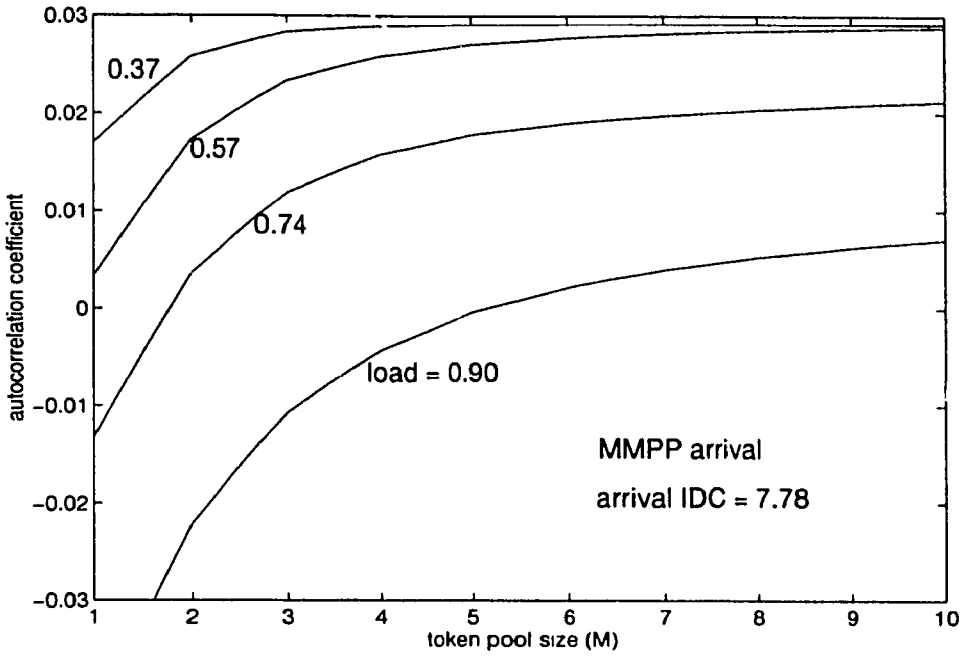

Figure 2.40 Autocorrelation coefficient between consecutive interdeparture times vs. pool size M

2.6 Conclusions

The Leaky Bucket scheme as a policing function in ATM networks must be available for every connection during the entire active phase and must operate in real-time. In this chapter, we have proposed a Modified Geometric (MGeo) model for the interdeparture time of a buffered Leaky Bucket scheme. The detailed mapping procedure to fit the interdeparture time to MGeo model is provided. The MGeo model is verified under a wide range of traffic sources such as Poisson, GGeo (Generalized Geometric) and MMPP (Markov Modulated Poisson Process) arrival processes. Numerical results and simulation show the MGeo approach provides a good approximation for the interdeparture time distribution of the Leaky Bucket and is very computationally efficient for real-time control.

The control effects of the Leaky Bucket are extensively examined from the view point of smoothing out the burstiness of the input traffic, thereby making it easier for the network to handle large amounts of traffic without undue delay, congestion, or buffer overflow. The smoothing effect is characterized by the Squared Coefficient of Variation (SCV) of the interdeparture time of the Leaky Bucket, and is analyzed under the Poisson, GGeo and MMPP arrival processes. Through the numerical examples, we investigate how the traffic characteristics for the designated traffic flow are affected by the traffic load, token pool size and the burstiness of the traffic source. The trade-off between the burstiness of the departure process and the cell delay is examined. We present results for both finite and infinite input buffer sizes.

By using the proposed MGeo departure model, we can analyze performance of the Leaky Bucket scheme with different parameter settings. Such results are useful for system designers to set the various parameters of the Leaky Bucket mechanism in accordance with the Quality of Service (QoS) requirement.

We also have looked at the correlation filtering effect of the Leaky Bucket. The autocorrelation coefficient between two consecutive interdeparture times is derived by using a similar mapping procedure. It is interesting to note that the Leaky Bucket has stronger burstiness and correlation control for heavily loaded systems. For lightly loaded systems, the burstiness and the correlation between two consecutive interdeparture times of the departure from the Leaky Bucket tends to be preserved from the input flow.

In this chapter, the correlation effect is studied in terms of covariance between two consecutive interdeparture times (at lag 1). In order to accurately characterize the departure process of the Leaky Bucket scheme, this measure is not sufficient to capture the correlation. Further study on the long term Index of Dispersion for Counts (IDC) will be carried out in the next chapter.

Chapter 3

STATISTICAL CHARACTERIZATION OF THE NUMBER OF DEPARTURES FROM A LEAKY BUCKET

In this chapter, we focus our analysis on the number of departures (counts) from a Leaky Bucket. Most of the previous work on the Leaky Bucket departure characteristics deal with the interdeparture time, and only focus on the coefficient of variation and short term correlation (correlation at lag 1). Only a few looked at the number of departures [8]. Wu et. al [8] present a procedure for calculating the mean, variance and autocovariance of the number of departures from the Leaky Bucket. A two mini-source model is proposed to characterize the Leaky Bucket departure process and evaluate the network performance. We note that the calculation of long term autocovariance with a large buffer and token pool sizes are very time consuming.

The characterizations of burstiness and correlation are not only captured by simple burstiness indexes such as the coefficient of variation, and the short term covariance (e.g. at lag 1). It is necessary to look at the long term variance such as long term Index of Dispersion for Counts (IDC) in order to accurately characterize the departure process of the Leaky Bucket.

The objective of this chapter is to fit the departure process of the Leaky Bucket to a two-state MMPP process by considering both variance and long term covariance. The detailed mapping procedures for the probability distribution of the number of departures and the correlation of the number of departures between two consecutive slots are provided in Section 3.1 and Section 3.2 respectively. The autocovariance function of the number of departures at arbitrary lags is carried out in Section 3.3. In Section 3.4, we discuss the Index of Dispersion for Counts (IDC) for the departure process of the Leaky Bucket. A statistical matching method is given in Section 3.5. Section 3.6 conclude this chapter.

3.1 Distribution of the Number of Departures from a Leaky Bucket

3.1.1 Mapping Procedure

First we consider the case of an infinite input buffer. As before, our assumption is based on a discrete slot boundary which means cells arrive and depart only at the slot boundaries. A slot is equivalent to a token generation interval. The arrivals at the end of a slot is independent from slot to slot. Further, we assume that tokens are also generated and depart at the slot boundaries, and depart in a FIFO order. Our embedded point is the slot boundary, just after the token's departure.

We will look at the number of cells departing at the end of a slot. Here we give a more general derivation of the vector version. The scalar version is a special case with dimension of one element.

In order to have the mapping procedure, some notation is given below:

m: number of tokens in the bucket;

n: number of cells in the input buffer;

M: token pool size;

J: number of arrival phases;

x_i: steady-state probability of the system in state i, $(i = M - m + n)$;

A_s: probability of s arrivals during a token generation interval with $J \times J$ elements;

e: column vector of 1's, with J elements;

I: $J \times J$ identity matrix;

D: number of cells departing from the Leaky Bucket at the end of a slot (Figure 3.1).

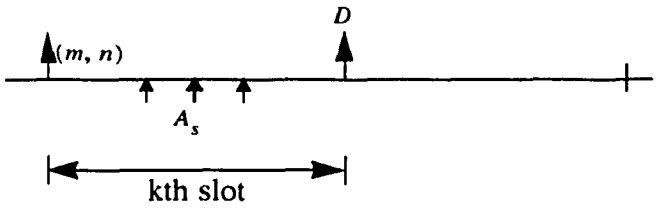

Figure 3.1

At the embedded point, we may find the system in one of the following states.

1. The queue is not empty and the token pool is empty ($m = 0, n \geq 1$):

There are n $(n \geq 1)$ cells and no tokens in the system.

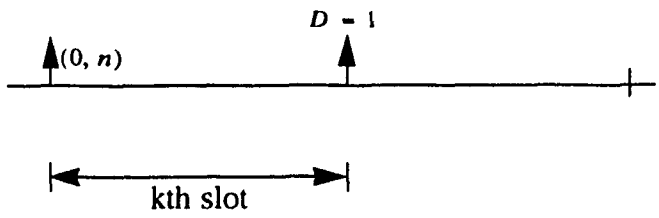

Figure 3.2

As shown in Figure 3.2, the new token generated at the next slot boundary will add to the empty bucket and there is only one token in the bucket. Then the number of cell departures at this slot boundary is one, the probability of this event is:

$$P(D = 1) = Pr[\text{no tokens in the system}] = \left(\sum_{i = M+1}^{\infty} x_i \right) e \tag{3.1}$$

2. *The queue is empty* ($0 \le m \le M-1, n = 0$)*:*

There are m ($0 \le m \le M-1$) tokens and no cells in the system.

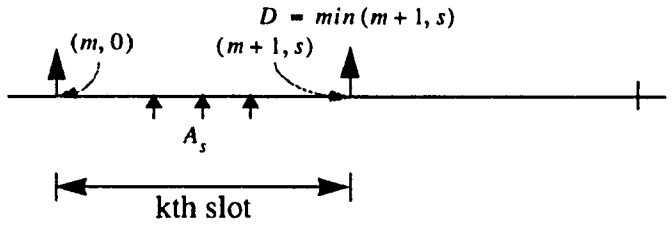

Figure 3.3

At the end of current slot, there are $m + 1$ tokens and s cells in the system if s cells arrive at the slot boundary with probability of A_s, see Figure 3.3. Then the number of cell departures at this slot boundary is $min(m + 1, s)$, the probability of this event is:

$$P[D = min(m + 1, s)] = x_{M-m} A_s e \qquad m = 0, 1, 2, \ldots, M-1;\ s = 0, 1, 2, \ldots \tag{3.2}$$

3. *The queue is empty and the token pool is full* ($m = M, n = 0$)*:*

There are M tokens and no cells in the system.

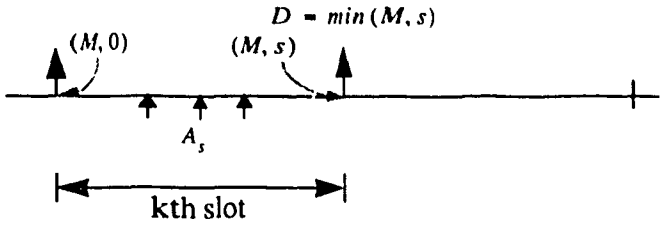

Figure 3.4

As depicted in Figure 3.4, at the end of current slot, there are still M tokens (since the bucket is full and the newly generated token will be dropped) and s cells in the system if s cells arrive at the slot boundary with probability of A_s. Then the number of cell departures at this slot boundary is $min\,(M, s)$, the probability of this event is:

$$P\,[D = min\,(M, s)\,] = x_0 A_s e \qquad s = 0, 1, 2, \ldots \tag{3.3}$$

In summary, the probabilities of having D departures at the end of a slot are given by:

$$P\,(D = 1) = \left(\sum_{i = M+1}^{\infty} x_i \right) e \tag{3.4}$$

$$P\,[D = min\,(m + 1, s)\,] = x_{M-m} A_s e \qquad m = 0, 1, 2, \ldots, M-1;\ s = 0, 1, 2, \ldots \tag{3.5}$$

$$P\,[D = min\,(M, s)\,] = x_0 A_s e \qquad s = 0, 1, 2, \ldots \tag{3.6}$$

For the finite input buffer size of N, we just replace ∞ by $M + N$ in (3.4).

Using equation (3.4)-(3.6), we can have the probability distribution of the number of departures from the Leaky Bucket. The first two moments, $\bar{D}$ and $\bar{D^2}$, of the number of departures are:

$$\bar{D} = \sum_{k=0}^{M} kP(D=k) \tag{3.7}$$

$$\overline{D^2} = \sum_{k=0}^{M} k^2 P(D=k) \tag{3.8}$$

Then the variance of the number of departures is given:

$$Var(D) = \overline{D^2} - (\bar{D})^2 \tag{3.9}$$

For the convenience of the discussion later in this chapter, we define Variance to Mean Ratio (VMR) of the number of departures as

$$VMR(D) = \frac{Var(D)}{\bar{D}} \tag{3.10}$$

We will see later VMR is one of the main terms in Index Dispersion of Count (IDC). Like SVC of the interdeparture time, VMR reflects the burstiness of the departure flow in terms of number of departures.

3.1.2 Numerical Results

In this section, we give some numerical results to illustrate probability distribution and the Variance to Mean Ratio (VMR) of number of departures from the Leaky Bucket described in the previous section. We consider different kinds of arrival processes such as Poisson, GGeo and MMPP. Numerical examples are given under the various parameter settings.

Figure 3.5 shows the probability distribution of number of departures from the Leaky Bucket at the end of a slot for different system loads for Poisson arrivals. As the traffic

load increases, token generation slows down, the probability of one departure per slot increases. That means cells depart more evenly and smoothly, and the Leaky Bucket has more burstiness control on the departure flow. This is the same conclusion we have drawn in Chapter 2.

Figure 3.6, Figure 3.7 and Figure 3.8 show the probability distributions of number of departures for GGeo arrival process. We find that the probability distribution of number of departures is also very sensitive to the traffic load, token pool size and the squared coefficient of variation of the interarrival time.

For the MMPP arrival process, similar results (Figure 3.9 and Figure 3.10) are obtained as those for the interdeparture time distribution discussed in Chapter 2. The departure probability distribution pattern either for the intervals or for the counts is not very sensitive to the IDC parameter of the MMPP arrival process.

Figure 3.11, Figure 3.12 and Figure 3.13 show the effect of traffic load and token pool size (M) on the Variance to Mean Ratio (VMR) of number of departures from the Leaky Bucket for Poisson, GGeo and MMPP respectively. As before, the VMR of the number of departures is greatly affected by traffic load and token pool size. It is obvious again that the throttle effect on burstiness is stronger in heavily loaded systems than in lightly loaded ones. In Figure 3.12, it is interesting to notice that the VMR can also be greatly reduced by choosing proper value of token pool size M, even in the lightly loaded system for GGeo arrival process. A value of $M = 0$, relates to the rate-based control, maximizes the Leaky Bucket's burstiness control effect in terms of VMR.

Figure 3.14, Figure 3.15 and Figure 3.16 plot the VMR of the number of departures versus the token pool size M for Poisson, GGeo and MMPP arrival processes, respectively. We find that the control effects on VMR for Poisson and MMPP arrival are similar when changing the token pool size and the traffic load. For large token pool sizes

($M \rightarrow 10$), the burstiness control effects at various traffic loads show no big differences, and the Leaky Bucket has less smoothing control on the output flow. But for GGeo arrival process, at the large token pool sizes ($M \rightarrow 10$), the VMR is more sensitive to the traffic load. By setting a proper value of token generation rate, certain degree of burstiness reduction can be achieved.

In Figure 3.5 - Figure 3.10, the lines between points are only used to identify a particular set of results. There are no values between two consecutive integers.

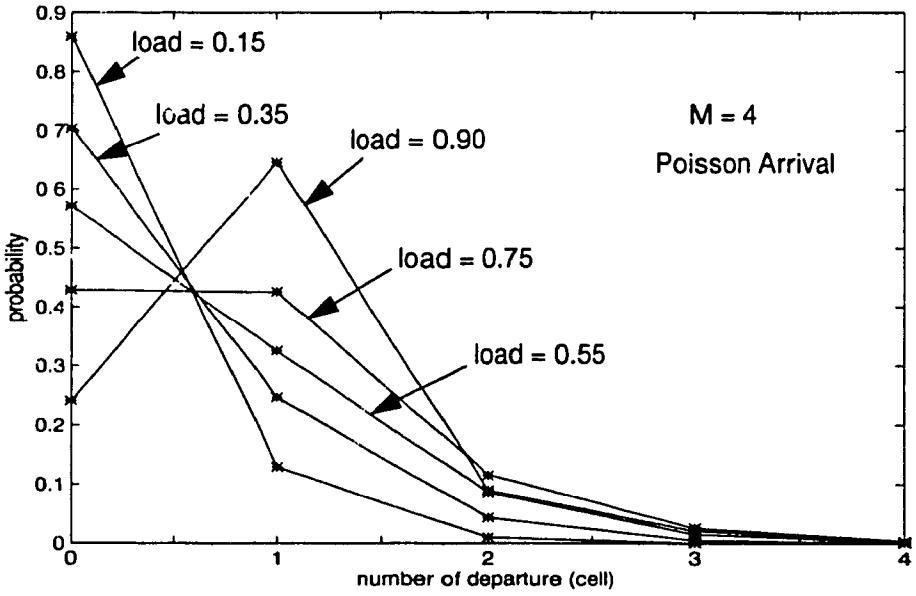

Figure 3.5 Probability distribution of no. of departures during a slot from Leaky Bucket at different system load (Poisson arrival)

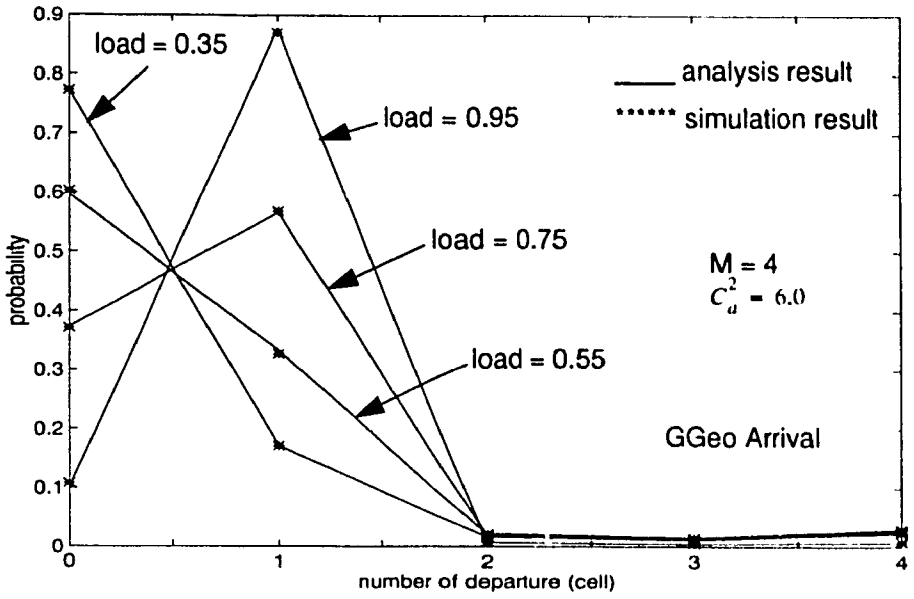

Figure 3.6 Probability distribution of no. of departures during a slot at different system load for GGeo arrival

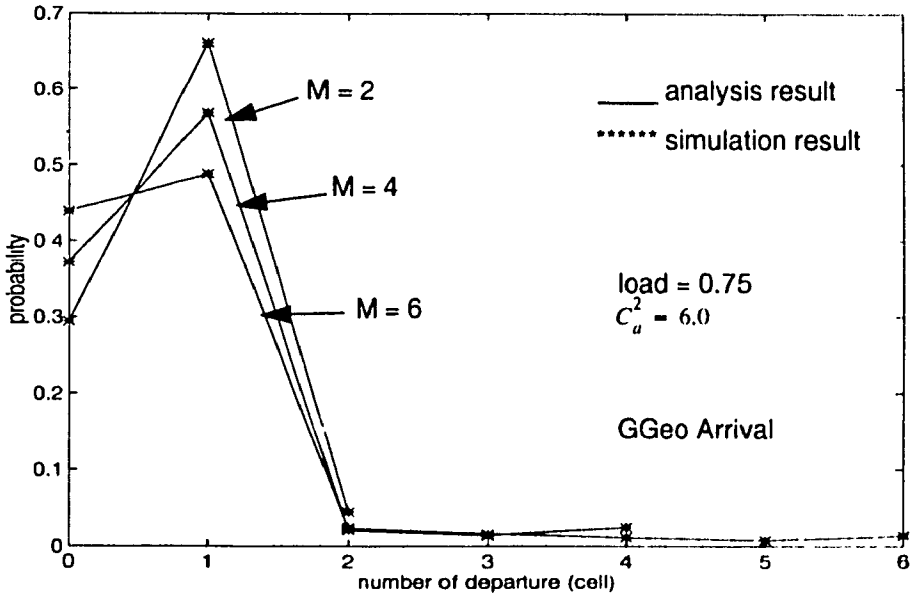

Figure 3.7 Probability distribution of no. of departures during a slot at different token pool size M for GGeo arrival

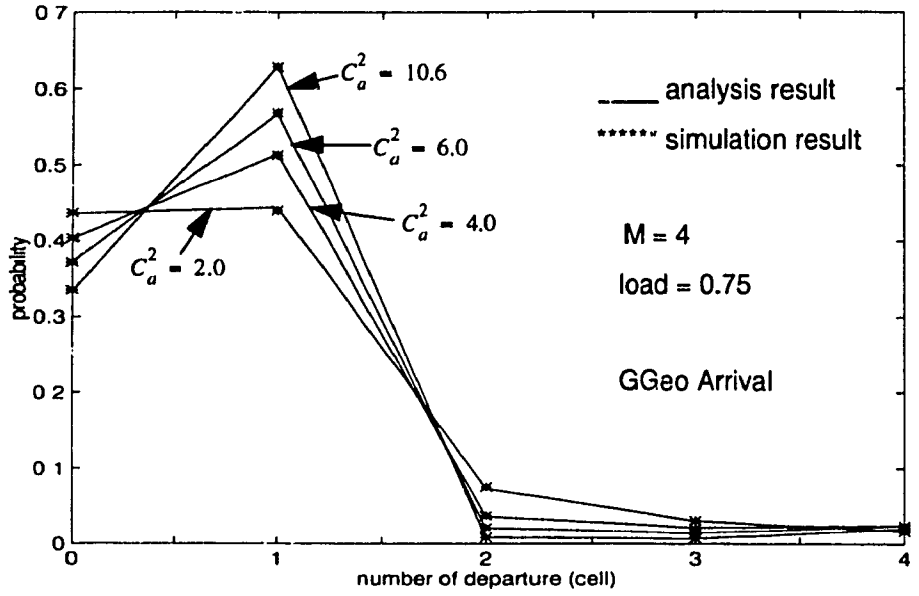

Figure 3.8 Probability distribution of no. of departures during a slot at different SCV of interarrival time for GGeo arrival process

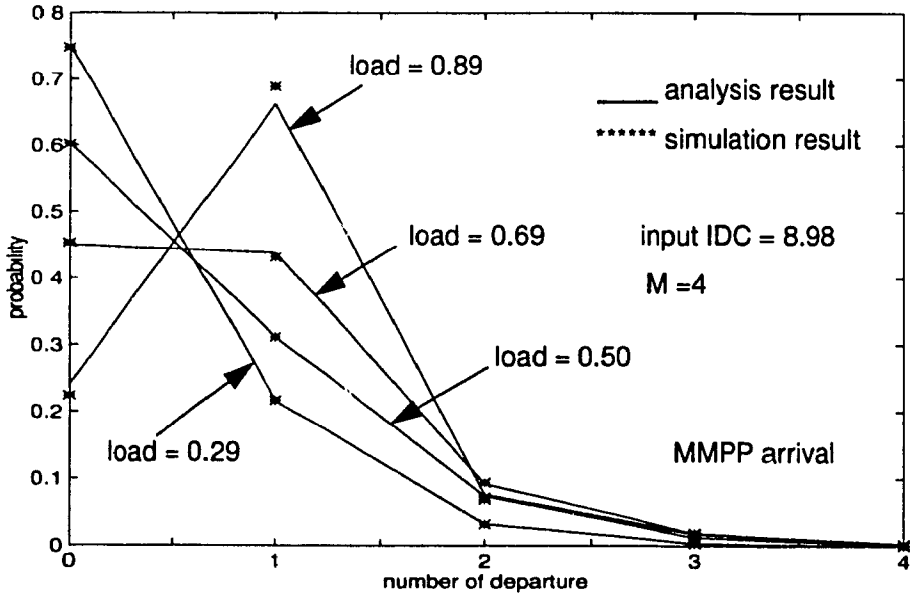

Figure 3.9 Probability distribution of no. of departures during a slot from Leaky Bucket at different system load (MMPP arrival)

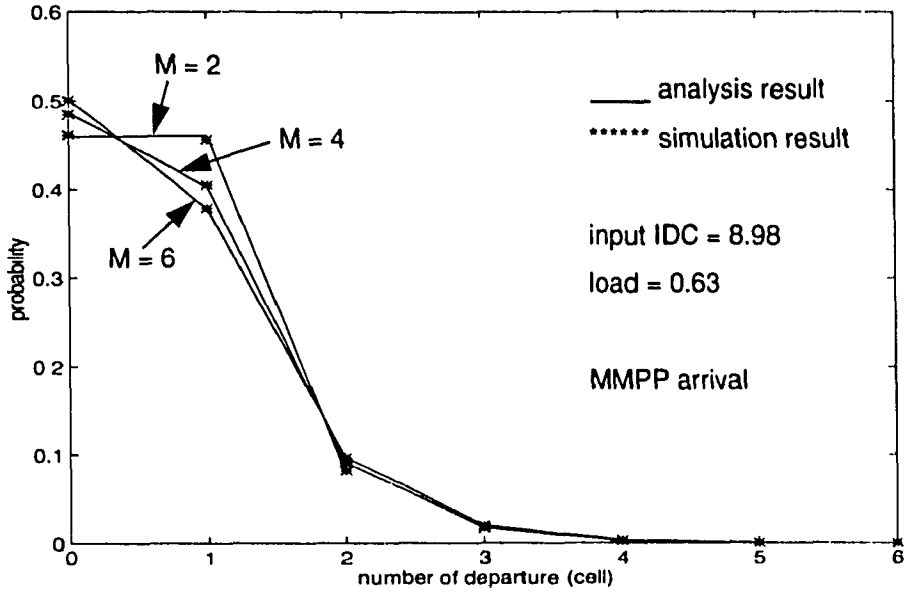

Figure 3.10 Probability distribution of no. of departures during a slot at different token pool size M for MMPP arrival

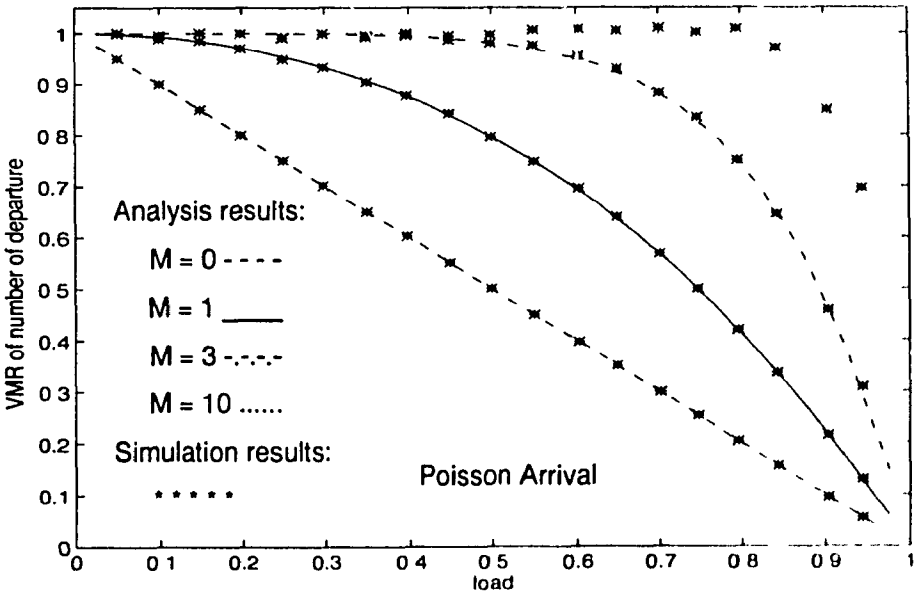

Figure 3.11 Comparison of the analytical results with simulation results for VMR of the no. of departures in a slot (Poisson arrival)

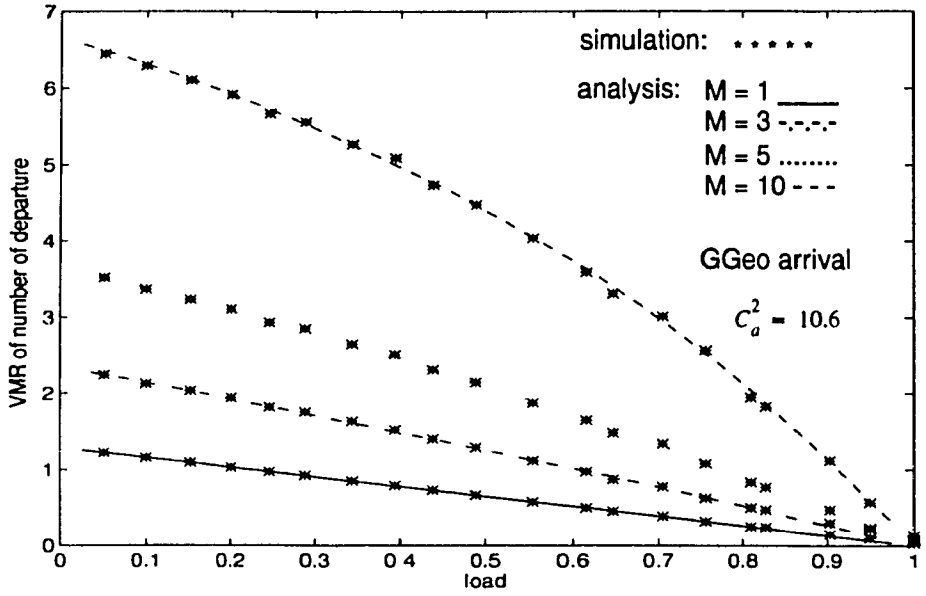

Figure 3.12 Comparison of the analysis results with simulation results for VMR of the no. of departures in a slot (GGeo arrival)

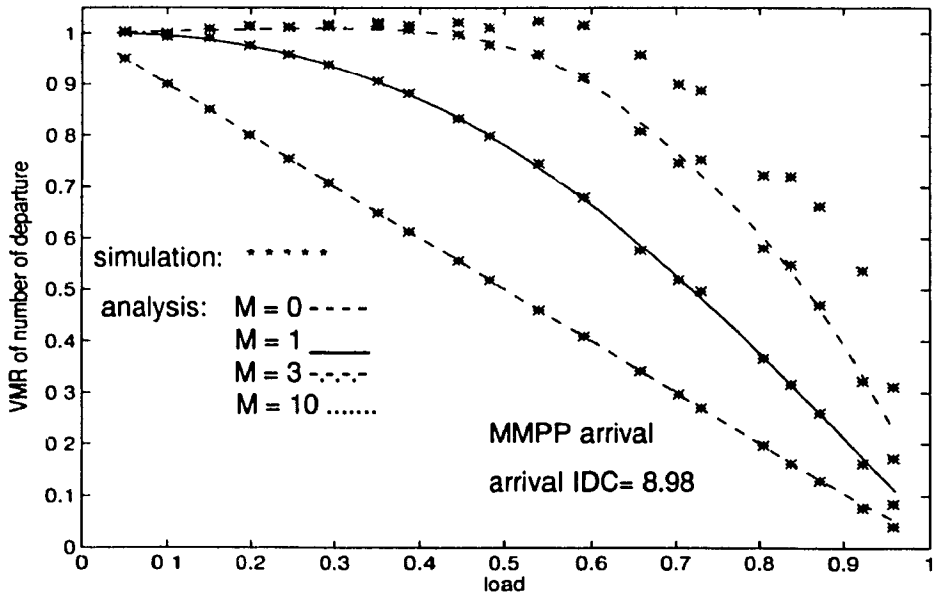

Figure 3.13 Comparison of the analysis results with simulation results for VMR of the no. of departures in a slot (MMPP arrival)

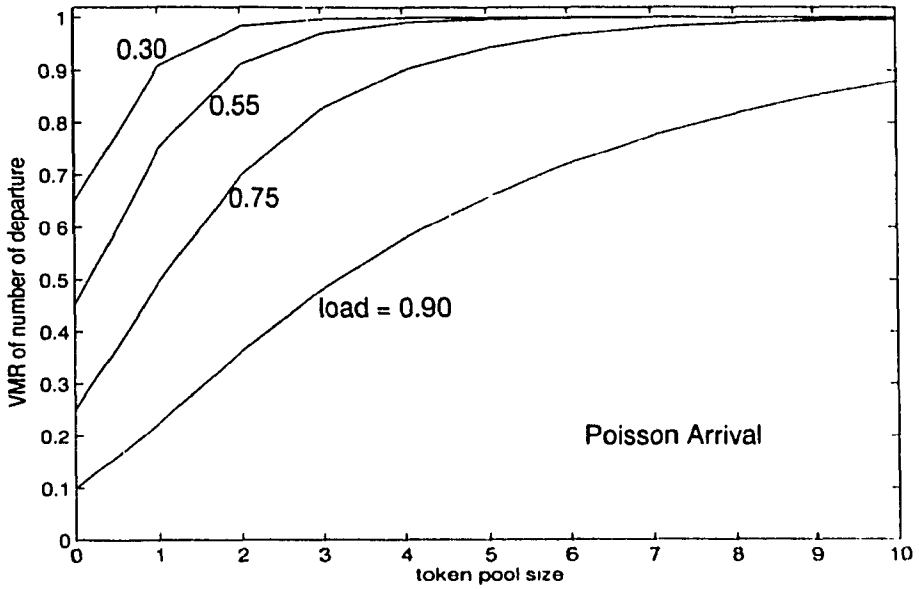

Figure 3.14 VMR of the no. of departures in a slot vs. token pool size M for different loads (Poisson arrival)

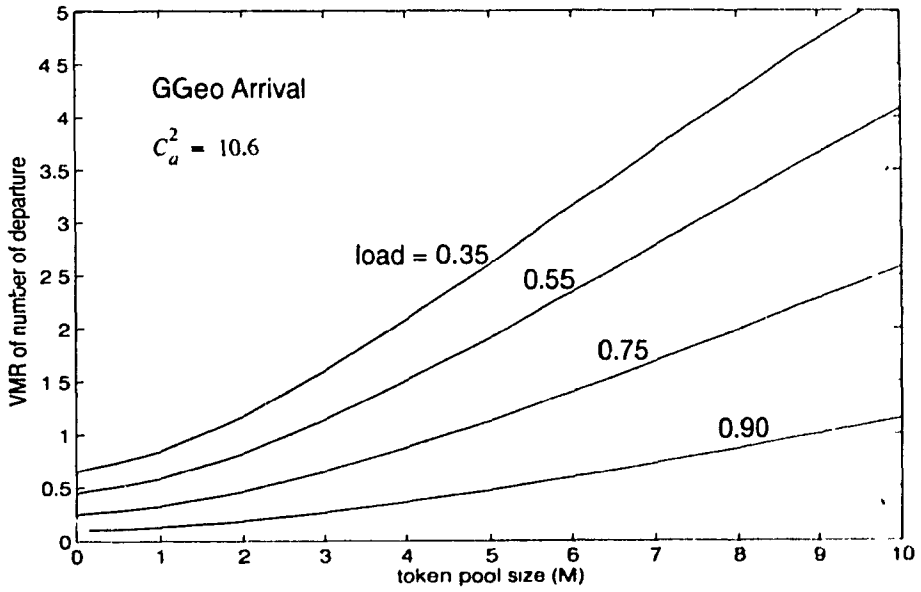

Figure 3.15 VMR of the no. of departures in a slot vs. token pool size M for different loads (GGeo arrival)

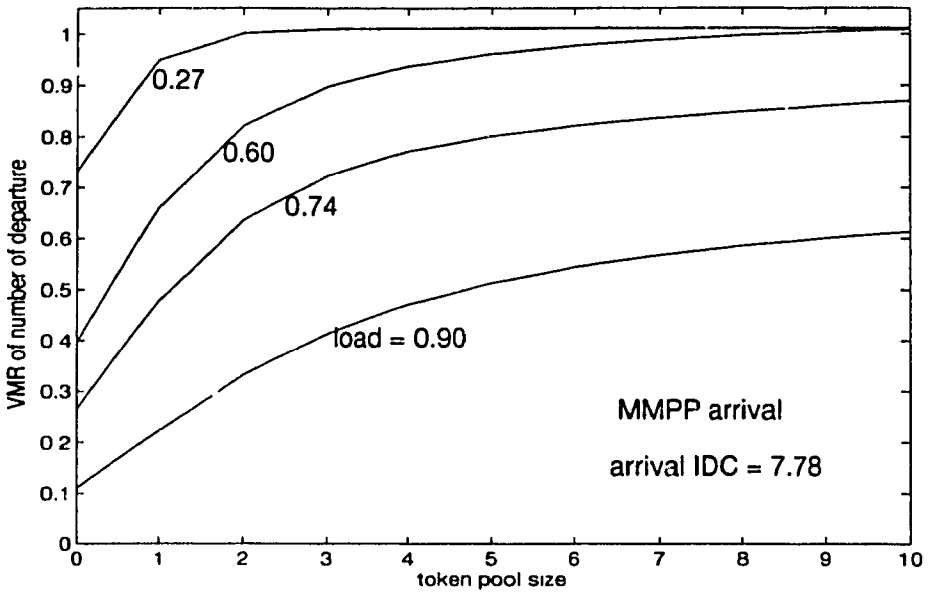

Figure 3.16 VMR of the no. of departures in a slot vs. token pool size M for different loads (MMPP arrival)

3.2 The Autocorrelation of the Number of Departures between Two Consecutive Slots

The correlation control effect of the Leaky Bucket for intervals at lag 1 is presented in Chapter 2. In this section, we are going to look at the correlation control effect for counts at lag 1 by using a similar mapping procedure given in the previous section.

3.2.1 Mapping Procedure

In order to see the correlation effect on the number of cell departures from a Leaky Bucket, we will look at the autocorrelation of the number of departures between the two consecutive slots (at lag 1). We make the same assumptions as before. Our embedded point is at the slot boundary, just after the token's departure. The cells and tokens only

arrive and depart at the slot boundary. The cell arrival process is independent from slot to slot and tokens depart in a FIFO order.

From the definition of autocorrelation, we know the autocorrelation of the number of departures between two consecutive slots can be determined by the joint probability of the number of departures at two consecutive slots $Q_C(i,j) = Pr[D^k = i, D^{k+1} = j]$.

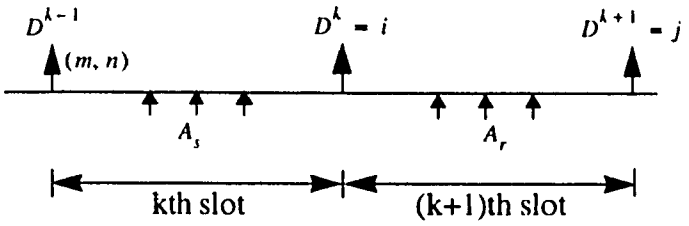

As before, at the embedded point, we may find the system in one of the following states.

1. The queue is not empty and the token pool is empty $(n \geq 1, m = 0)$*:*

a) There are $n = 1$ *cell and no tokens in the system.*

i) If there are no arrivals (A_0) *during the kth slot:*

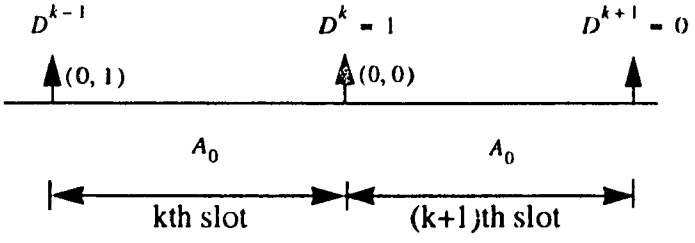

Figure 3.17

In the case there are no arrivals at the end of $(k+1)$th slot boundary shown in Figure 3.17, the number of departures at the kth slot boundary is one after the newly generated token is added to the empty bucket, and the number of departures at the $(k+1)$th slot boundary is zero with probability $A_0 A_0$. Then the joint probability of this event is:

$$Q_C(1,0) = Pr[D^k = 1, D^{k+1} = 0] = x_{M+1} A_0 A_0 e \tag{3.11}$$

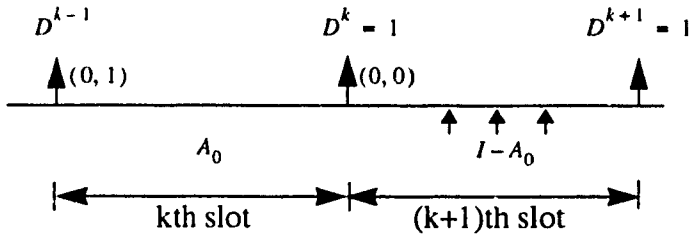

Figure 3.18

In the case of at least one arrival at the end of $k+1$ th slot boundary (Figure 3.18), both the number of departures at the kth and the $k+1$ th slot boundary are one with probability $A_0(I - A_0)$. Then the joint probability is:

$$Q_C(1,1) = Pr[D^k = 1, D^{k+1} = 1] = x_{M+1} A_0 (I - A_0) e \tag{3.12}$$

ii) If there is at least one arrival $(I - A_0)$ during the kth slot:

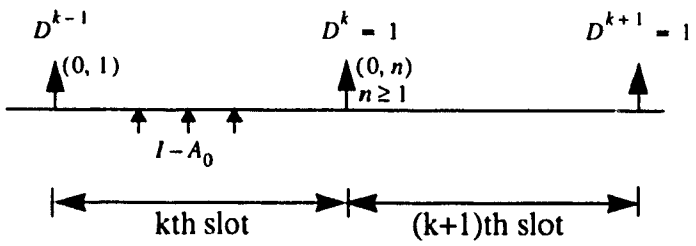

Figure 3.19

In this case shown in Figure 3.19, the number of departures at the kth slot boundary is one after the newly generated token is added to the bucket and the number of departures at the $k+1$ th slot boundary is one with probability since there are cells but no tokens in the bucket at the beginning of $k+1$ th slot and there will be only one newly generated token in the bucket at the end of $k+1$ th slot. The joint probability of this event is:

$$Q_C(1,1) = Pr[D^k = 1, D^{k+1} = 1] = x_{M+1}(1-A_0)e \tag{3.13}$$

b) There are n $(n \geq 2)$ cells and no tokens in the system.

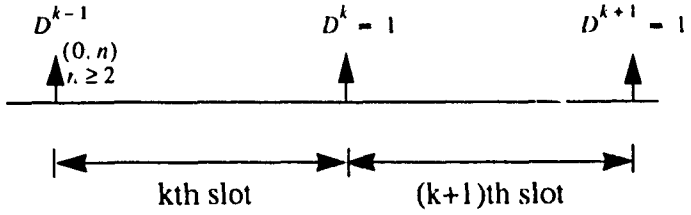

Figure 3.20

In this case (Figure 3.20), both the number of departures at the kth and $(k+1)$th slot boundary are one since the cells in the system are waiting for the tokens in order to depart from the system. The joint probability of this event is:

$$Q_C(1,1) = Pr[D^k = 1, D^{k+1} = 1] = \left(\sum_{i=M+2}^{\infty} x_i\right)e \tag{3.14}$$

2. *The queue is empty $(0 \leq m \leq M-2, n = 0)$:*

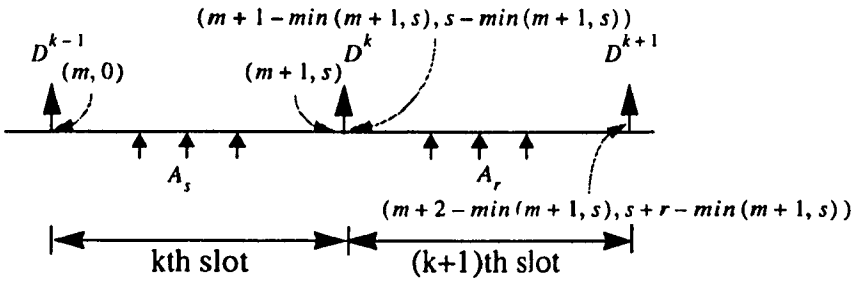

$$D^k = min(m+1, s)$$

$$D^{k+1} = min[m+2-min(m+1,s), s+r-min(m+1,s)]$$

Figure 3.21

As shown in Figure 3.21, at the end of kth slot, there are $m+1$ tokens and s cells in the system if s cells arrive at the kth slot with probability of A_s. In this case, the number of cell departures at this slot boundary is $min(m+1, s)$. There will be $m+1-min(m+1, s)$ tokens and $s-min(m+1, s)$ cells left in the system after the departure at the kth slot boundary. At the end of the $k+1$ th slot, there will be $m+2-min(m+1, s)$ tokens and $s+r-min(m+1, s)$ cells in the system if r cells arrive at the $(k+1)$th slot with probability of A_r; consequently, the number of departures at the $(k+1)$th slot boundary is $min[m+2-min(m+1, s), s+r-min(m+1, s)]$. The joint probability of having D^k and D^{k+1} departures at the kth and $(k+1)$th slot boundaries is:

$$Q_C(D^k, D^{k+1}) = x_{M-m} A_s A_r \qquad s, r = 0, 1, 2, 3, \ldots \tag{3.15}$$

where $D^k = min(m+1, s)$ and $D^{k+1} = min[m+2-min(m+1, s), s+r-min(m+1, s)]$.

3. The queue is empty and there are $M-1$ tokens in the bucket ($m = M-1, n = 0$):

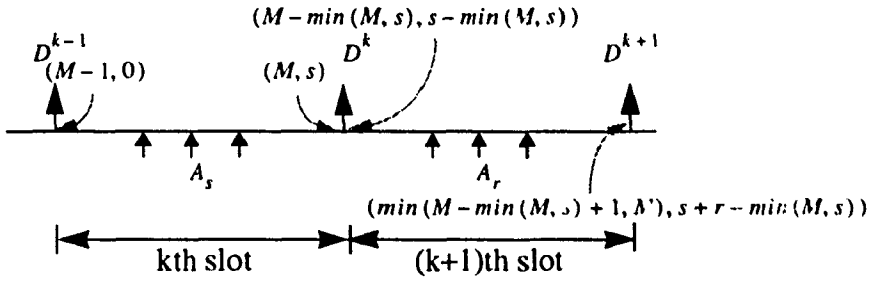

$D^k = min(M, s)$

$D^{k+1} = min[min(M - min(M, s) + 1, M), s + r - min(M, s$

Figure 3.22

At the end of kth slot, there are M tokens and s cells in the system if s cells arrive at the kth slot with probability of A_s, shown in Figure 3.22. In this case, the number of cell departures at this slot boundary is $min(M, s)$. There will be $M - min(M, s)$ tokens and $s - min(M, s)$ cells in the system at the beginning of the $(k+1)$th slot. At the end of the $(k+1)$th slot, there will be $min(M - min(M, s) + 1, M)$ tokens and $s + r - min(M, s)$ cells in the system if r cells arrive at the $(k+1)$th slot with probability of A_r. Then the number of departures at the $(k+1)$th slot boundary is $min(min(M - min(M, s) + 1, M), s + r - min(M, s))$. The joint probability of having D^k and D^{k+1} departures at the kth and $(k+1)$th slot boundaries is:

$$Q_C(D^k, D^{k+1}) = x_1 A_s A_r \qquad s, r = 0, 1, 2, 3, \ldots \tag{3.16}$$

where $D^k = min(M, s)$ and

$D^{k+1} = min(min(M - min(M, s) + 1, M), s + r - min(M, s))$.

4. *The queue is empty and the pool is full ($m = M, n = 0$):*

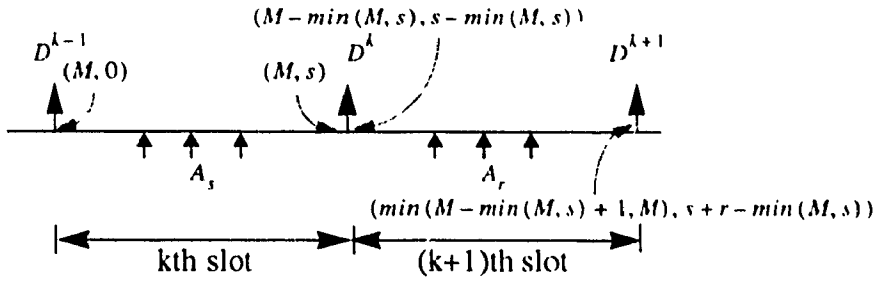

$D^k = min(M, s)$

$D^{k+1} = min[min(M - min(M, s) + 1, M), s + r - min(M, s)]$

Figure 3.23

This case is same as the case 3., except the initial state is different (see Figure 3.23). The joint probability of having D^k and D^{k+1} departures at the kth and $(k+1)$th slot boundaries is:

$$Q_C(D^k, D^{k+1}) = x_0 A_s A_r \qquad s, r = 0, 1, 2, 3, \ldots \tag{3.17}$$

where $D^k = min(M, s)$ and

$D^{k+1} = min[min(M - min(M, s) + 1, M), s + r - min(M, s)]$.

Then the autocorrelation of the number of departures between two consecutive slot (at lag 1) is

$$R_{C1} = E\{D^k D^{k+1}\} = \sum_{i=0}^{M} \sum_{j=0}^{M} ijPr[D^k = i, D^{k+1} = j] = \sum_{i=0}^{M} \sum_{j=0}^{M} ijQ_C(i, j) \tag{3.18}$$

The autocovariance at lag 1 is

$$\begin{aligned} C_{C1} &= R_{C1} - (\bar{D})^2 \\ &= \sum_{i=0}^{M} \sum_{j=0}^{M} ijQ_C(i,j) - (\bar{D})^2 \end{aligned} \tag{3.19}$$

Finally, the autocorrelation coefficient is given by

$$r_{C1} = \frac{C_{C1}}{Var(D)} = \frac{\sum_{i=0}^{M} \sum_{j=0}^{M} ijQ_C(i,j) - (\bar{D})^2}{Var(D)} \tag{3.20}$$

where $\bar{D}$ and $Var(D)$ are given in (3.7) and (3.9).

3.2.2 Numerical Results

Figure 3.24-Figure 3.29 show the autocorrelation coefficient of the number of departures between two consecutive slots, at various values of traffic load, token pool size M and arrival IDC for Poisson and MMPP arrival processes.

The autocorrelation coefficient of the number of departures between two consecutive slots is greatly affected by the traffic load and token pool size M as depicted in Figure 3.24 and Figure 3.25. It is interesting to note that the setting token pool size to one has different correlation control effect from other values of pool size as traffic load changes for Poisson arrival. The Leaky Bucket amplifies the correlation on counts at lag one when the token pool size is set to one.

Figure 3.26 shows the autocorrelation coefficient of the number of departures at lag one versus arrival IDC for the MMPP traffic. The main difference between the correlation (at lag 1) for counts and for intervals (Figure 2.37) is that the Leaky Bucket with token

pool size of one increases the short term correlation on counts. We have observed that the autocorrelation coefficient of the number of departures at lag 1 becomes less sensitive to arrival IDC value after it reaches to 20. We have similar results for the interdeparture time presented in Chapter 2.

Figure 3.27, Figure 3.28 and Figure 3.29 plot the effect of token pool size on the auto-correlation of the number of departures. As we mentioned before setting token pool size to one results in more correlated departure flow in terms of count at lag 1.

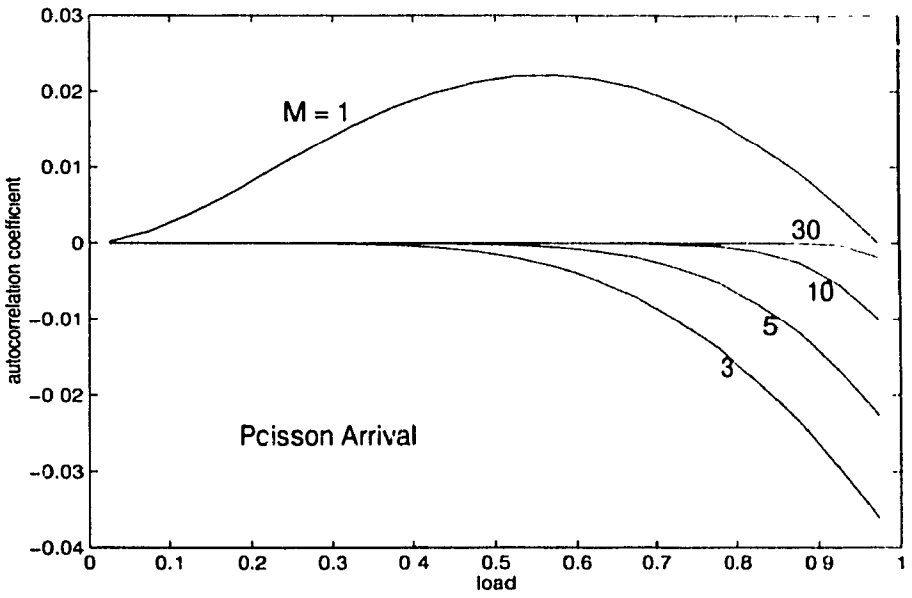

Figure 3.24 Autocorrelation coefficient of number of departures between two consecutive slots vs. load for different token pool size M (Poisson arrival)

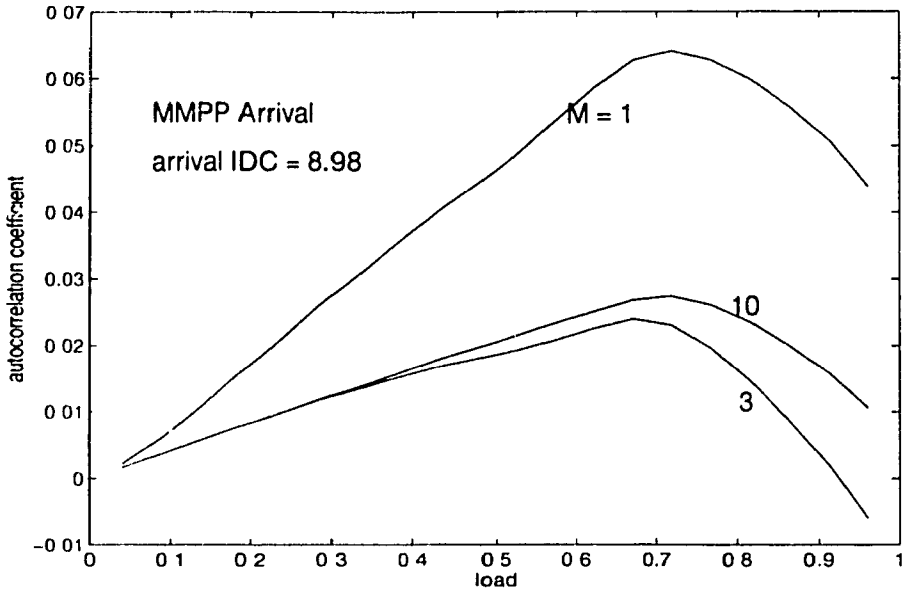

Figure 3.25 Autocorrelation coefficient of number of departures between two consecutive slots vs. load for different token pool size M (MMPP arrival)

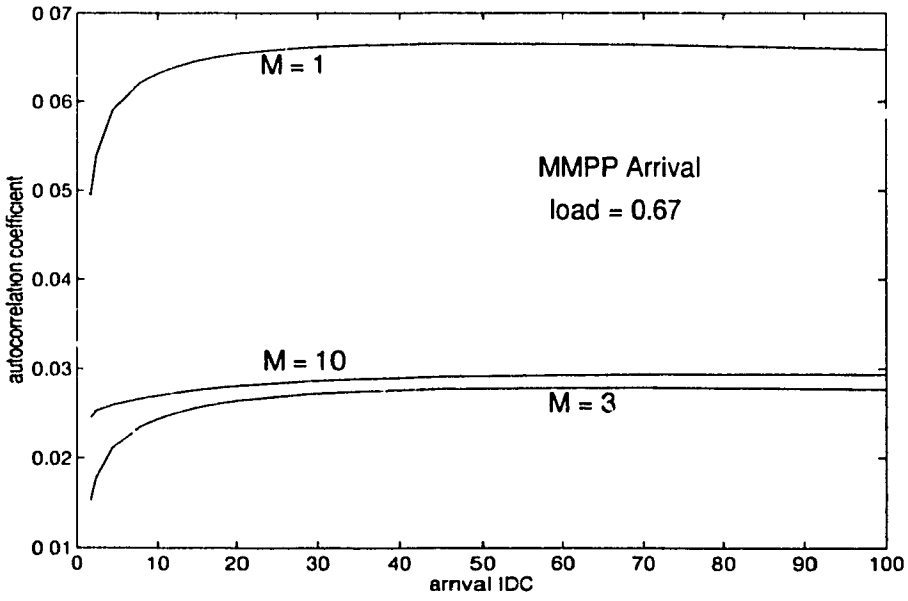

Figure 3.26 Autocorrelation coefficient of number of departures between two consecutive slots vs. token pool size M for different loads (MMPP arrival)

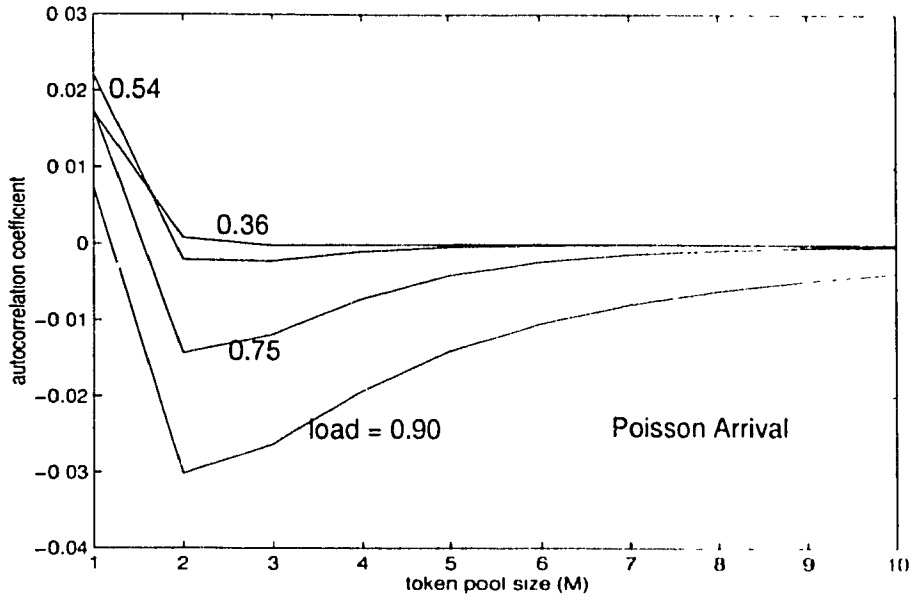

Figure 3.27 Autocorrelation coefficient of number of departures between two consecutive slots vs. token pool size M for different load (Poisson arrival)

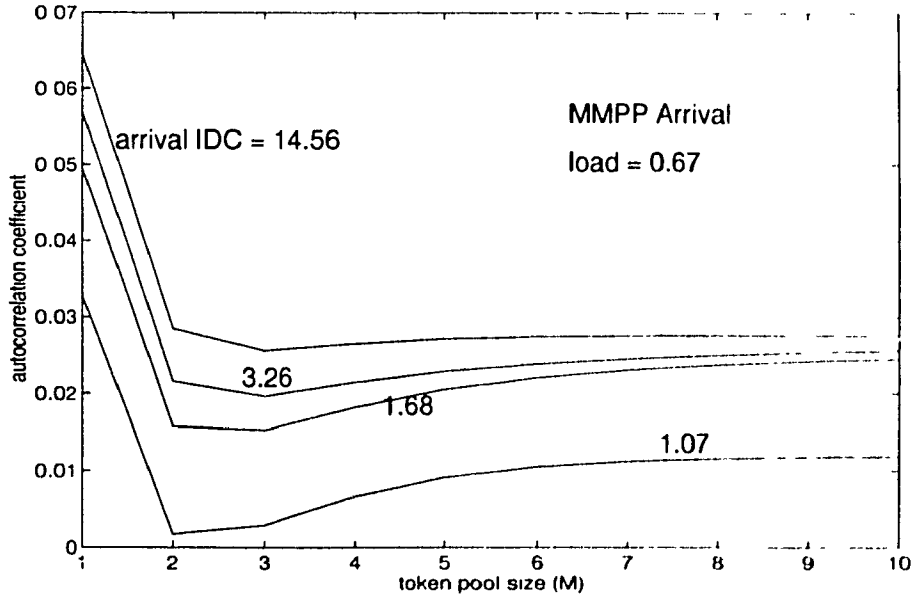

Figure 3.28 Autocorrelation coefficient of number of departures between two consecutive slots vs. token pool size M for different arrival IDC (MMPP arrival)

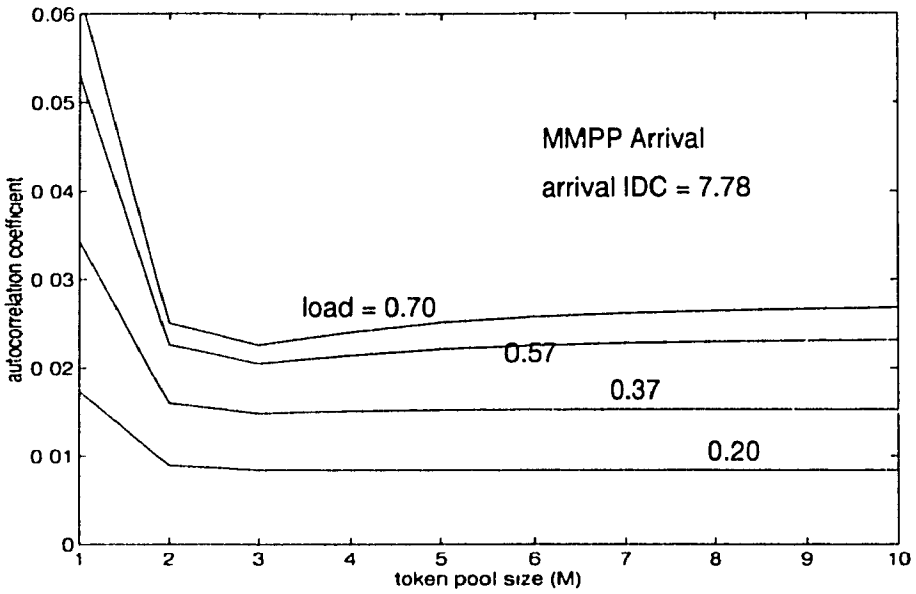

Figure 3.29 Autocorrelation coefficient of number of departures between two consecutive slots vs. arrival IDC for different token pool size M (MMPP arrival)

3.3 Autocovariance of the Number of Departures from a Leaky Bucket

The burstiness and correlation characteristics of the traffic are not only captured by simple burstiness index such as VMR and the short term covariance (e.g. at lag 1). In order to model the departure process accurately, it is necessary to look at the long term variance. In this section, the mean, variance and autocovariance of the number of departures at different lags are presented.

3.3.1 Number of Cell Departures from Leaky Bucket During a Slot

We let $D_{i,j}$ denote the number of cells departing at the end of a slot due to the $i \rightarrow j$ state transition (Figure 3.30), i and j are states of the system which reflect both number of tokens and cells. The relationship among the number of tokens (m), the number of cells (n) and the state of the system $(i = M - m + n)$ is listed in Table 2.1.

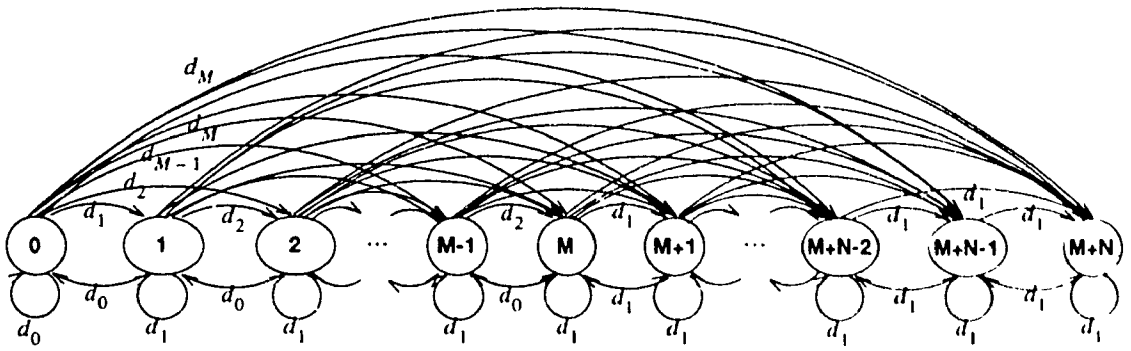

$d_i (0 \le i \le M)$: i cells departing from the Leaky Bucket at certain state transition

Figure 3.30 State Transition Diagram for Leaky Bucket Output

For $i \ge M + 1$, there is only one departure, then

$$D_{i,j} = \begin{cases} 1, & i-1 \le j \\ 0, & i-1 > j \end{cases}; \tag{3.21}$$

For $0 < i \le M$,

$$D_{i,j} = \begin{cases} j-i+1, & i-1 \le j \le M \\ M-i+1, & j > M \\ 0, & i-1 > j \end{cases}, \tag{3.22}$$

For $i = 0$,

$$D_{0,j} = \begin{cases} j, & j \le M \\ M, & j > M \end{cases} \tag{3.23}$$

In summary, the number of departures ($D_{i,j}$) at the end of a slot due to the $i \rightarrow j$ state transition could be written in the following form:

$$D_{i,j} = \begin{cases} min(M,j) - i, & i = 0 \\ min(M,j) - i + 1, & 0 < i \le M \\ 1, & i \ge M+1 \\ 0, & i - 1 > j \end{cases} \tag{3.24}$$

$$D = [D_{i,j}] = \begin{bmatrix} 0 & 1 & 2 & \dots & M-1 & M & M & \dots & M & M & M \\ 0 & 1 & 2 & \dots & M-1 & M & M & \dots & M & M & M \\ 0 & 0 & 1 & \dots & M-2 & M-1 & M-1 & \dots & M-1 & M-1 & M-1 \\ \dots & \dots & \dots & \dots & \dots & \dots & \dots & \dots & \dots & \dots & \dots \\ 0 & 0 & 0 & \dots & 1 & 2 & 2 & \dots & 2 & 2 & 2 \\ 0 & 0 & 0 & \dots & 0 & 1 & 1 & \dots & 1 & 1 & 1 \\ 0 & 0 & 0 & \dots & 0 & 1 & 1 & \dots & 1 & 1 & 1 \\ \dots & \dots & \dots & \dots & \dots & \dots & \dots & \dots & \dots & \dots & \dots \\ 0 & 0 & 0 & \dots & 0 & 0 & 0 & \dots & 1 & 1 & 1 \\ 0 & 0 & 0 & \dots & 0 & 0 & 0 & \dots & 1 & 1 & 1 \\ 0 & 0 & 0 & \dots & 0 & 0 & 0 & \dots & 0 & 1 & 1 \end{bmatrix} \tag{3.25}$$

3.3.2 The Mean, Variance and the Third Moment

Then the mean $\bar{D}$, the second moment $\overline{D^2}$, the variance $Var(D)$, and the third moment $\overline{D^3}$ of the number of cell departures at the end of a slot are obtained as follows:

$$\bar{D} = \sum_{i=0}^{M+N} x_i \sum_{j=0}^{M+N} D_{i,j} p_{i,j} \tag{3.26}$$

$$\overline{D^2} = \sum_{i=0}^{M+N} x_i \sum_{j=0}^{M+N} D_{i,j}^2 p_{i,j} \tag{3.27}$$

$$Var(D) = \overline{D^2} - (\overline{D})^2$$
$$= \sum_{i=0}^{M+N} x_i \sum_{j=0}^{M+N} D_{i,j}^2 p_{i,j} - (\overline{D})^2 \tag{3.28}$$

$$\overline{D^3} = \sum_{i=0}^{M+N} x_i \sum_{j=0}^{M+N} D_{i,j}^3 p_{i,j} \tag{3.29}$$

where $p_{i,j}$ is the i,jth entry of the state transition probability matrix P given in (2.3), x_i is the steady state probability given in (2.4).

The Variance to Mean Ratio (VMR) of the number of departures from the Leaky Bucket is given by:

$$VMR = \frac{Var(D)}{\overline{D}} = \frac{\sum_{i=0}^{M+N} x_i \sum_{j=0}^{M+N} D_{i,j}^2 p_{i,j} - \left(\sum_{i=0}^{M+N} x_i \sum_{j=0}^{M+N} D_{i,j} p_{i,j} \right)^2}{\sum_{i=0}^{M+N} x_i \sum_{j=0}^{M+N} D_{i,j} p_{i,j}} \tag{3.30}$$

3.3.3 Autocovariance of the Number of Departures at Different Lags

Let $i(k)$ denote the state of system at the end of $(k-1)$th slot and just before the beginning of the kth slot, and $j(k)$ be the state of the system at the end of kth slot, just before the beginning of the $(k+1)$th slot.

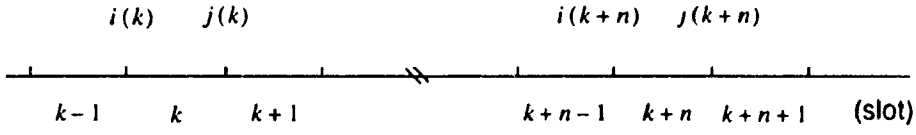

For simplifying the documentation, let $i(k) = i$, $j(k) = j$, $i(k+n) = l$ and $j(k+n) = m$.

The autocorrelation function of the number of cell departures at the end of the two slots with lag of n slots is

$$\begin{aligned} R_{Cn} &= E[D_{i(k),j(k)} D_{i(k+n),j(k+n)}] \\ &= \sum_{i=0}^{M+N} x_i \sum_{j=0}^{M+N} D_{i,j} p_{i,j} \sum_{l=0}^{M+N} p_{j,l}^{(n-1)} \sum_{m=0}^{M+N} D_{l,m} p_{l,m} \end{aligned} \tag{3.31}$$

where $p_{j,l}^{(i)}$ is the j,lth entry of the multiple step transition probability matrix $P^{(i)}$. P is the state transition probability matrix given in (2.3), and $P^{(i)} = P \times P^{(i-1)}$.

Then the autocovariance of the number of cell departures at lag n is given by:

$$\begin{aligned} C_{Cn} &= R_{Cn} - (\bar{D})^2 \\ &= \sum_{i=0}^{M+N} x_i \sum_{j=0}^{M+N} D_{i,j} p_{i,j} \sum_{l=0}^{M+N} p_{j,l}^{(n-1)} \sum_{m=0}^{M+N} D_{l,m} p_{l,m} \\ &\quad - \left(\sum_{i=0}^{M+N} x_i \sum_{j=0}^{M+N} D_{i,j} p_{i,j} \right)^2 \end{aligned} \tag{3.32}$$

The autocorrelation coefficient at lag n is:

$$r_{Cn} = \frac{C_{Cn}}{Var(D)} \tag{3.33}$$

where C_{Cn} and $Var(D)$ are given in (3.32) and (3.28).

Some numerical examples are given for the autocorrelation coefficient of the number of departures from the Leaky Bucket. Figure 3.31-Figure 3.38 show the autocorrelation coefficient at different lags for Poisson, GGeo and MMPP arrival processes. The effects of

traffic load, token pool size, SCV of the interarrival time and IDC of arrival process on the correlation of departure flow are presented. We have observed that autocorrelation coefficient function is unstable before lag 10. It is clear that only taking correlation statistics at lag 1 or 2 to mapping the output traffic is very approximate.

For the Poisson arrival process and lightly loaded or large token pool size systems, the departure flow has the same correlation characteristics as the arrival process as shown in Figure 3.31 and Figure 3.32.

The numerical results shown in Section 3.2 for lag 1 are verified the same as using the method in this section by setting lag to 1.

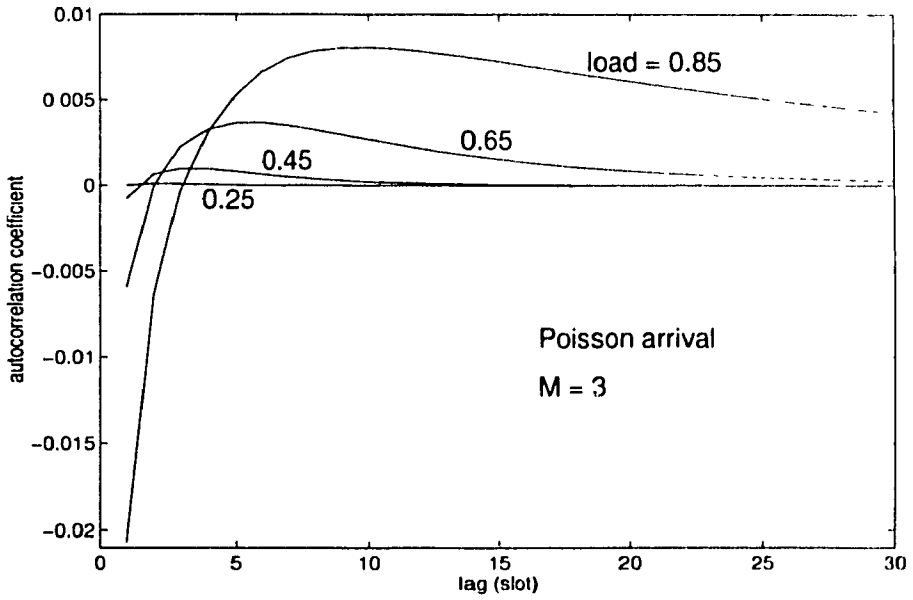

Figure 3.31 Autocorrelation coefficient of number of departures at different loads for Poisson arrival

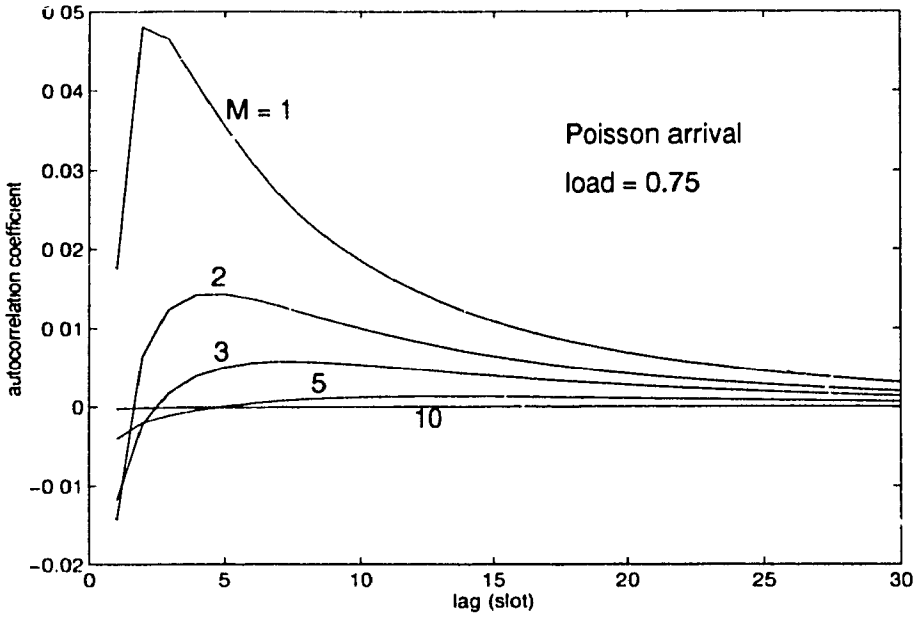

Figure 3.32 Autocorrelation coefficient of number of departures for different token pool size M for Poisson arrival

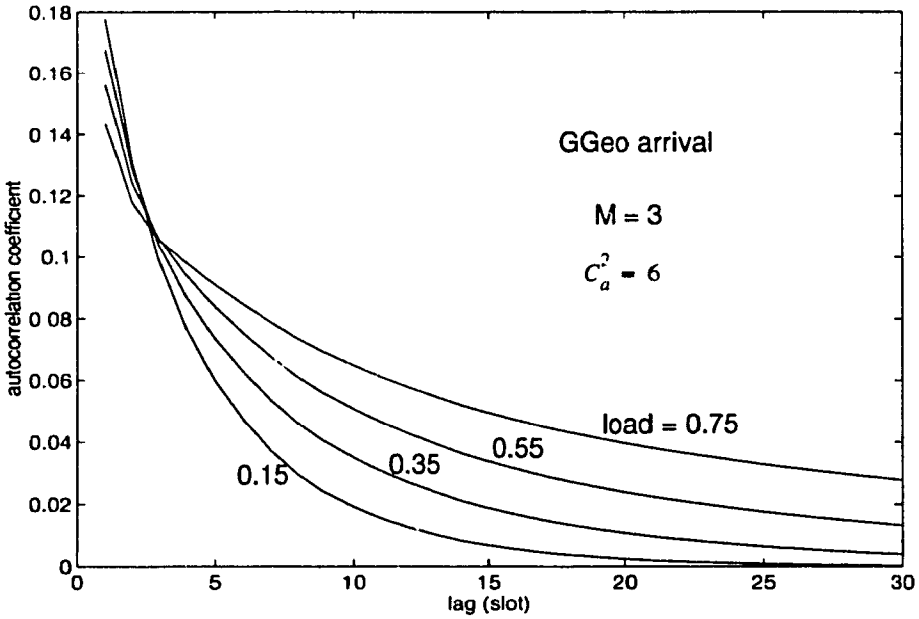

Figure 3.33 Autocorrelation coefficient of number of departures for different loads for GGeo arrival

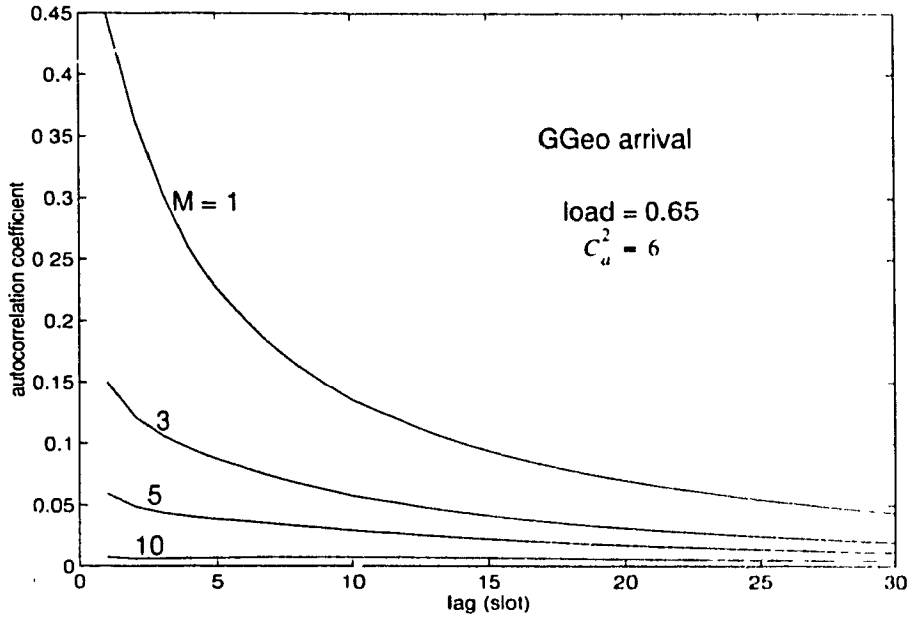

Figure 3.34 Autocorrelation coefficient of number of departures for different token pool size for GGeo arrival

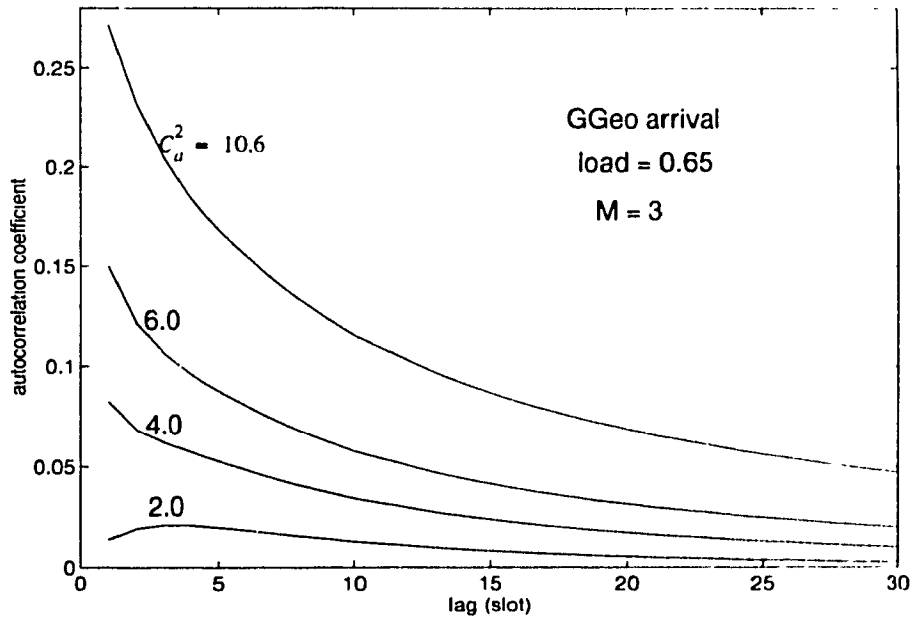

Figure 3.35 Autocorrelation coefficient of number of departures for different C_a^2 for GGeo arrival

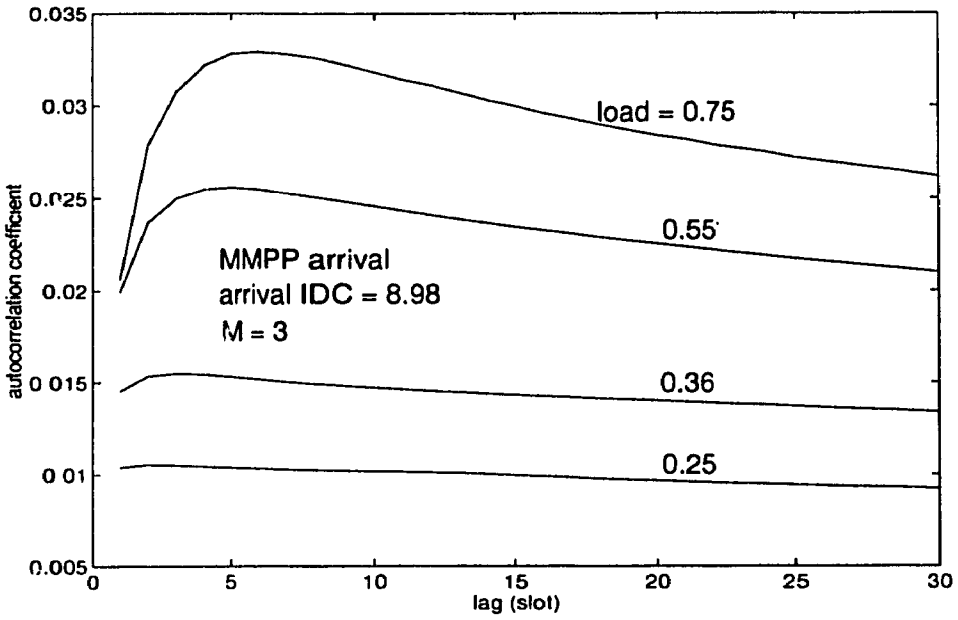

Figure 3.36 Autocorrelation coefficient of number of departures for different loads for MMPP arrival

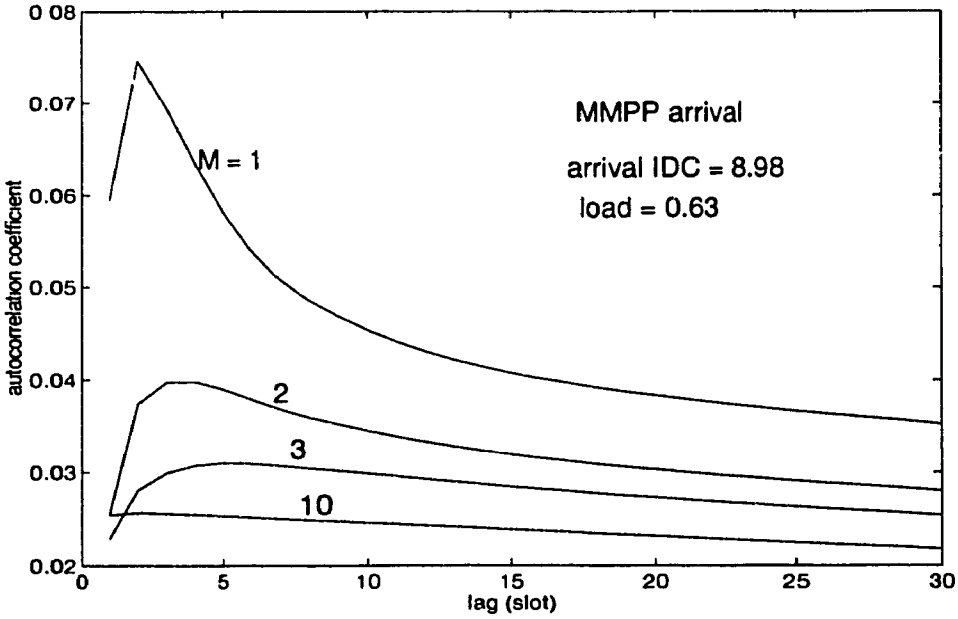

Figure 3.37 Autocorrelation coefficient of number of departures for different token pool size for MMPP arrival

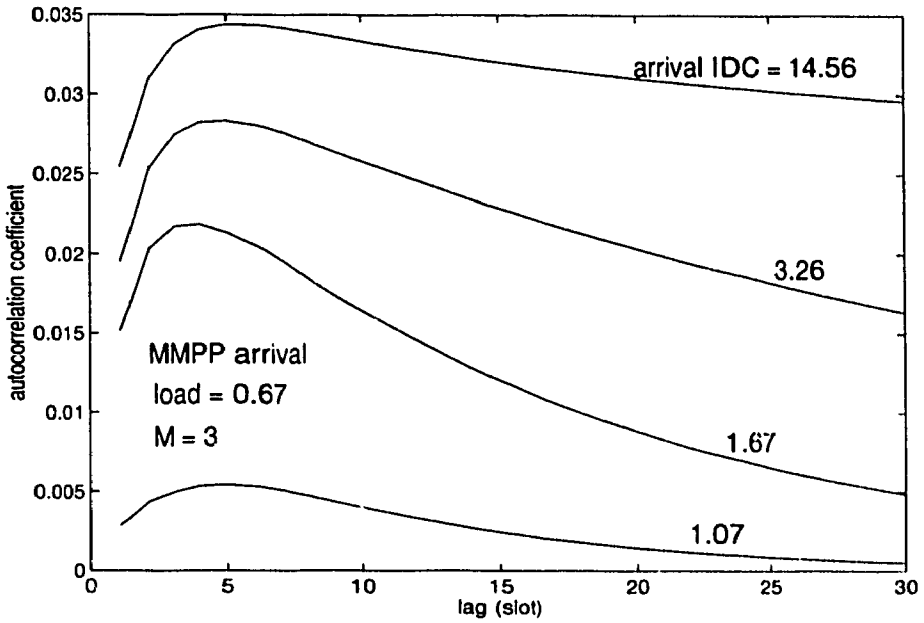

Figure 3.38 Autocorrelation coefficient of number of departures for different arrival IDC for MMPP arrival

3.4 Index of Dispersion for Counts (IDC) of the Departure Process of a Leaky Bucket

Gusella [35] demonstrates that Indexes of Dispersion of Counts (IDC) is a valuable and valid tool for characterizing the variability of a process. The IDC is relatively straightforward to estimate and conveys much more information than simpler indexes such as the coefficient of variation, that are often used to describe burstiness quantitatively. The IDC at lag n can be expressed in terms of VMR and the autocorrelation coefficient at lag k:

$$IDC_n = VMR\left[1 + 2\sum_{k=1}^{n-1}\left(1 - \frac{k}{n}\right)r_{Ck}\right] \tag{3.34}$$

where VMR and r_{Ck} is given in (3.30) and (3.33), respectively.

Figure 3.39-Figure 3.47 show departure IDC versus lag at different traffic loads, token pool sizes under Poisson, GGeo and MMPP arrival process. From these figures, we can see the departure IDC becomes closer to the arrival IDC when lag increases. It seems that the long term IDC (lag $\rightarrow \infty$) is likely to be preserved, same conclusion is obtained by Saito [36]. However, the reduction of Variance to Mean Ratio (IDC at lag 1) under the heavily loaded systems is larger than that under the lightly loaded systems, and that through the system with smaller token pool size is likely to be larger than that with a larger token pool size. These results are very helpful to us to do the statistical matching of the departure process of the Leaky Bucket.

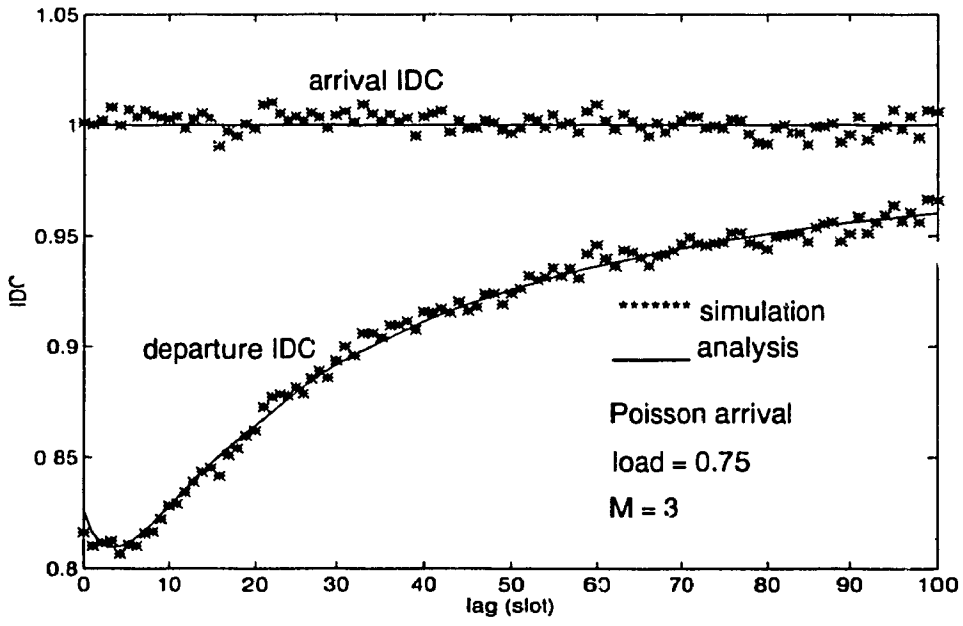

Figure 3.39 Comparison of the analysis results with simulation results for arrival and departure IDC (Poisson arrival)

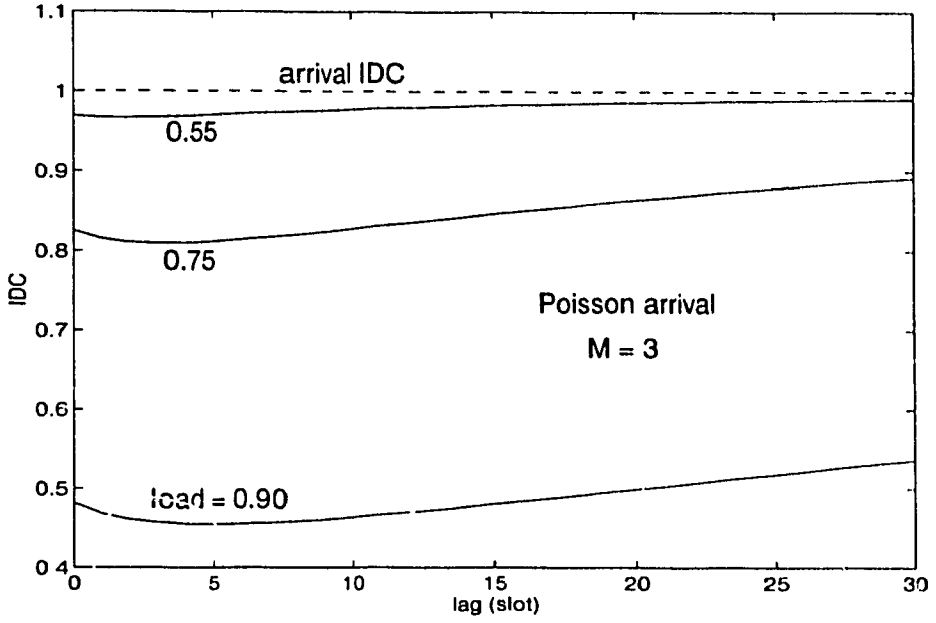

Figure 3.40 Departure IDC for different loads for Poisson arrival

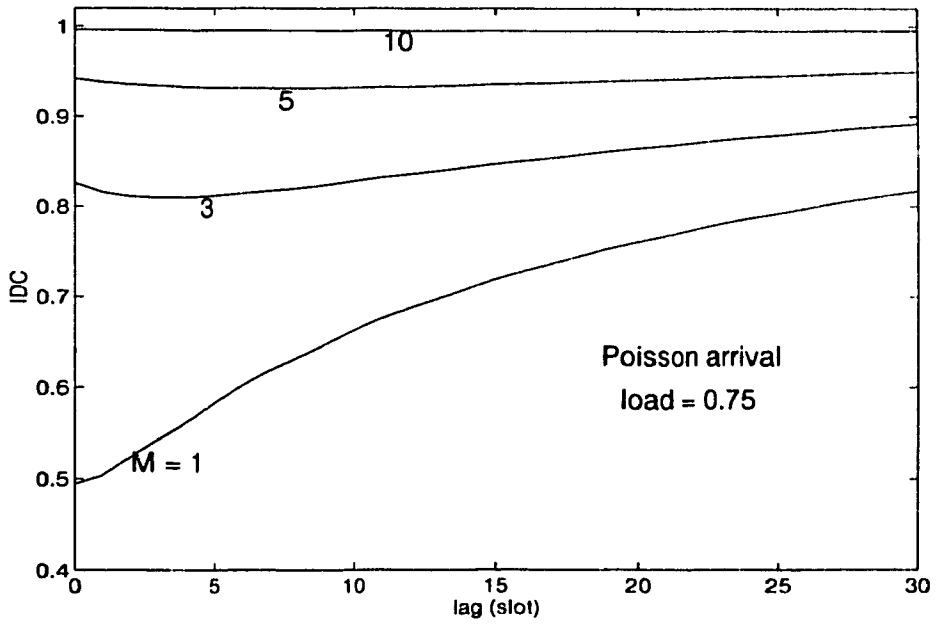

Figure 3.41 Departure IDC for different token pool size for Poisson arrival

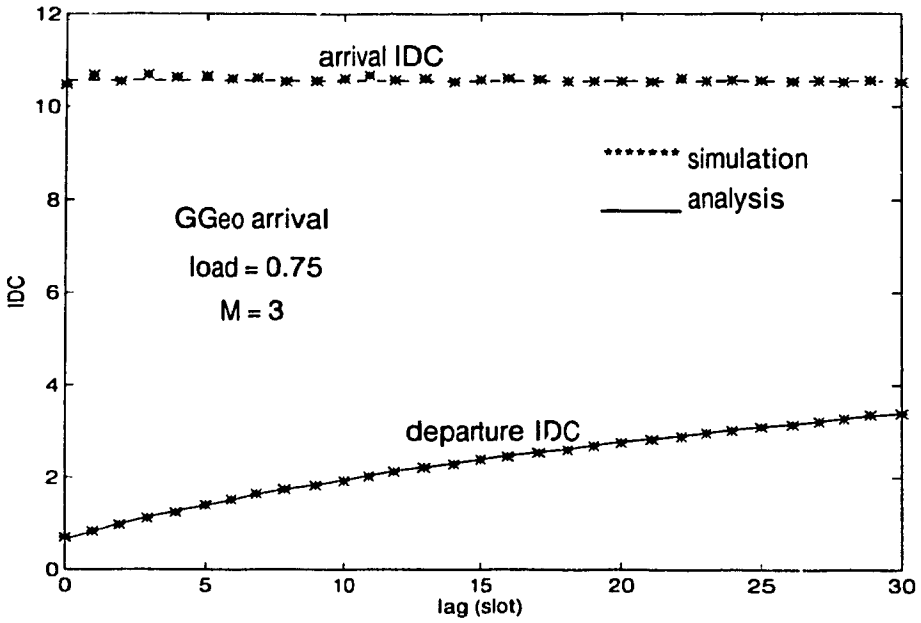

Figure 3.42 Comparison of the analysis results with simulation results for arrival and departure IDC (GGeo arrival)

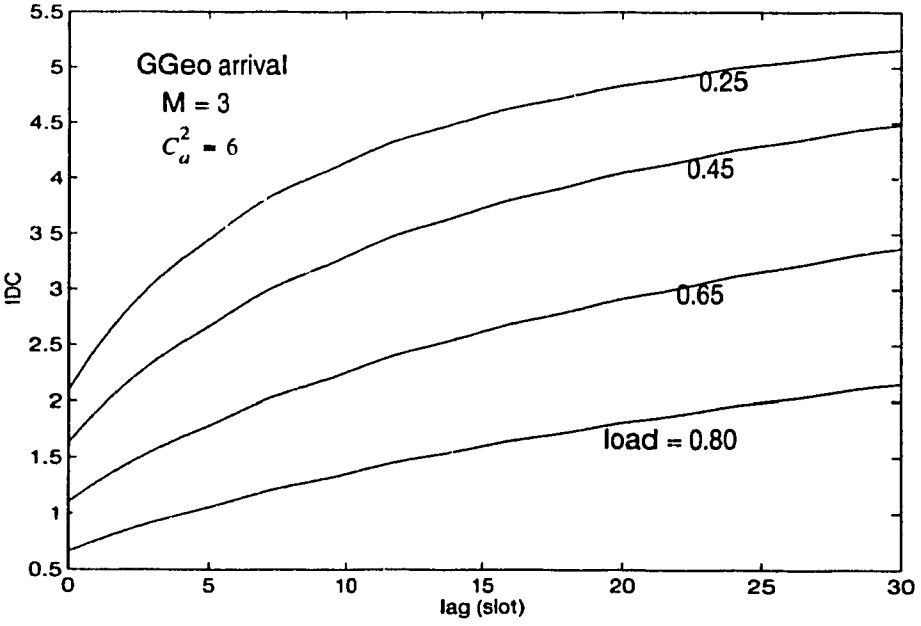

Figure 3.43 Departure IDC for different loads for GGeo arrival

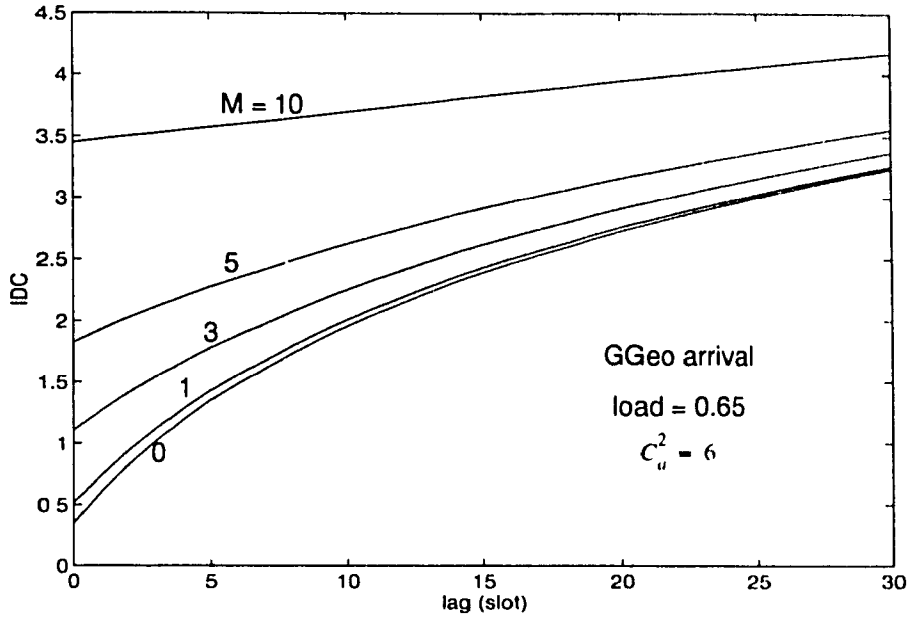

Figure 3.44 Departure IDC for different token pool size for GGeo arrival

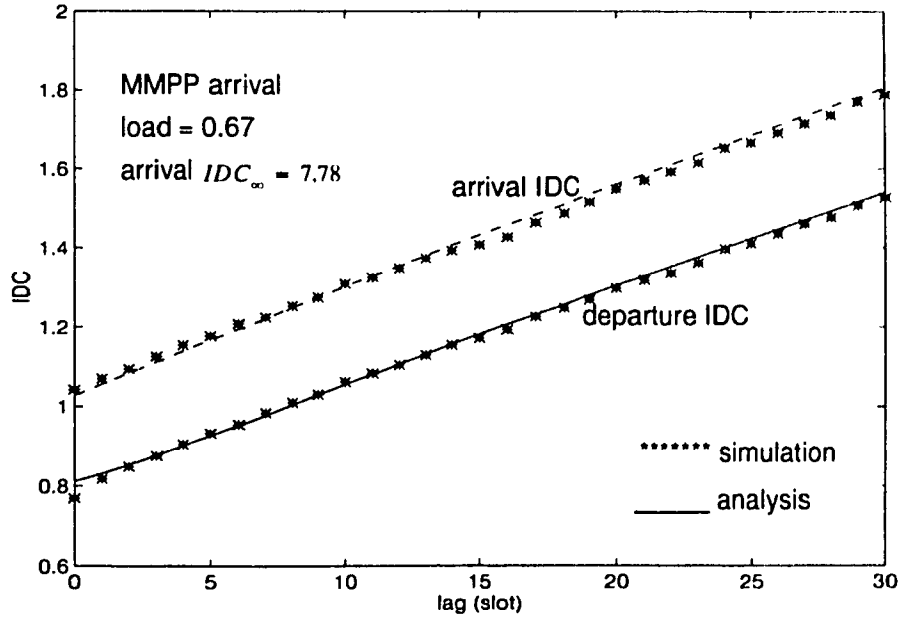

Figure 3.45 Comparison of the analysis results with simulation results for arrival and departure IDC (MMPP arrival)

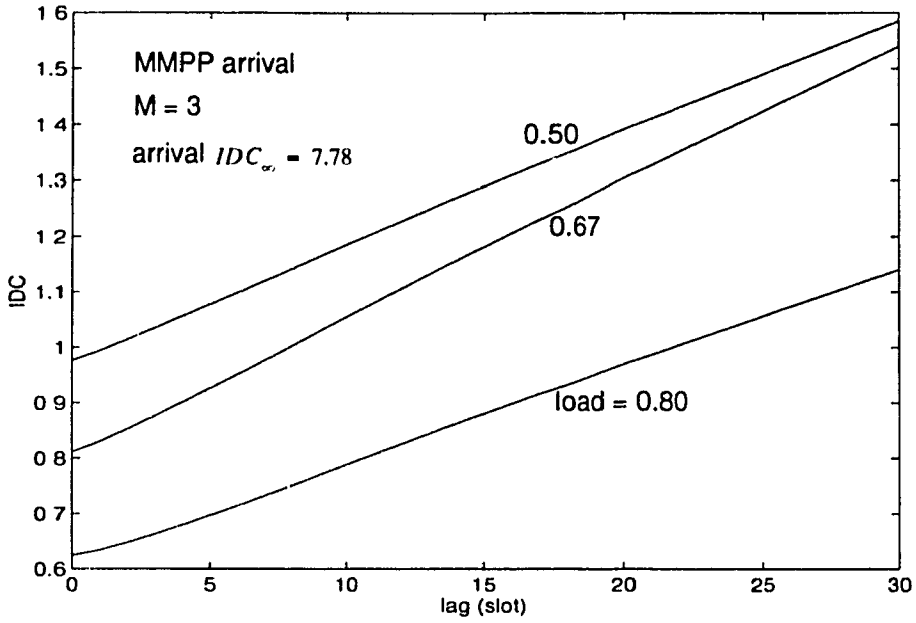

Figure 3.46 Departure IDC for different loads for MMPP arrival

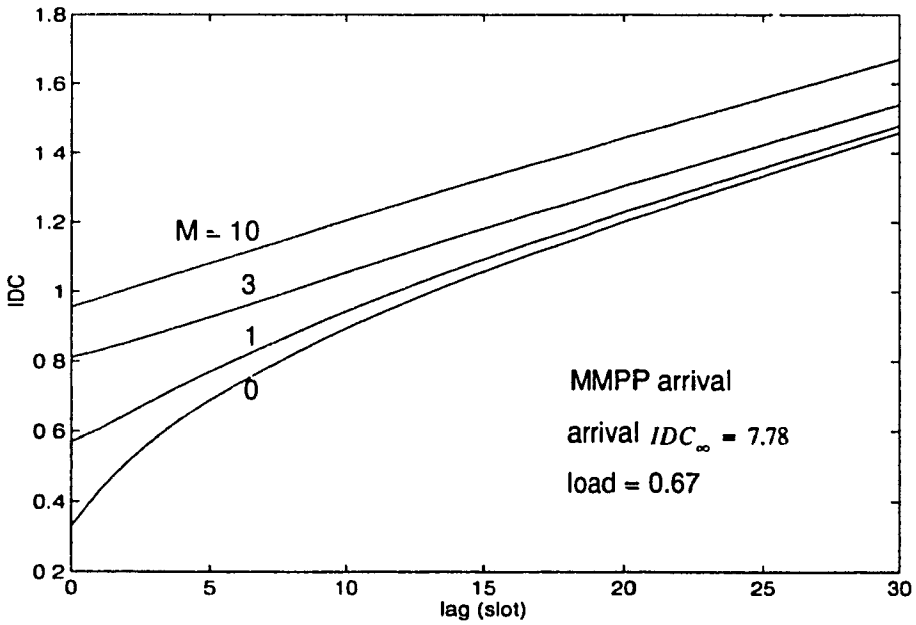

Figure 3.47 Departure IDC for different token pool size for MMPP arrival

The calculation of IDC in (3.34) is very time consuming because of those seven summations [(3.30), (3.32)-(3.34)], especially when the Leaky Bucket has large dimensions of M and N. Since the autocorrelation coefficient r_{Ck}, autocovariance C_{Ck} and the autocorrelation R_{Ck} have the following relations:

$$r_{Ck} = \frac{C_{Ck}}{Var(D)}, \qquad C_{Ck} = R_{Ck} - (\bar{D})^2 \tag{3.35}$$

we make some modifications to the equation (3.34) in order to speed up the calculation.

$$\begin{aligned} IDC_{n+1} &= VMR\left[1 + 2\sum_{k=1}^{n}\left(1 - \frac{k}{n+1}\right)r_{Ck}\right] \\ &= VMR\left[1 + \frac{2}{v_d}\sum_{k=1}^{n}\left(1 - \frac{k}{n+1}\right)C_{Ck}\right] \\ &= VMR\left[1 + \frac{2}{v_d}\left(\sum_{k=1}^{n} R_{Ck} - \frac{1}{n+1}\sum_{k=1}^{n} kR_{Ck} - \frac{n}{2}(\bar{D})^2\right)\right] \\ &= VMR\left[1 + \frac{2}{v_d}\left(\Phi - \frac{n}{2}(\bar{D})^2\right)\right] \end{aligned} \tag{3.36}$$

where $\Phi = \sum_{k=1}^{n} R_{Ck} - \frac{1}{n+1}\sum_{k=1}^{n} kR_{Ck}$.

$$\begin{aligned} \sum_{k=1}^{n} R_{Ck} &= \sum_{k=1}^{n}\left(\sum_{j=0}^{M+N}\sum_{i=0}^{M+N} x_i D_{i,j} p_{i,j} \sum_{l=0}^{M+N} p_{j,l}^{(k-1)} \sum_{m=0}^{M+N} D_{l,m} p_{l,m}\right) \\ &= \sum_{j=0}^{M+N}\sum_{i=0}^{M+N} x_i D_{i,j} p_{i,j} \sum_{l=0}^{M+N}\left(\sum_{k=1}^{n} p_{j,l}^{(k-1)}\right)\sum_{m=0}^{M+N} D_{l,m} p_{l,m} \\ &= \sum_{j=0}^{M+N}\sum_{i=0}^{M+N} x_i D_{i,j} p_{i,j} \sum_{l=0}^{M+N} C_l \sum_{m=0}^{M+N} d_{l,m} p_{l,m} \end{aligned} \tag{3.37}$$

$$\sum_{k=1}^{n} kR_k = \sum_{j=0}^{M+N}\sum_{i=0}^{M+N} x_i D_{i,j} p_{i,j} \sum_{l=0}^{M+N}\left(\sum_{k=1}^{n} kp_{j,l}^{(k-1)}\right)\sum_{m=0}^{M+N} D_{l,m}p_{l,m}$$
$$= \sum_{j=0}^{M+N}\sum_{i=0}^{M+N} x_i D_{i,j} p_{i,j} \sum_{l=0}^{M+N} C_2 \sum_{m=0}^{M+N} D_{l,m}p_{l,m} \qquad (3.38)$$

where $C_1 = \sum_{k=1}^{n} p_{j,l}^{(k-1)}$ and $C_2 = \sum_{k=1}^{n} kp_{j,l}^{(k-1)}$.

Then we have Φ as:

$$\Phi = \sum_{k=1}^{n} R_{Ck} - \frac{1}{n+1}\sum_{k=1}^{n} kR_{Ck}$$
$$= \sum_{j=0}^{M+N}\sum_{i=0}^{M+N} x_i D_{i,j} p_{i,j} \sum_{l=0}^{M+N}\left(C_1 - \frac{C_2}{n+1}\right)\sum_{m=0}^{M+N} D_{l,m}p_{l,m} \qquad (3.39)$$
$$= \sum_{j=0}^{M+N}\sum_{i=0}^{M+N} x_i D_{i,j} p_{i,j} \sum_{l=0}^{M+N} C \sum_{m=0}^{M+N} D_{l,m}p_{l,m}$$

where

$$C = C_1 - \frac{C_2}{n+1} = \sum_{k=1}^{n} p_{j,l}^{(k-1)} - \frac{1}{n+1}\sum_{k=1}^{n} kp_{j,l}^{(k-1)}$$
$$= \sum_{k=1}^{n}\left(1 - \frac{k}{n+1}\right)p_{j,l}^{(k-1)} \qquad (3.40)$$

Finally, IDC at lag $n+1$ is given by

$$IDC_{n+1} = VMR\left[1 + \frac{2}{Var(D)}\left(\sum_{j=0}^{M+N}\sum_{i=0}^{M+N} x_i D_{i,j} p_{i,j} \sum_{l=0}^{M+N} C \sum_{m=0}^{M+N} D_{l,m}p_{l,m} - \frac{n}{2}(\bar{D})^2\right)\right] \qquad (3.41)$$

Figure 3.48-Figure 3.53 give departure IDC at lag 20, 40 and 80 versus traffic load. At smaller lag, IDC has the similar control effect as VMR. However, when lag is set to a

larger value (e.g. at 80), the control effect becomes less. From these results, the same conclusion can be drawn as before. The long term IDC of the arrival process seems to be preserved by the Leaky Bucket mechanism.

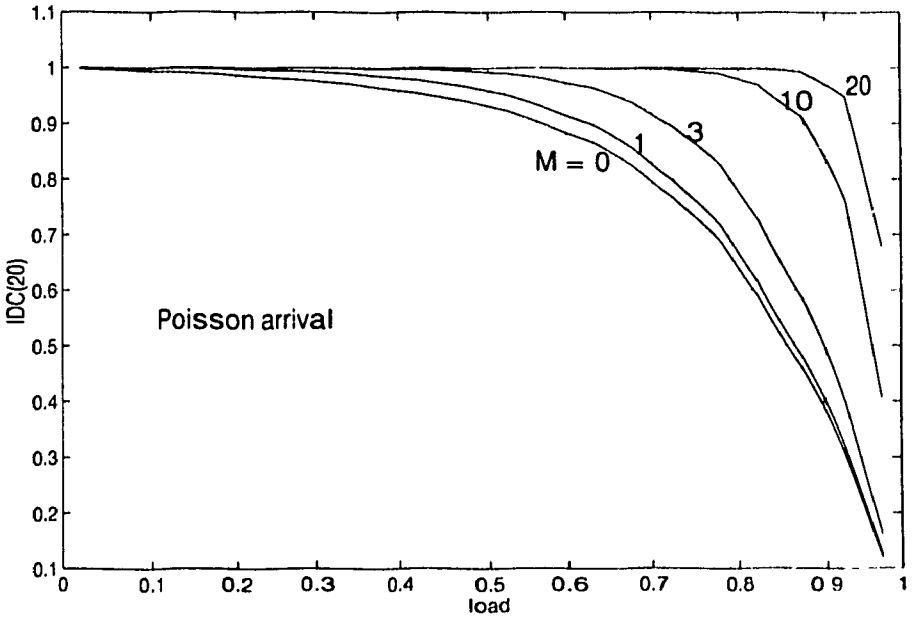

Figure 3.48 Departure IDC(20) vs. load for different token pool size M (Poisson arrival)

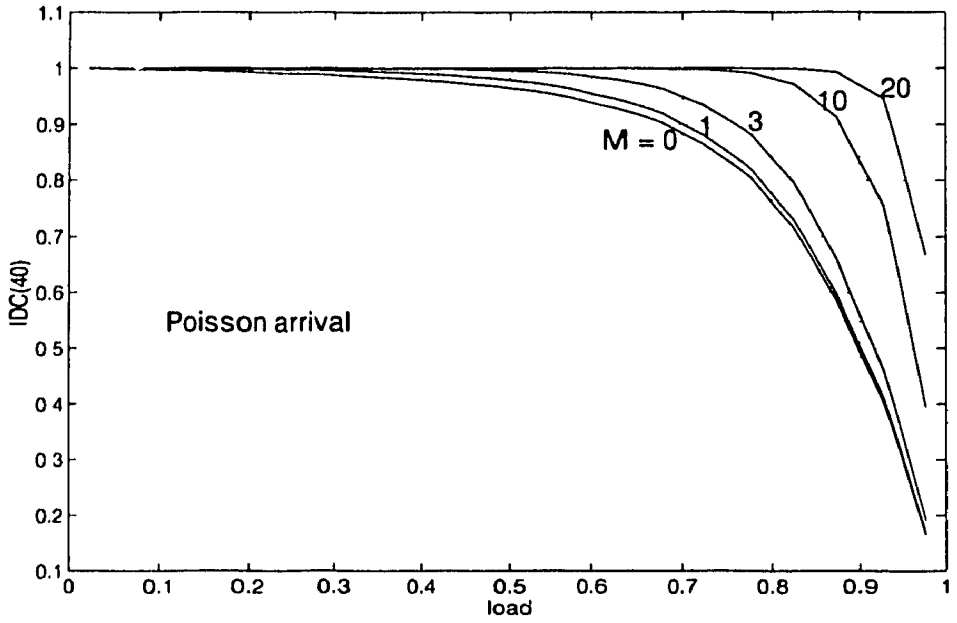

Figure 3.49 Departure IDC(40) vs. load for different token pool size M (Poisson arrival)

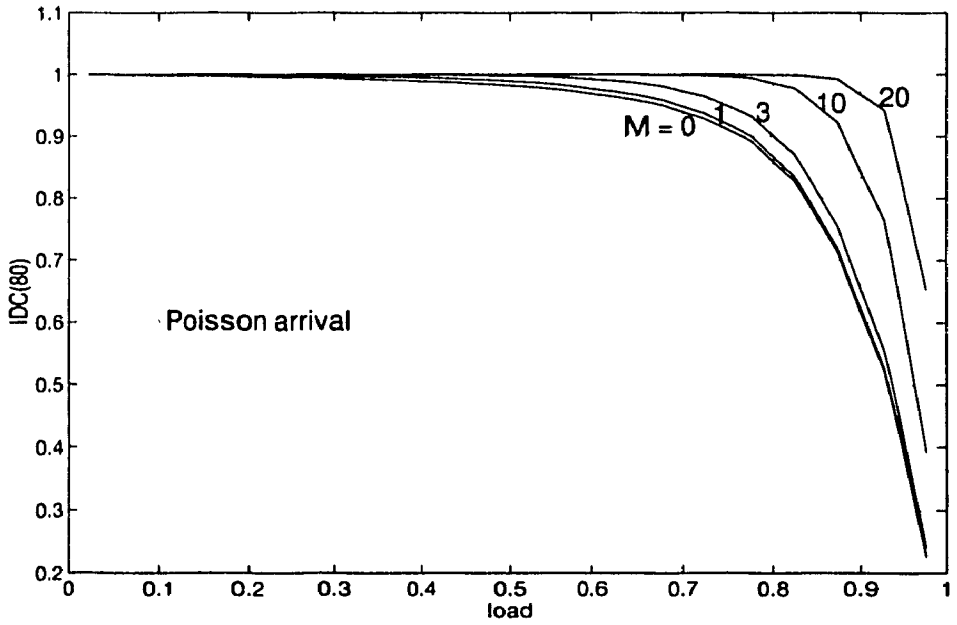

Figure 3.50 Departure IDC(80) vs. load for different token pool size M (Poisson arrival)

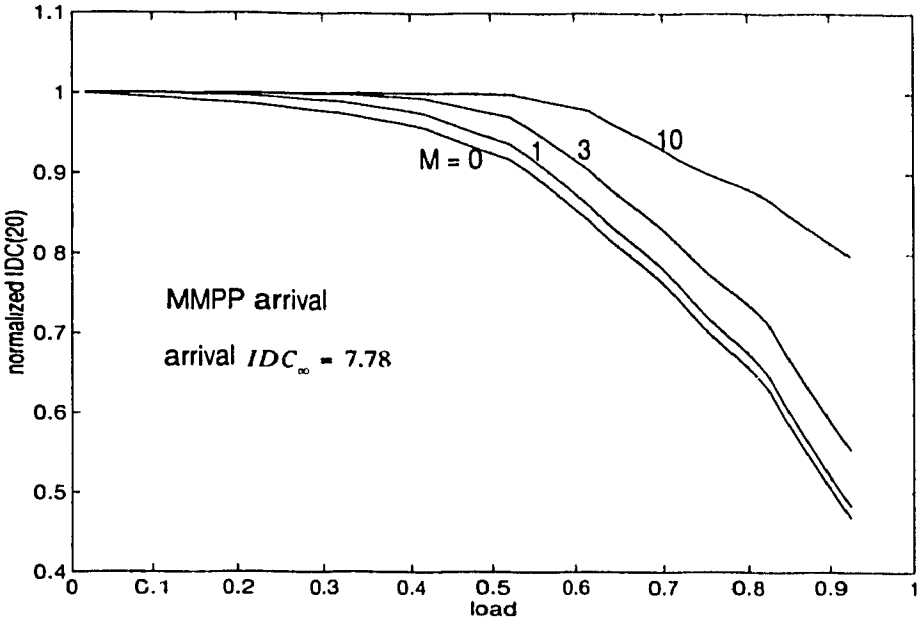

Figure 3.51 Normalized departure IDC(20) vs. load for different token pool size M (MMPP arrival)

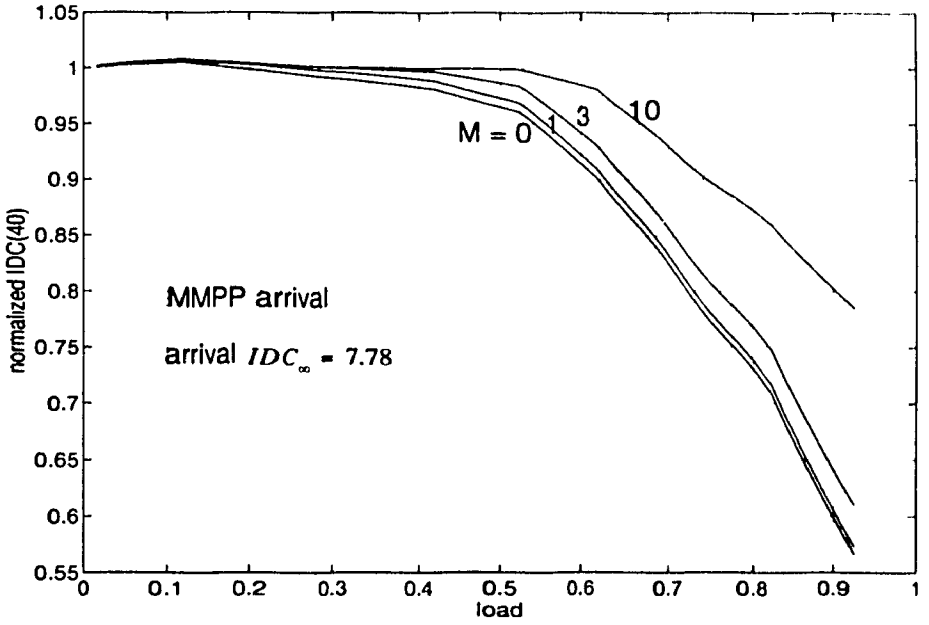

Figure 3.52 Normalized departure IDC(40) vs. load for different token pool size M (MMPP arrival)

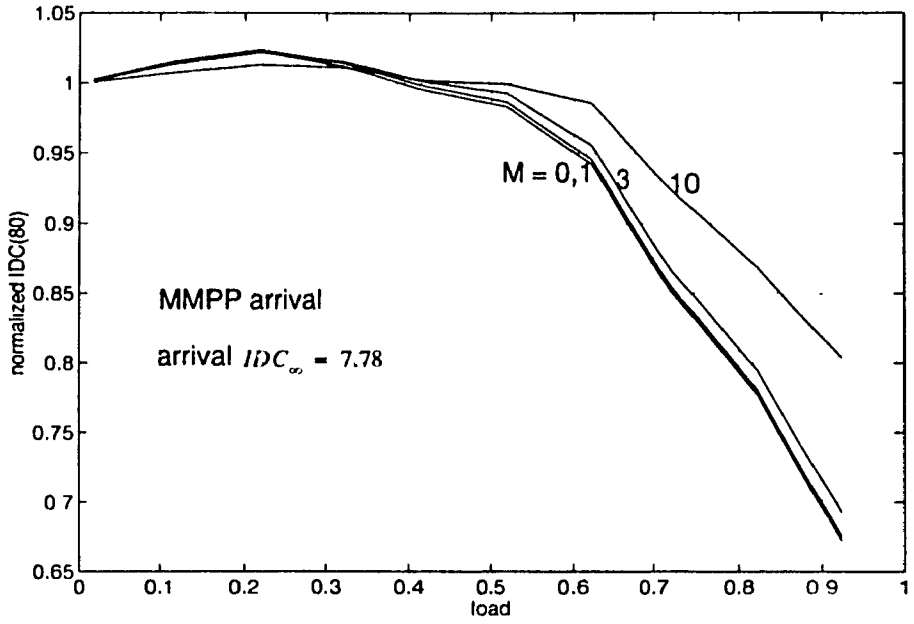

Figure 3.53 Normalized departure IDC(80) vs. load for different token pool size M (MMPP arrival)

3.5 Statistical Matching Procedure of the Departure Process to a two-state MMPP Model

Finding an appropriate representation for the output process of a Leaky Bucket is of paramount importance for network performance evaluation. With the correlated input, we are facing the challenge of obtaining a suitable traffic model for the departure process of the Leaky Bucket which can capture both the burstiness and the correlation. Recently, some studies analyze the statistical properties of the departure process of the Leaky Bucket. Only few [8] [33] presents a traffic model to approximate the departure process. Wu et.al [8] use a two-mini-source model to characterize the departure process of a Leaky Bucket by considering the autocovariance. But determining the parameters of the two-minisource model is very complicated and time consuming. As demonstrated earlier in Section 2.3, our MGeo model gives very good results for modeling the interdeparture time

distribution of the Leaky Bucket scheme. However, the MGeo model only captures the burstiness of the departure process. From the results shown in Section 3.3, we know that considering the long term correlation is very necessary for appropriate modeling the departure process.

The MMPP is a model that has received much attention in recent years. It is a powerful, analytically treatable model that can capture the burstiness and correlation. To reduce the complexity of solving queues, the departure process may be approximated by a simpler process such as two-state MMPP that can capture the important characteristics of the departure flow from the Leaky Bucket as closely as possible. The two-state MMPP is defined by four parameters $(\hat{\lambda}_1, \hat{\lambda}_2)$ and $(\hat{\sigma}_1, \hat{\sigma}_2)$. Then the problem is reduced to choosing the parameters of the two-state MMPP using four metrics of the departure process of the Leaky Bucket. For example, let us assume that the first four moments of the departure process are known. Then, using the equations of the first four moments of the two-state MMPP and the given values, we have four equations and four unknowns, which can be solved to obtain the required unknowns. However, in general, there is no guarantee that there is a two-state MMPP that matches the first four moments of the departure process exactly. Even if there is an exact match, we have a nonlinear system of equations to work with. Hence, most often the matching has to be done approximately.

In order to accurately model the departure process of the Leaky Bucket, it is important to capture both the variance and the long term covariance. In our procedure, we chose to match the Variance-to-Mean Ratio (VMR) and the long term autocorrelation coefficient (r_{Cn}) of the number of departures.

We assume the arrival process is the 2-state MMPP with parameters (λ_1, λ_2) and (σ_1, σ_2). Then

$$\Lambda = \begin{bmatrix} \lambda_1 & 0 \\ 0 & \lambda_2 \end{bmatrix}, \qquad R = \begin{bmatrix} -\sigma_1 & \sigma_1 \\ \sigma_2 & -\sigma_2 \end{bmatrix} \tag{3.42}$$

In order to capture variance of the number of departures of a Leaky Bucket, we denote

$$\frac{VMR_{\text{departure}}}{VMR_{\text{arrival}}} = \theta \tag{3.43}$$

where parameter θ is the ratio of departure VMR given in (3.30) to arrival VMR.

By definition of VMR:

$$VMR_{\text{arrival}} = \frac{Var(a)}{\lambda_a}, \qquad VMR_{\text{departure}} = \frac{Var(D)}{\lambda_d} \tag{3.44}$$

where $Var(a)/Var(D)$ is the variance of arrival/departure process and λ_a/λ_d is the average arrival/departure rate of the Leaky Bucket. In addition we know

$$\lambda_d = \lambda_a (1 - P_L) \tag{3.45}$$

where P_L is the cell loss probability.

Then the variance ($Var(D)$) of departure process can be obtained from

$$\left(\frac{Var(D)}{\lambda_d}\right) / \left(\frac{Var(a)}{\lambda_a}\right) = \theta \tag{3.46}$$

Substituting (3.45) into above equation, we have

$$Var(D) = \theta Var(a)\,(1 - P_L) \tag{3.47}$$

From [36] and the conclusion we reached in Section 3.4, we know that for the MMPP/D/1 queue, the covariance structure of the departure process are likely to be preserved even when the variance is controlled by the Leaky Bucket. To simplify calculations we assume that the parameters $\hat{R}$ and R which reflect the correlation structure have the following relation,

$$\frac{\hat{R}}{R} = \frac{\hat{\tau}}{\tau} = \gamma \tag{3.48}$$

where $\tau = 1/(\sigma_1 + \sigma_2)$, $\hat{\tau} = \sum_{n=0}^{\infty} r_{Cn}$ (refer to[41]), and γ is the normalized autocorrelation coefficient. The calculation of the autocorrelation coefficient r_{Cn} is very complicated and time consuming as we discussed in Section 3.3. For real-time system control, we suggest using the calculated curves (Figure 3.54) to find the value of γ at different traffic loads and token pool sizes. Then $\hat{R} = \gamma R$, $\hat{\sigma}_1$ and $\hat{\sigma}_2$ are given by

$$\hat{\sigma}_1 = \gamma\sigma_1, \qquad \hat{\sigma}_2 = \gamma\sigma_2 \tag{3.49}$$

We notice that from [41] for the 2-state MMPP,

$$Var(D) = \frac{(\hat{\lambda}_1 - \hat{\lambda}_2)^2 \hat{\sigma}_1 \hat{\sigma}_2}{(\hat{\sigma}_1 + \hat{\sigma}_2)^2}, \qquad Var(a) = \frac{(\lambda_1 - \lambda_2)^2 \sigma_1 \sigma_2}{(\sigma_1 + \sigma_2)^2} \tag{3.50}$$

$$\lambda_d = \frac{\hat{\lambda}_1 \hat{\sigma}_2 + \hat{\lambda}_2 \hat{\sigma}_1}{\hat{\sigma}_1 + \hat{\sigma}_2}, \qquad \lambda_a = \frac{\lambda_1 \sigma_2 + \lambda_2 \sigma_1}{\sigma_1 + \sigma_2} \tag{3.51}$$

Substitute (3.50) into (3.47) and (3.51) to (3.45), then $\hat{\lambda}_1$ and $\hat{\lambda}_2$ are found to be

$$\hat{\lambda}_1 = \lambda_a (1 - P_L) + \frac{(\lambda_1 - \lambda_2)\sigma_1}{\sigma_1 + \sigma_2} \sqrt{\theta (1 - P_L)} \tag{3.52}$$

$$\hat{\lambda}_2 = \lambda_a(1-P_L) - \frac{(\lambda_1-\lambda_2)\sigma_2}{\sigma_1+\sigma_2}\sqrt{\theta(1-P_L)} \tag{3.53}$$

where θ is the ratio of departure VMR to arrival VMR and P_L is the cell loss probability given in (2.6).

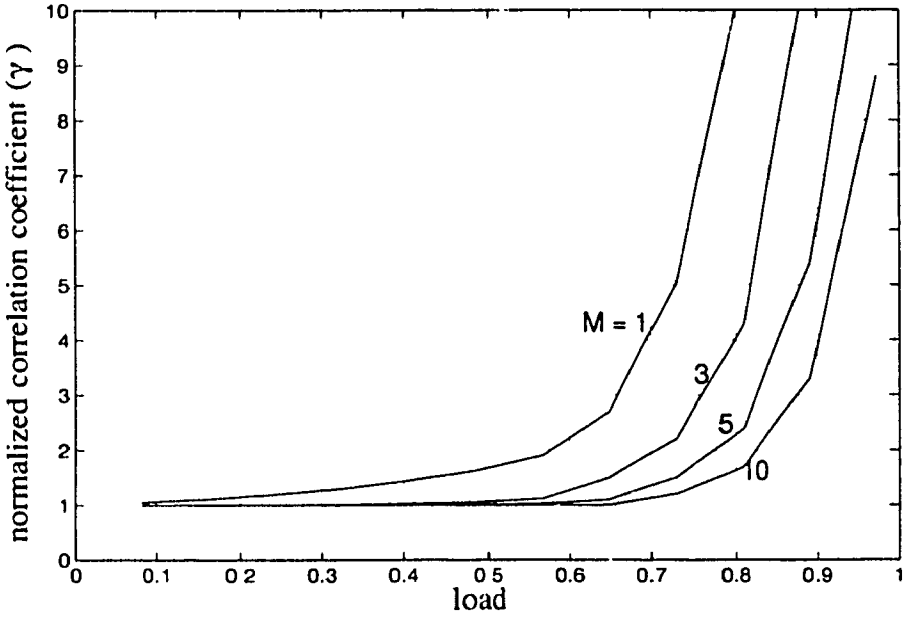

Figure 3.54 Normalized autocorrelation coefficient vs. traffic load

3.6 Conclusions

In this chapter, the characterizations of burstiness and correlation are discussed in terms of number of departures from a Leaky Bucket. The probability of the number of departures and the correlation of the number of departures between two consecutive slots are derived by using similar mapping procedures. We also consider the long term covariance in terms of autocovariance at arbitrary lags and IDC for the departure process of the

Leaky Bucket. Finally a two-state MMPP approximate model is suggested for future study to model the departure process of the Leaky Bucket. Further studies and verifications are needed through analysis and simulation work.

Chapter 4

CONCLUSIONS AND FUTURE WORK

The Leaky Bucket mechanism is widely considered to be the most promising approach for congestion control in the high-speed ATM networks. The study of the departure process of a Leaky Bucket is very important for the network performance evaluation. In this thesis, we have discussed various statistics of the departure process of a buffered Leaky Bucket scheme.

The Leaky Bucket scheme as a policing function in ATM networks must be available for every connection during the entire active phase and must operate in real-time. Our MGeo approach provides a good approximate model for the interdeparture time distribution of the Leaky Bucket and is computationally very efficient for real-time control.

The burstiness and correlation control effects are extensively examined in terms of SCV of interdeparture time, VMR of number of departures, and autocorrelation coefficient of two consecutive interdeparture times/number of cell departures between two consecutive slots.

The analyses are carried out under a wide range of traffic sources such as Poisson, Generalized Geometric (GGeo) and Markov Modulated Poisson Process (MMPP). Simulation results are provided to verify the accuracy of the various mapping procedures.

Numerical results are obtained in order to investigate how the traffic characteristics of the departure process of the Leaky Bucket are affected by the token pool size, the token generation rate, the burst a. d correlation degree of the arrival process. Based on the results we find that by decreasing the token generation rate the traffic flow gets smoother but cells may experience longer delay in input buffer. By increasing token pool size, smaller cell delay but higher bursty traffic flow may obtained. These results give the design engineer an idea of how to set the various parameters of a Leaky Bucket in accordance with the agreement between network and users.

We also look at the covariance function and Index Dispersion for Counts (IDC) of the departure process of a Leaky Bucket. Various numerical results are provided under the different arrival processes for further study. Finally, a two-state MMPP approximation is suggested for the departure process of the Leaky Bucket.

Although the results discussed in Chapter 2 and Chapter 3 are promising, there is still a number of issues that remain to be investigated and studied further.

- Modified Geometric (MGeo) model is demonstrated to be suitable for the interdeparture time distribution of the Leaky Bucket. A more general model based on MGeo which can also capture the correlation effect may be investigated.

- The calculations of the covariance function and Index of Dispersion for Counts (IDC) is complicated and time consuming. Simplification of those calculations is possible, and useful for the real-time control.

- The 2-state MMPP approximate model will be verified through simulation under the different traffic sources such as voice, video and data. This may result in more precise matching procedure.

Appendix A:

SIMULATION MODEL

Simulation of the departure process characterization of a Leaky Bucket under different traffic arrival processes is implemented in the UNIX environment using C. The flowchart of the simulation program for the Leaky Bucket is shown in Figure A.1.

In the simulation, time is segmented into fixed size of slots, and a slot is the minimum duration of any event. Cells arrive to the input buffer of the Leaky Bucket according to a Poisson or GGeo or two-state MMPP process. And tokens are generated at a fixed rate and stored in the token pool, if the token pool is not full. An arriving cell that finds the token pool non-empty departs the system and one token is removed from the token pool. An arriving cell that finds the token pool empty joins the input queue if buffer is not full, otherwise it is lost. The simulation is made over a specified number of cells generated to the system at each simulating point. The simulation yields a set of performance measures: system load, queue length and queue length variation; and output statistics: mean, variance, SCV of interdeparture time, VMR of the number of departures and IDC.

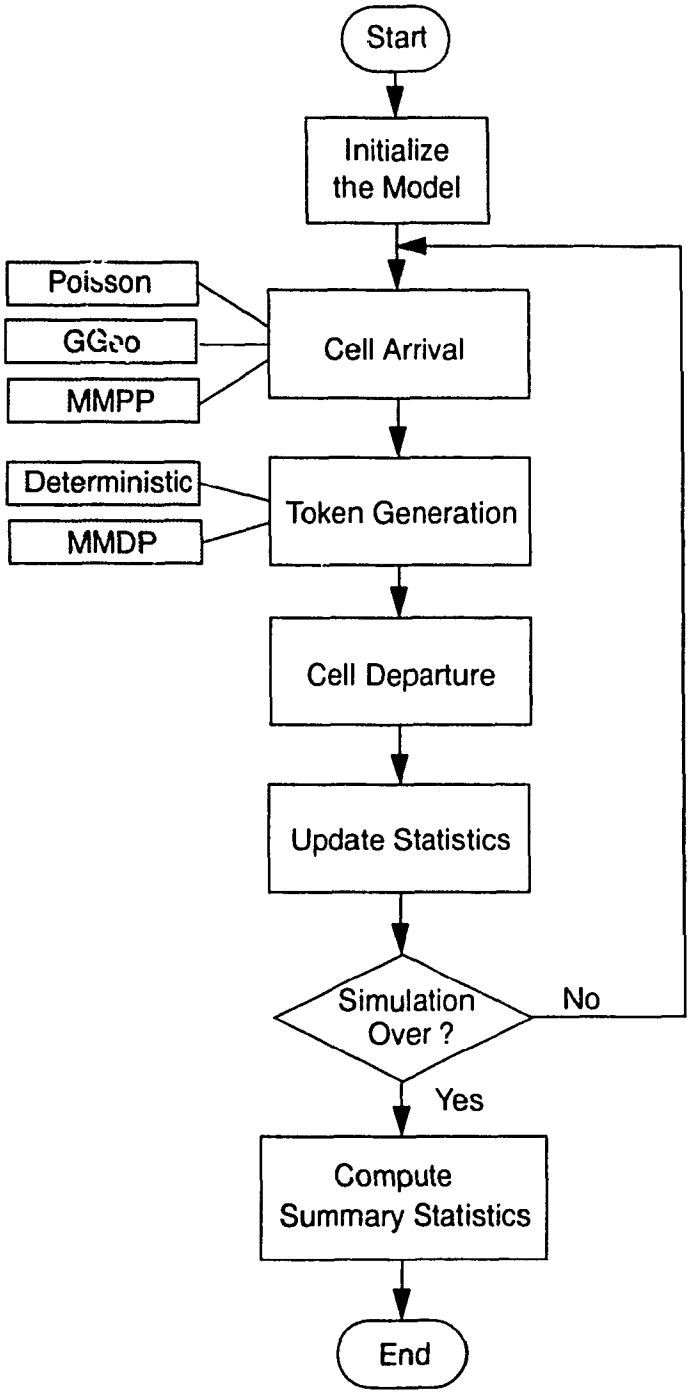

Figure A.1 Flowchart of the simulation program for the Leaky Bucket scheme

Appendix B:

CONFIDENCE INTERVAL AND MAXIMUM ERROR OF ESTIMATE

For each simulation used in this thesis, the method of repeating the simulation experiment is used for analyzing the data. The experiment is run many times using different (and presumedly independent) streams of random numbers for different runs.

Let m be the number of runs, and n be the observations in each run. Let $d_i^{(j)}$ be the delay of the ith cell in the jth run. $d_i^{(j)}$; $1 \le i \le n$, $1 \le j \le m$. The total number of cells generated is $m \cdot n$. We have total of $m \cdot n$ observations for each statistics analysis.

We denote the sample mean delay of the jth run by

$$\overline{d^{(j)}} = \frac{\sum_{i=1}^{n} d_i^{(j)}}{n}, \qquad j = 1, 2, \ldots, m \tag{B.1}$$

Then the set $\{\overline{d^{(j)}},\ 1 \le j \le m\}$ forms m independent and identically distributed random variables. The best estimates of the mean $\bar{d}$ and variance σ_d^2 of the variables $\overline{d^{(j)}}$ are given by the overall sample mean delay

$$\bar{d} = \frac{1}{m}\sum_{j=1}^{m}\overline{d^{(j)}} = \frac{1}{mn}\sum_{j=1}^{m}\sum_{i=1}^{n} d_i^{(j)} \tag{B.2}$$

and the sample variance

$$\sigma_d^2 = \frac{1}{m-1}\sum_{j=1}^{m}\left(\overline{d^{(j)}} - \bar{d}\right)^2 \tag{B.3}$$

respectively.

Since the number of cells generated is sufficiently large, the variables $\overline{d^{(j)}}$ are approximately normally distributed. Then, the distribution of the variable $\bar{d} - mean\left(\sigma_d^2/m\right)^{1/2}$ can be approximated by the t-distribution with $m-1$ degrees of freedom. Thus, the confidence interval for the mean is given by $\bar{d} \pm E$, where E is the maximum error of estimate and can be obtained by

$$E = \frac{t_{\alpha/2,\, m-1}}{m^{1/2}}\sigma_d \tag{B.4}$$

The value of $t_{\alpha/2}$ can be found in Table B.1.

Taking 95% confidence interval obtained from 20 runs as an example, we know from the figure on the next page that $\alpha = 1 - 95\% = 0.05$. Then $\alpha/2 = 0.025$ and $m = 20$. So the parameter $t_{\alpha/2}$ in (B.4) is given as $t_{0.025,\,19} = 2.093$.

In our experiment, the simulations results are obtained from total of 20 runs for each token generation rate $1/\alpha$ and each token pool size of M considered. We generate over 50K cells to the system for each run. The mean values are within 2% of the true mean with 95% confidence.

Table B.1. Table of Percentage Points of the t-Distribution

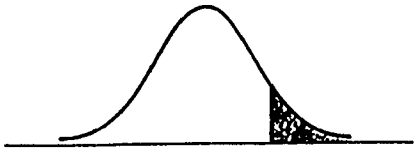

Degrees of Freedom	$t_{0.100}$	$t_{0.050}$	$t_{0.025}$	$t_{0.010}$	$t_{0.005}$
1	3.078	6.314	12.706	31.821	63.657
2	1.886	2.920	4.303	6.695	9.925
3	1.638	2.353	3.182	4.541	5.841
4	1.533	2.132	2.776	3.747	4.604
5	1.476	2.015	2.571	3.365	4.032
6	1 440	1.943	2.447	3.143	3.707
7	1.415	1.895	2.365	2.998	3.499
8	1.397	1.860	2.306	2.896	3.355
9	1.383	1.833	2.262	2.821	3.250
10	1.372	1.812	2.228	2.764	3.169
11	1.363	1.796	2.201	2.718	3.106
12	1.356	1.782	2.179	2.681	3.055
13	1 350	1.771	2.160	2.650	3.012
14	1.345	1.761	2.145	2.624	2.977
15	1.341	1.753	2.131	2.602	2.947
16	1.337	1.746	2.120	2.583	2.921
17	1.333	1.740	2.110	2.567	2.898
18	1.330	1.734	2.101	2.552	2.878
19	1.328	1.729	2.093	2.539	2.861
20	1.325	1.725	2.086	2.528	2.845
21	1.323	1.721	2.080	2.518	2.831
22	1.321	1.717	2.074	2.508	2.819
23	1.319	1.714	2.069	2.500	2.807
24	1.318	1.711	2.064	2.492	2.797
25	1.316	1.708	2.060	2.485	2.787
26	1.315	1.706	2.056	2.479	2.779
27	1.314	1.703	2.052	2.473	2.771
28	1.313	1.701	2.048	2.467	2.763
29	1.311	1.699	2.045	2.462	2.756
∞	1.282	1.645	1.960	2.326	2.576

Source: From M Merrington, "Table of Percentage Points of the *t*-Distribution," *Biometrika*, 32, 1941, p. 300 Reproduced by permission of the *Biometrika* Trustees.

Bibliography

[1] "CCITT: COM 18-228-E", Geneva, March, 1984.

[2] R. Handel and M.N. Huber, "*Integrated Broadband Networks: An Introduction to ATM-Based Networks*", Addison-Wesley Publishing Co., 1991.

[3] J.J. Bae and T. Suda, "Survey of Traffic Control Schemes and Protocols in ATM Networks", Proc. IEEE, Vol. 79, No. 2, pp. 170-189, February 1991.

[4] J. Turner, "New Directions in Communications (or Which Way to the Information Age?)", IEEE. Magazine, vol. 25, pp. 8-15, October 1986.

[5] W. Matragi and K. Sohraby, "Combined Reactive/Preventive Approach for Congestion Control in ATM Networks", IEEE INFOCOM'93, pp. 1336-1342, San Francisco, March 1993.

[6] M. Sidi, Wen-Zu Liu, I. Cidon and I. Gopal, "Congestion Control Through Input Rate Regulation", pp. 471-477. IEEE Transaction on Communications, Vol. 41, No.3, March 1993.

[7] K. K. Leung, B. Sengupta and R. W. Yeung, "A Credit Manager for Traffic Regulation in High-Speed Networks: A Queueing Analysis", IEEE/ACM Trans. on Networking, Vol. 1, No. 2, pp. 236-245, April 1993.

[8] X. Wu, I. Lambadaris, H. Lee and A. R. Kaye, "Output Process Characterization and Performance Analysis of a Leaky Bucket Access Scheme", Manuscript, Carleton University, 1993.

[9] I. Cidon and I.S. Gopal, "PARIS: An Approach to Integrated High-speed Private Networks", International Journal of Digital and Analog Cabled Systems, vol. 1, pp. 77-86, April-June 1988.

[10] A.W. Berger, "Performance Analysis of a Rate Control Throttle Where Tokens and Jobs Queue", IEEE INFOCOM'90, pp. 30-38, San Francisco, June 1990.

[11] A.E. Eckberg, D.T. Luan and D.M. Lucantoni, "Meeting the Challenge: Congestion and Flow Control Strategies for Broadband Information Transport", GLOBRCOM'89, pp. 49.3.1-49.3.5, Dallas, November 1989.

[12] K. Bala, I. Cidon and K. Sohraby, "Congestion Control for High-speed Packet Switch", INFOCOM'90, pp.520-526, San Francisco, June 1990.

[13] K.S. Sohraby and M. Sidi, "On the Performance of Bursty and Correlated Sources Subject to Leaky Bucket Rate-based Access Control Schemes", INFOCOM'91, pp. 426-434, Florida, 1991.

[14] J. Huang, Y. Chen, J.F. Hayes and M. Mehmet Ali, "Performance Analysis of Tunable Leaky Bucket in ATM Networks", ITC International Teletraffic Seminar, Russia, 1995.

[15] X. Wu, I. Lambadaris, H. Lee and A.R. Kaye, "A Comparative Study of Some Leaky Bucket Network Access Schemes", IEEE ICC'94, pp. 1586-1591, New Orleans, May 1994.

[16] H.R. Mehrvar and Tho Le-Ngoc, "ANN Approach for Congestion Control in Packet Switch OBP Satellite", IEEE ICC'95, Seattle, Washington, June 1995.

[17] D.M. Lucantoni, "New Results on the Single Server Queue with a Batch Markovian Arrival Process", Stochastic Models, Vol. 7, no.1, pp. 1-46, 1991.

[18] M.F. Neuts, "*Structured Stochastic Matrices of M/G/1 Type and their Applications*", New York & Basel: Marcel Dekker Inc., 1989.

[19] D.M. Lucantoni, K.S. Meier-Hellstern and M.F. Neuts, "A Single Server Queue with Server Vacations and a Class of Non-renewal Arrival Processes", Advanced Applied Probability, vol. 22, pp. 676-705, 1990.

[20] J. Huang and J.F. Hayes, "A Study of the Matrix Analytic Method and its Application in Performance Evaluation of Broadband and Related System", ISORA'95, Beijing, August 1995

[21] H. Bruneel and B. G. Kim, "*Discrete-time Models for Communication System Including ATM*", London: Kluwer Academic Publisher, 1993.

[22] J.N. Daigle, "*Queueing Theory for Telecommunications*", Addison-Wesley, 1992.

[23] J. W. Lee and B.G. Lee, "Performance analysis of ATM Cell Multiplexer with MMPP Input", IEICE Trans. Commun., Vol. E75-B, No. 8, August 1992.

[24] H. Heffes and D.M. Lucantoni, "A Markov Modulated Characterization of Packetized Voice and Data Traffic and Related Statistical Multiplexer Performance", IEEE Journal on Selected Areas in Comm., Vol. SAC-4, No. 6, pp.856-868, September 1986.

[25] S. Verma, "Matrix Geometric Technique: Theory and Application to Queueing Problems", Report, Dept. of ECE., Concordia University, April 1993.

[26] J. Huang, T. Zhu and J.F. Hayes, "An Efficient Computational Method for Solving Nonlinear Matrix Equation and its Application in Complicated Queueing Analysis", International Workshop on High Performance Computing, Beijing, July 1995.

[27] V. Ramaswami, "A Stable Recursion for the Steady State Vector in Markov chains of M/G/1 Type", Stochastic Models, Vol. 4, No. 1, pp. 183-188, 1988.

[28] D. D. Kouvatsos, "Maximum Entropy Analysis of Queueing Network Models", Performance Evaluation, No. 17, pp. 245-290, 1993.

[29] E. P. Rathgeb, "Modeling and Performance Comparison of Policing Mechanisms for ATM Networks", IEEE Journal on Selected Areas in Commun., Vol. 9, No. 3, pp. 325-334, April 1991.

[30] D. D. Kouvatsos, N. M. Tabet-Aouel and S.G. Denazis, "ME-based Approximations for general Discrete-time Queueing Model", Performance Evaluation, No. 21, pp. 81-109, 1994.

[31] G. Latouche and V. Ramaswami, "A Unified Stochastic Model for the Packet Stream from Periodic Sources", Performance Evaluation, No. 14, pp. 103-121, 1992.

[32] S. Wittevrongel and H. Bruneel, "Output Traffic Analysis of a Leaky Bucket Traffic Shaper Fed by a Bursty Source", IEEE ICC'94, pp.1581-1585, New Orleans, May 1994.

[33] Y. Chen, J. Huang, J.F. Hayes and M. Mehmet Ali, "Departure Process Characterization of the Leaky Bucket with Modified Geometric Model", CCECE'95, pp. 971, Montreal, September 1995.

[34] Y. Ohba, M. Muraata and H. Miyahara, "Analysis of Interdeparture Processes for Bursty Traffic in ATM Networks", IEEE Journal on Selected Areas in Comm., Vol. 9, No. 3, April 1991.

[35] Riccardo Gusella, "Characterizing the Variability of Arrival Processes with Indexes of Dispersion", IEEE Journal on Selected Areas in Comm., Vol. 9, No. 2, pp. 203-211, February 1991.

[36] H. Saito, "The Departure Process of an N/G/1 Queue", Performance Evaluation, No. 11, pp. 241-251, 1990.

[37] N.L.S. Fonseca and J.A. Silvester, "Modelling the Output Process of an ATM Multiplexer with Markov Modulated Arrivals", IEEE ICC'94, pp. 721-725, New Orleans, May 1994.

[38] T. Takine, T. Suda and T. Hasegawa, "Cell Loss and Output Process Analysis of a Finite-Buffer Discrete Time ATM Queueing System with Correlated Arrivals", IEEE INFOCOM'93, pp. 1259-1269, San Francisco, March 1993.

[39] M. Mehmet Ali and F. Kamoun, "ANew Approach in the Transient Analysis of ATM Multiplexers with Bursty Sources", IEEE GLOBECOM'94, pp.1060-1064, San Francisco, 1994.

[40] J. Huang, Tho Le-Ngoc and J.F. Hayes, "Performance of a Broadband Satellite Communications System", Canadian Conference on ECE., pp. 141-144, Montreal, September 1995.

[41] R. O. Onvural, "*Asynchronous Transfer Mode Networks Performance Issues*", Artech House Inc., 1994.

[42] H. Heffes, "A Class of Data Traffic Process - Covariance Function Characterization and Related Queueing Results", BSTJ, Vol. 59, No. 6, pp. 897-929, July-August 1980.

[43] J.F. Hayes, "*Modelling and Analysis of Computer Communications Networks*", New York: Plenum Publishing Co., 1984.

[44] L. Kleinrock, "*Queueing Systems*", Vol. 1: Theory, John Wiley & Sons Inc., 1975.

[45] A. Papoulis, "*Probability, Random Variables, and Processes*", 3rd Edition, McGraw-Hill, Inc., 1991.

[46] D. Hong, T. Suda and J. J. Bae, "Survey of Techniques for Prevention and Control of Congestion in an ATM Network", IEEE ICC'91, pp. 204-210, Denver, June 1991.

[47] M. Butto, E. Cavallero and A. Tonietti, "Effectiveness of the 'Leaky bucket' Policing Mechanism in ATM Networks", IEEE Journal on Selected Areas in Comm., Vol. 9, No. 3, pp. 335-342, April 1991.

[48] J. Ren and J.W. Mark, "Design and Analysis of a Credit-Based Controller for Congestion Control in B-ISDN/ATM Networks", IEEE INFOCOM'95, pp. 40-48, Boston, April 1995.

[49] V. Bemmel, "A Unified Congestion Control Strategy in ATM Networks", IEEE ICC'94, pp. 1600-1604, New Orleans, May 1994.

[50] J. Banks and J. Carson, "*Discrete-event System Simulation*", Prentice-Hall, 1984.

[51] R.E. Walpole and R.H. Myers, "*Probability and Statistics for Engineers and Scientists*", Macmillan Publishing Company.